

## Linear elastic theories of plates for in-plane (membrane) loading

We need to understand the relations between stresses, both normal and shear components, and the corresponding strains and subsequent deflections of a plate. This understanding is essential in the use of finite element methods for the analysis of plates when treated as linear elastic structures.

The in-plane (or planar) behaviour of a thin plate can be regarded as one of “plane stress”, i.e. we assume that there is no variation in stress through the thickness of the plate, and only the 3 planar components of stress are non-zero. So we now have a 2D problem.

Compatibility of strains and displacements - stretching and shearing of a plate

Each point in a plate has 2 degrees of freedom, described by components of displacement  $u$  and  $v$  in directions parallel to the  $x$  and  $y$  axes. It is convenient to use vectors and matrices when dealing with quantities which have many components, so:

$$\mathbf{u} = \begin{Bmatrix} u \\ v \end{Bmatrix}, \quad \boldsymbol{\varepsilon} = \begin{Bmatrix} \varepsilon_x \\ \varepsilon_y \\ \gamma \end{Bmatrix} = \begin{Bmatrix} \frac{\partial u}{\partial x} \\ \frac{\partial v}{\partial y} \\ \frac{\partial u}{\partial y} + \frac{\partial v}{\partial x} \end{Bmatrix} = \begin{bmatrix} \frac{\partial}{\partial x} & 0 \\ 0 & \frac{\partial}{\partial y} \\ \frac{\partial}{\partial y} & \frac{\partial}{\partial x} \end{bmatrix} \begin{Bmatrix} u \\ v \end{Bmatrix} = \mathbf{d} \cdot \mathbf{u} \quad (1)$$

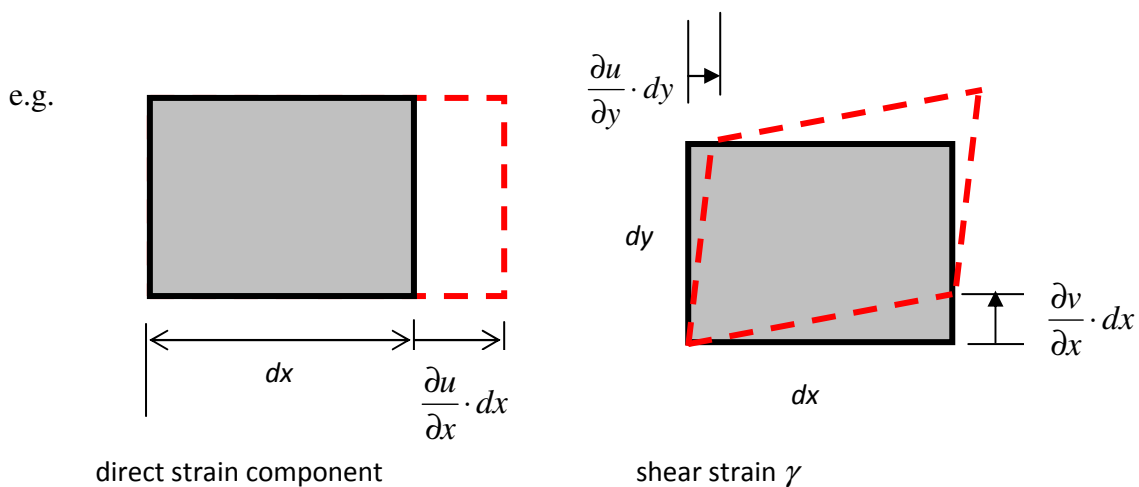


Figure 1: strain components for 2D deformation

## Equilibrium of stresses with body loads

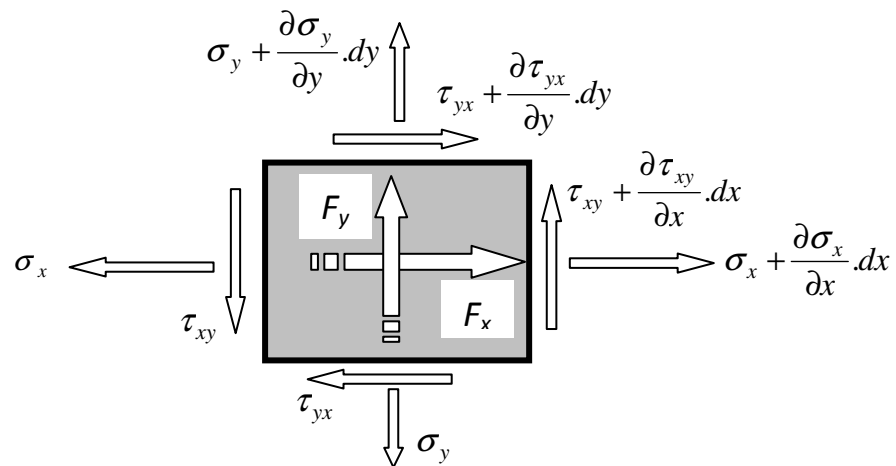


Figure 2: stresses and body forces

## Moment equilibrium

$$\left( \tau_{xy} + \frac{\partial \tau_{xy}}{\partial x} \cdot dx \right) t \cdot dy \cdot \frac{dx}{2} + \tau_{xy} \cdot t \cdot dy \cdot \frac{dx}{2} - \left( \tau_{yx} + \frac{\partial \tau_{yx}}{\partial y} \cdot dy \right) t \cdot dx \cdot \frac{dy}{2} - \tau_{yx} \cdot t \cdot dx \cdot \frac{dy}{2} = 0$$

Neglecting higher order terms involving  $dx \cdot dx \cdot dy$  we find

$$(\tau_{xy} - \tau_{yx}) t \cdot dx \cdot dy = 0 \quad \text{OR} \quad \boxed{\tau_{xy} = \tau_{yx} \equiv \tau} \quad (2)$$

## Force equilibrium

$$\left( \sigma_x + \frac{\partial \sigma_x}{\partial x} \cdot dx \right) t \cdot dy + \left( \tau + \frac{\partial \tau}{\partial y} \cdot dy \right) t \cdot dx - \sigma_x \cdot t \cdot dy - \tau \cdot t \cdot dx + F_x \cdot t \cdot dx \cdot dy = 0$$

i.e.

$$\frac{\partial \sigma_x}{\partial x} + \frac{\partial \tau}{\partial y} + F_x = 0 \quad \text{and similarly} \quad \frac{\partial \sigma_y}{\partial y} + \frac{\partial \tau}{\partial x} + F_y = 0 \quad \text{OR} \quad \boxed{\mathbf{\sigma}^T + \mathbf{F} = \mathbf{0}} \quad (3)$$

## Equilibrium of stresses with boundary tractions

### Force equilibrium

$$\Phi_n \cdot ds = \sigma_x \cdot dy \cdot \cos \alpha + \sigma_y \cdot dx \cdot \sin \alpha + \tau \cdot dx \cdot \cos \alpha + \tau \cdot dy \cdot \sin \alpha$$

$$\Phi_n = \sigma_x \cdot \cos^2 \alpha + \sigma_y \cdot \sin^2 \alpha + \tau \cdot \sin 2\alpha$$

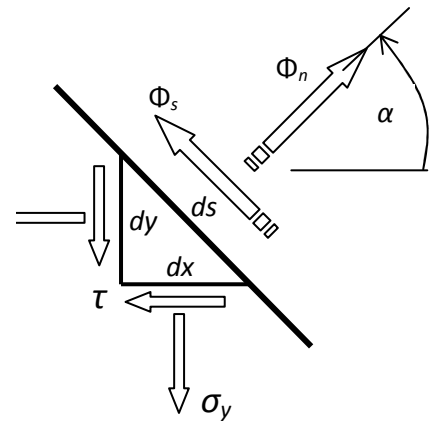


Figure 3: boundary tractions

$$\Phi_s \cdot ds = -\sigma_x \cdot dy \cdot \sin \alpha + \sigma_y \cdot dx \cdot \cos \alpha - \tau \cdot dx \cdot \sin \alpha + \tau \cdot dy \cdot \cos \alpha$$

$$\Phi_s = -0.5\sigma_x \cdot \sin 2\alpha + 0.5\sigma_y \cdot \sin 2\alpha + \tau \cdot \cos 2\alpha$$

$$\begin{Bmatrix} \Phi_n \\ \Phi_s \end{Bmatrix} = \begin{bmatrix} \cos^2 \alpha & \sin^2 \alpha & \sin 2\alpha \\ -0.5 \sin 2\alpha & 0.5 \sin 2\alpha & \cos 2\alpha \end{bmatrix} \begin{Bmatrix} \sigma_x \\ \sigma_y \\ \tau \end{Bmatrix} \quad \text{OR} \quad \boxed{\Phi = R \cdot \sigma} \quad (4)$$

### Hooke's law for plane stress

$$\begin{Bmatrix} \epsilon_x \\ \epsilon_y \\ \gamma_{xy} \end{Bmatrix} = \frac{1}{E} \begin{bmatrix} 1 & -\nu & 0 \\ -\nu & 1 & 0 \\ 0 & 0 & 2(1+\nu) \end{bmatrix} \begin{Bmatrix} \sigma_x \\ \sigma_y \\ \tau_{xy} \end{Bmatrix} \quad \text{OR} \quad \begin{Bmatrix} \sigma_x \\ \sigma_y \\ \tau_{xy} \end{Bmatrix} = \frac{E}{(1-\nu^2)} \begin{bmatrix} 1 & \nu & 0 \\ \nu & 1 & 0 \\ 0 & 0 & 0.5(1-\nu) \end{bmatrix} \begin{Bmatrix} \epsilon_x \\ \epsilon_y \\ \gamma_{xy} \end{Bmatrix}$$

$$\epsilon = E^{-1} \cdot \sigma$$

$$\text{OR} \quad \sigma = E \cdot \epsilon$$

(5)

## References

Structures, M.S. Williams & J.D. Todd, Macmillan Press, 2000,

Section 4.4 for two-dimensional elasticity, and Chapter 10 for an outline of the finite element method.

Concepts and applications of finite element analysis, R D Cook, D S Malkus, M E Plesha, R J Witt. 4<sup>th</sup> ed Wiley 2002,

Section 3.1 for plane stress.

Mechanics of Structures, Variational and Computational Methods, W. Wunderlich & W.D. Pilkey, 2<sup>nd</sup> ed., CRC Press, 2003.

Section 13.1.1 for plane stress.

**Use of finite elements for plane stress – formative exercise to familiarise students with Oasys GSA and learn about the significance of shear deformations in beams.**

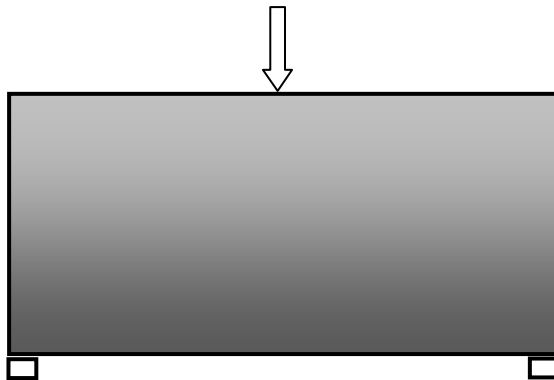



Figure 4: deep beam problem with varying span-depth ratios

### **Guidance for using Oasys GSA version 8.3 in modelling rectangular plates.**

- **Create a finite element model**
- Select Structure Type: **Plane Stress** and check default units or select different ones.
- Note arrangement of axes, by default x and y lie in the plane of the structure and the z axis is positive out of the screen. Choose a point of your plate as the origin and choose the directions of the x,y axes for your Global Coordinate system.
- Define 4 nodes at the corners of the rectangular plate – numbers and x,y coordinates, z = 0 by default.

- Define a single Quad 4 element connected to the 4 nodes. In the element table specify the Type as Quad 4, and input the node numbers under the Topology heading (use an anticlockwise sequence).
- Define the material properties with one of the standard Properties, use “steel”.
- Define 2D Element Properties
  - Input a name for 2D element property 1; Material: steel; and Thickness.
- Split element as required to create a finer mesh of elements
  - Select the element(s) with the mouse after activating the “Select elements” icon in the left hand menu.
  - Select Sculpt from the top menu, followed by 2D Element Operations → Split Quad Elements...
  - Input the numbers of Splits (or subdivisions) required along the 2 edges which define the rectangle (Edge 1 connects the 1<sup>st</sup> node in the sequence to the 2<sup>nd</sup> etc., following the sequence defined by the Topology of the original element) – then **Preview before accepting!!** E.g. split the vertical sides into 10 elements, and the horizontal sides to conform with square elements.
- Define supports
  - Select Nodes, Supports, and enter restraint direction in a Table
- Define loads
  - Select Loading, Nodal Loading, Node Loads, and enter node number(s), direction(s) and value(s) of forces applied to nodes.
- **Analyse the model**
  - Use the  $\Sigma$  icon on the top menu.
- **Examine the output**
  - Deflected shape – use the  button on the right hand side of the screen, also try animation with the button below. Deflections can be exaggerated or reduced by the use of the **x2** or **/2** buttons.
  - Select a column of nodes with a box in order to focus on the question of planarity, and zoom to enlarge view. Inspection should reveal the answer!
  - Display principal stress vectors in the complete structure by selecting the “Diagram settings” button on the right hand side. Then in the dialogue box select 2D Element Derived Stresses, and 2D Stress, Principal. Red vectors indicate tension and green vectors indicate compression. Use the **x2** or **/2** buttons to scale as appropriate.
  - Graphic views can be saved in different formats such as PNG or JPEG by selecting Graphics and then SaveImage.

Student data for a steel deep beam, all beams of depth 2m and thickness 0.04m, and carry a central vertical load on the top edge of 1000kN.

## Linear elastic theory of plates – Kirchhoff theory

We now need to understand the relations between moments, both bending and twisting, and shear forces and the corresponding deformations and subsequent deflections of a plate. This understanding is essential in the use of finite element methods for the analysis of plates when treated as linear elastic structures. In Kirchhoff theory we neglect deformations due to transverse shear forces, as we often do in the case of beams.

We can imagine a flat plate to be formed from a set of thin layers or laminas stuck together to form what is in reality a three dimensional structure. However if we can assume the thickness is relatively small, then we can proceed to assume that straight “fibres” aligned through the plate thickness normal to its surfaces remain straight after the plate has deformed. Furthermore we will assume that such fibres remain normal to the mid-surface of the plate. These sort of assumptions are similar to those commonly used for beams, i.e. plane sections remain plane.

Bending and twisting of plates – compatibility of strains and curvatures/twists

The deformed shape of a plate subjected to transverse loads can be thought of as occurring in beam strips where both bending and twisting becomes apparent, see Figure 5:

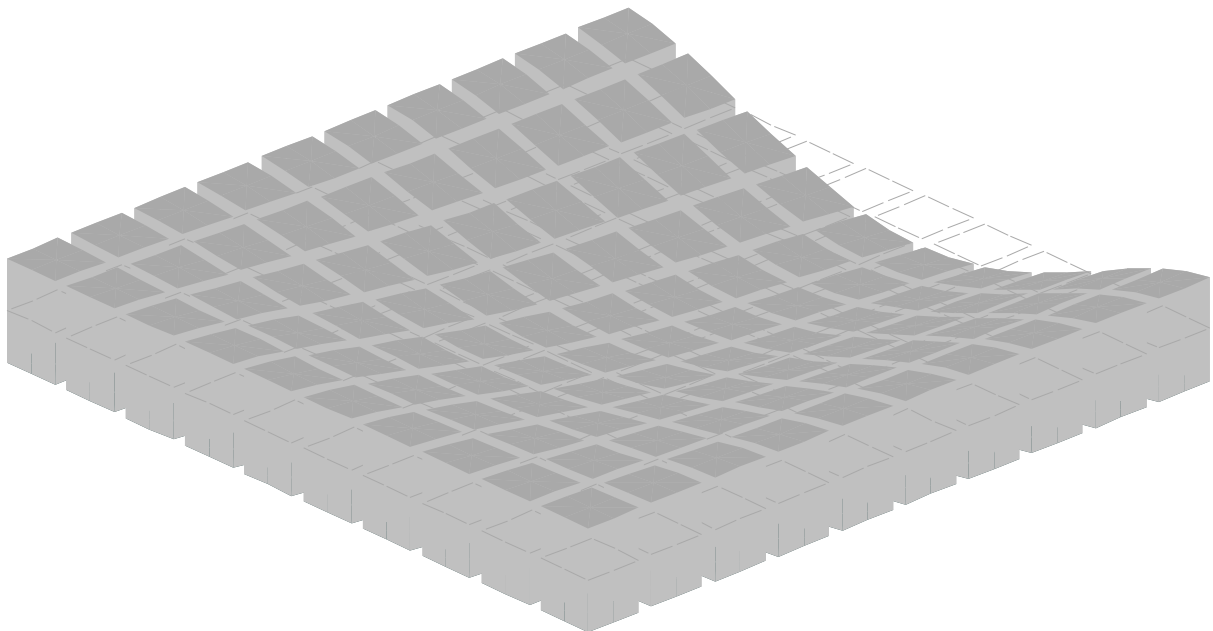


Figure 5: deformed view of a bent plate – simulated by Oasys GSA.

The fibres which are initially normal to the mid-surface rotate about the x and y axes as the plate bends and twists. The corresponding components of rotation are denoted by  $\psi_y$  and  $\psi_x$  respectively, and are illustrated in Figure 6 where it is very important to note their meaning and their positive senses!

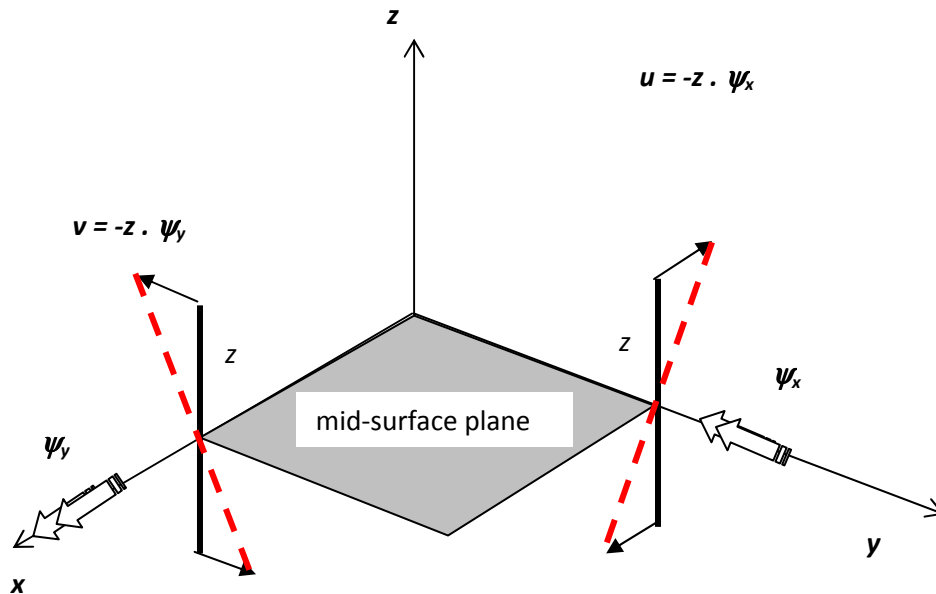


Figure 6: reference axes and components of rotation and displacement

The rotations produce displacements  $u$  and  $v$  in a lamina distance  $z$  from the mid-surface, and strains in the lamina:

$$\begin{Bmatrix} \epsilon_x \\ \epsilon_y \\ \gamma_{xy} \end{Bmatrix} = \begin{Bmatrix} -z \cdot \frac{\partial \psi_x}{\partial x} \\ -z \cdot \frac{\partial \psi_y}{\partial y} \\ -z \cdot \frac{\partial \psi_x}{\partial y} - z \cdot \frac{\partial \psi_y}{\partial x} \end{Bmatrix} = -z \begin{Bmatrix} \psi_{x,x} \\ \psi_{y,y} \\ (\psi_{x,y} + \psi_{y,x}) \end{Bmatrix} \quad \text{where e.g. } \psi_{x,x} \equiv \frac{\partial \psi_x}{\partial x}. \quad (6)$$

We term rates of rotations  $\psi_{x,x}$ ,  $\psi_{y,y}$  the “curvatures” in beam strips parallel to the x and y axes respectively, and  $(\psi_{x,y} + \psi_{y,x})$  the “twist” in these beam strips.

In Kirchhoff theory we assume that fibres normal to the mid-surface remain normal, so the rotations are equal to gradients of deflection  $w$ , i.e. curvatures and twists are also given by:

$$\mathbf{k} = \begin{Bmatrix} K_x \\ K_y \\ K_{xy} \end{Bmatrix} \equiv \begin{Bmatrix} \psi_{x,x} \\ \psi_{y,y} \\ \psi_{x,y} + \psi_{y,x} \end{Bmatrix} = \begin{Bmatrix} w_{,xx} \\ w_{,yy} \\ 2w_{,xy} \end{Bmatrix} \quad (7)$$

### Hooke's law in terms of moments and curvatures

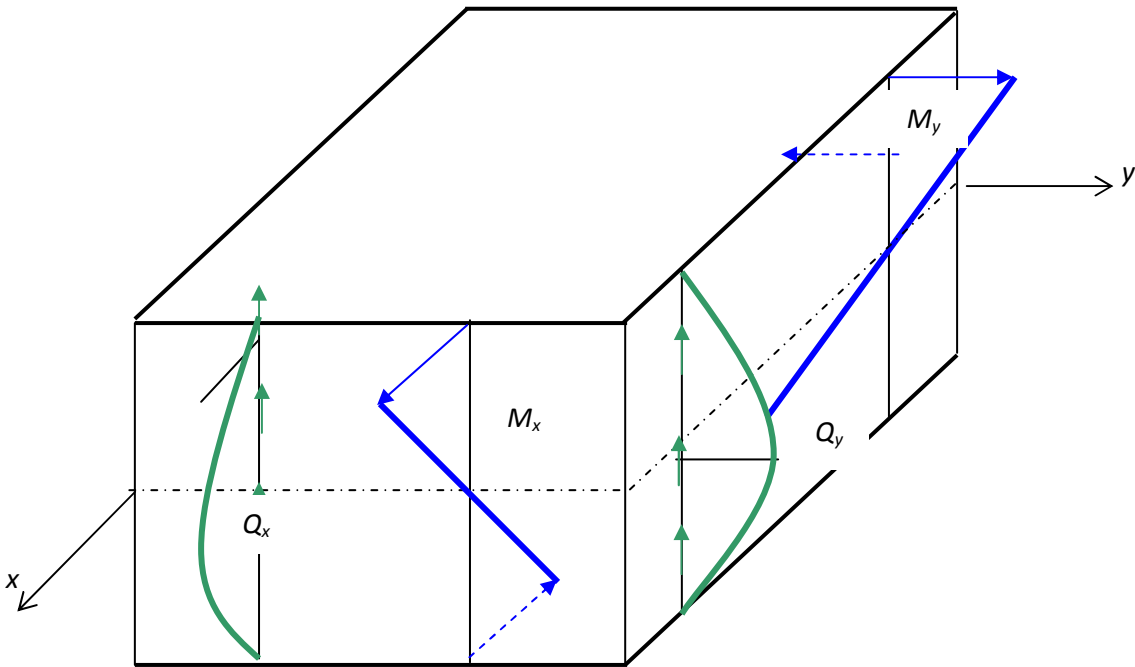
Stresses in a lamina are then expressed, as in plane stress, by:

$$\begin{Bmatrix} \sigma_x \\ \sigma_y \\ \tau_{xy} \end{Bmatrix} = -z \cdot \frac{E}{(1-\nu^2)} \begin{bmatrix} 1 & \nu & 0 \\ \nu & 1 & 0 \\ 0 & 0 & 0.5(1-\nu) \end{bmatrix} \begin{Bmatrix} \psi_{x,x} \\ \psi_{y,y} \\ (\psi_{x,y} + \psi_{y,x}) \end{Bmatrix} = -z \cdot \mathbf{E} \cdot \mathbf{k}$$

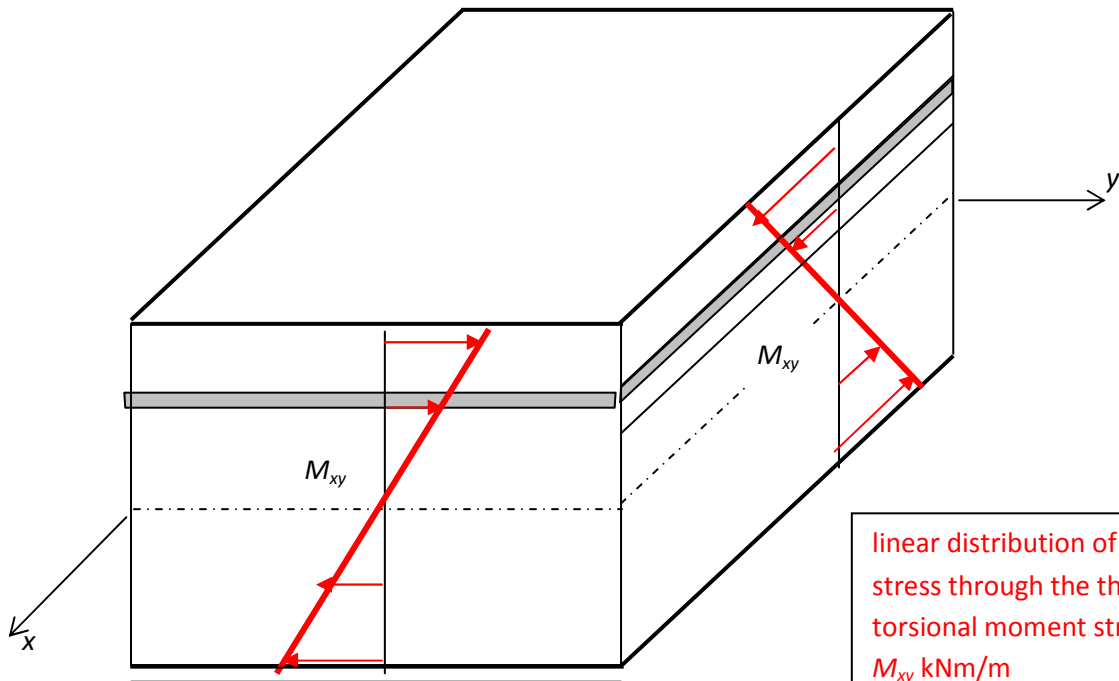
Bending and twisting moments can be expressed as the stress-resultants:



linear distributions of normal stress through the thickness  $\Rightarrow$   
 bending moment stress-resultants  $M_x$  and  $M_y$  kNm/m



parabolic distributions of transverse shear stress through the thickness  $\Rightarrow$  stress-resultants  $Q_x$  and  $Q_y$  kN/m



linear distribution of planar shear stress through the thickness  $\Rightarrow$   
 torsional moment stress-resultants  $M_{xy}$  kNm/m

Figure 7: stress distributions through the thickness and stress-resultants

$$M_x = \int_{-t/2}^{+t/2} \sigma_x \cdot z \cdot dz; \quad M_y = \int_{-t/2}^{+t/2} \sigma_y \cdot z \cdot dz; \quad M_{xy} = \int_{-t/2}^{+t/2} \tau_{xy} \cdot z \cdot dz$$

$$\begin{Bmatrix} M_x \\ M_y \\ M_{xy} \end{Bmatrix} = -\frac{E}{(1-\nu^2)} \begin{bmatrix} 1 & \nu & 0 \\ \nu & 1 & 0 \\ 0 & 0 & 0.5(1-\nu) \end{bmatrix} \int_{-t/2}^{+t/2} z^2 dz \begin{Bmatrix} \kappa_x \\ \kappa_y \\ \kappa_{xy} \end{Bmatrix}$$

Or  $\mathbf{M} = -\mathbf{D} \cdot \boldsymbol{\kappa}$  where  $\mathbf{D} = D \begin{bmatrix} 1 & \nu & 0 \\ \nu & 1 & 0 \\ 0 & 0 & 0.5(1-\nu) \end{bmatrix}$  and  $D \equiv \frac{Et^3}{12(1-\nu^2)}$ .

(8)

$D$  is usually termed the flexural rigidity of the plate in a similar way that  $EI$  is the flexural rigidity of a beam.

**Note:** the significance of the sign convention (taken to agree with that used by RD Cook et al [2]), means that with the  $z$  axis vertically upwards sagging curvatures are positive, but sagging moments are negative! Troublesome maybe, but these are quite common conventions.

### Equilibrium for an infinitesimal plate element

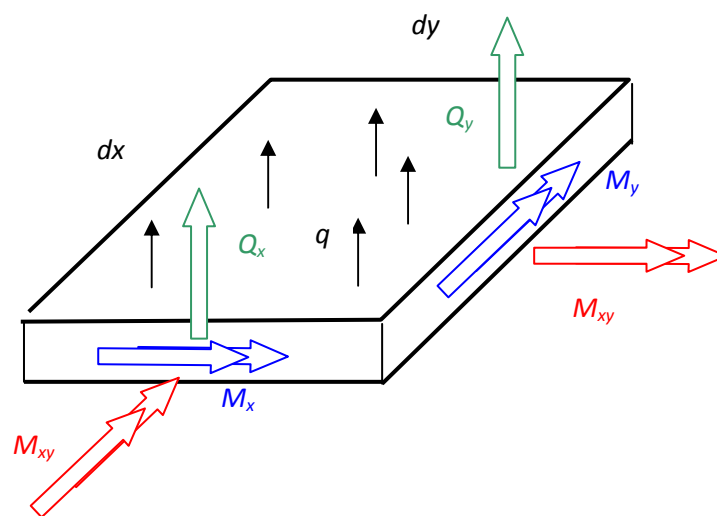


Figure 8: isometric view of stress-resultants and pressure load

- **Vertical equilibrium** of an infinitesimal element at the intersection of x- and y- direction beam strips:

$$\text{Increase in shear force in x-beam strip} = \left( \frac{\partial Q_x}{\partial x} dx \right) dy$$

$$\text{Increase in shear force in y-beam strip} = \left( \frac{\partial Q_y}{\partial y} dy \right) dx$$

$$\text{Vertical equilibrium requires: } \left( \frac{\partial Q_x}{\partial x} dx \right) dy + \left( \frac{\partial Q_y}{\partial y} dy \right) dx + q dx dy = 0 \text{ i.e.}$$

$$\boxed{\frac{\partial Q_x}{\partial x} + \frac{\partial Q_y}{\partial y} + q = 0} \quad (9)$$

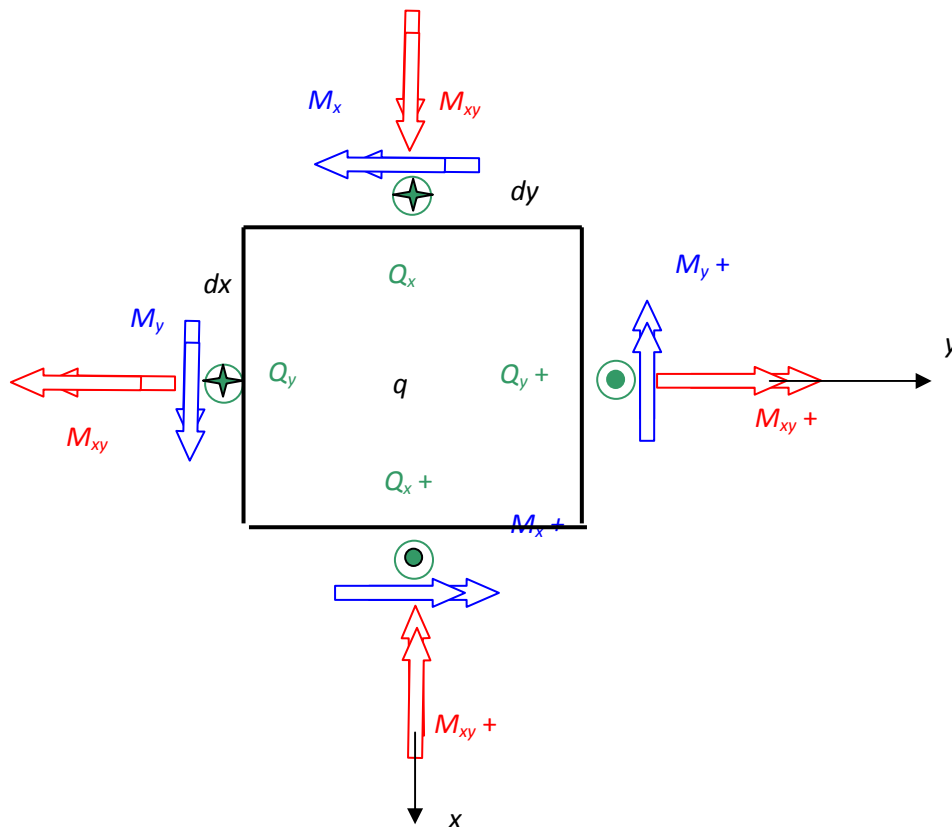


Figure 9: plan view of stress-resultants and pressure load

- **Moment equilibrium about the x- axis**

Increases in bending and torsional moments about the x-axis in a y-beam strip are balanced by the

couple formed by the  $Q_y$  shear forces:  $\left(\frac{\partial M_y}{\partial y} dy\right) dx + \left(\frac{\partial M_{xy}}{\partial x} dx\right) dy = (Q_y dx) dy$  , or

$$\boxed{\frac{\partial M_y}{\partial y} + \frac{\partial M_{xy}}{\partial x} = Q_y} \quad (10)$$

- **Moment equilibrium about the y-axis** in an x-beam strip

Similarly

$$\boxed{\frac{\partial M_x}{\partial x} + \frac{\partial M_{xy}}{\partial y} = Q_x} \quad (11)$$

- Combining the moment equilibrium equations with vertical equilibrium, we get:

$$\frac{\partial^2 M_x}{\partial x^2} + 2 \frac{\partial^2 M_{xy}}{\partial x \partial y} + \frac{\partial^2 M_y}{\partial y^2} = -q,$$

which leads on to governing partial differential equations in terms of displacements! Exact analytic solutions to such equations are sometimes possible, but for practical problems we usually resort to finite element methods.

### Boundary conditions

These come in two forms: static, e.g. distributions of shear forces or moments and kinematic, e.g. distributions of deflections or rotations. An example of a square plate simply supported (i.e. having zero deflections and zero bending moments at its edges) and supporting a uniformly distributed load (UDL) is illustrated below, and demonstrates that it can span in two directions. Consequently the load can be shared in each direction, thereby approximately halving the bending moments that would occur from spanning in one direction only.

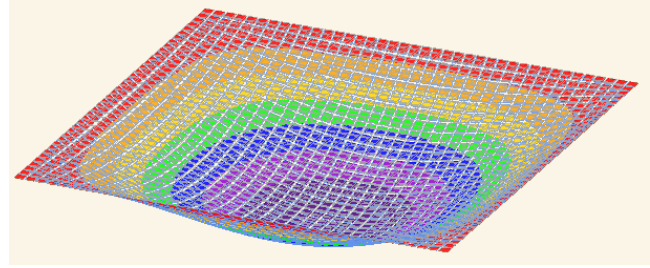
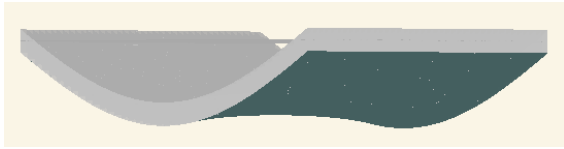


Plate spanning one way – note anticlastic curvature with  $\nu = 0.34$ .  
 Plate spanning two ways with contour lines of deflection – note maximum bending moment  $\leq 50\%$  of that from one way spanning.

Figure 10: deflected shapes of one way and two spanning plates.

When we consider purely static boundary conditions, we would expect to be able to specify 3 components of traction as shown indicated by the bending moment  $M_n$ , the torsional moment  $M_{ns}$  and the shear force  $Q_n$ .

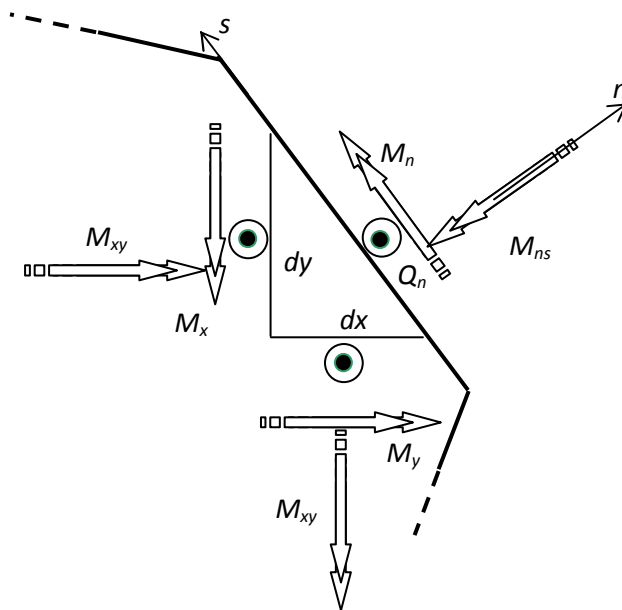


Figure 11: static boundary conditions

However, the assumption of no shear deformation leads the Kirchhoff theory to only allow 2 independent boundary conditions, e.g. tractions, to be applied. This is a similar situation as for normal beam theory where 2 conditions are specified at each support. For plates this could be troublesome!

## An anomaly

Consider again the square simply supported plate. The boundary conditions are zero deflection and zero bending moment, and we keep quiet about the torsional moment!! What deflected shape do we expect? A form of dishing, and  $w_{,n}$  (edge slope in the normal direction) isn't zero and it changes along a supported edge towards the corner where it should be zero. This implies that  $w_{,ns}$  is non-zero and so the torsional moment (proportional to the twist) should not be zero. An approximation to a solution based on Kirchhoff theory for a square plate with a UDL and simply supported on all 4 sides is shown in Figure 12 for a symmetric quadrant:

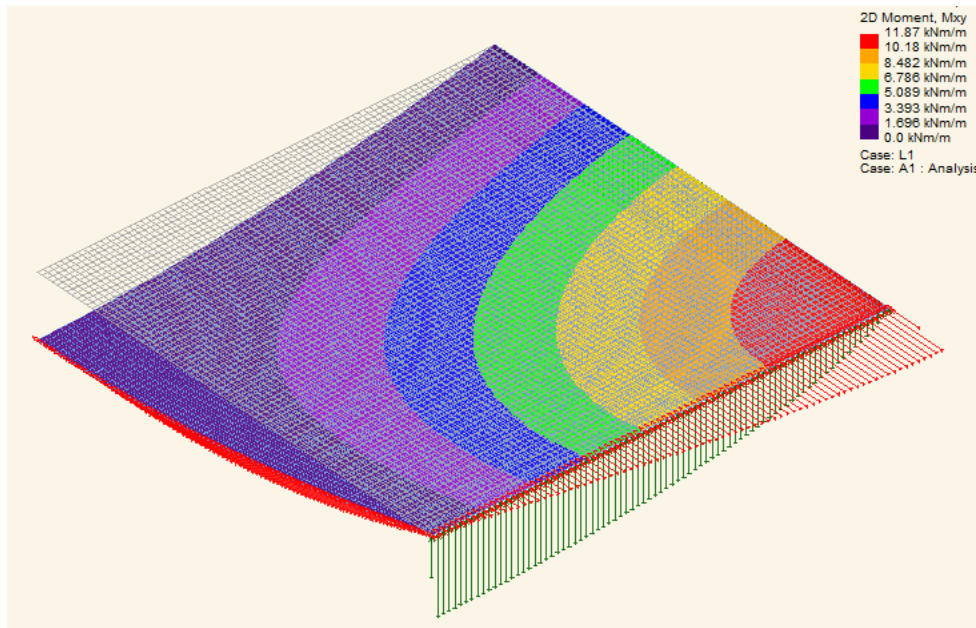


Figure 12: quadrant of a simply supported square plate, vertical deflections and reactions

We see that torsional moments are implied as part of the reactions (distribution shown by red vectors), and as the corner is approached the gradient of the torsional moment and the vertical shear reaction become zero. However, if we don't apply horizontal shear stresses  $\tau_{ns}$  on the boundary face, then how can torsional moments be present?

An answer to this is to argue that torsional moments could just as well be applied via couples formed by vertical shear forces (a narrow edge strip which is rigid with respect to shear stresses doesn't know the difference!). The way we could proceed is to replace the distribution of torsional moment  $M_{ns}$  along an edge between corners by a statically equivalent distribution of shear forces, and then apply the net shear forces.

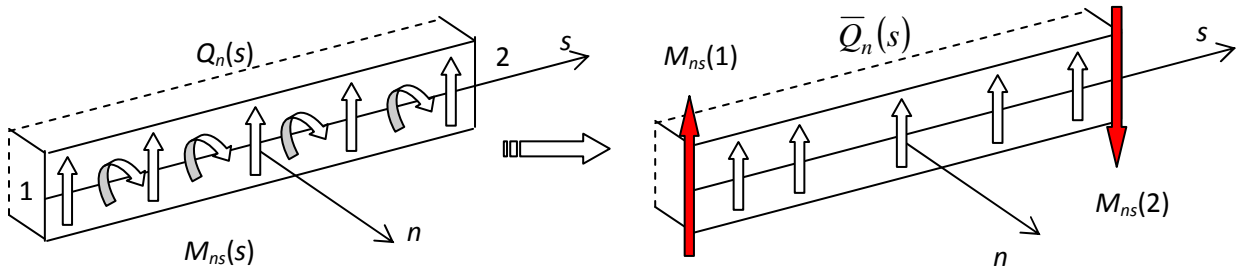


Figure 13: statically equivalent Kirchhoff shear forces

The net equivalent Kirchhoff shear forces then consist of a distribution of forces denoted by  $\bar{Q}_n(s)$  and a pair of concentrated forces  $M_{ns}(1)$  and  $M_{ns}(2)$  applied at the ends/corners 1 and 2, where:

$$\bar{Q}_n(s) = Q_n(s) + \frac{\partial M_{ns}(s)}{\partial s} \text{ and } M_{ns}(1) = M_{ns}(s) \text{ at end 1, } M_{ns}(2) = M_{ns}(s) \text{ at end 2.} \quad (12)$$

Replacement is carried out for the reactions shown in Figure 12, and results for the shear distribution and the total corner force are shown in Figure 14:

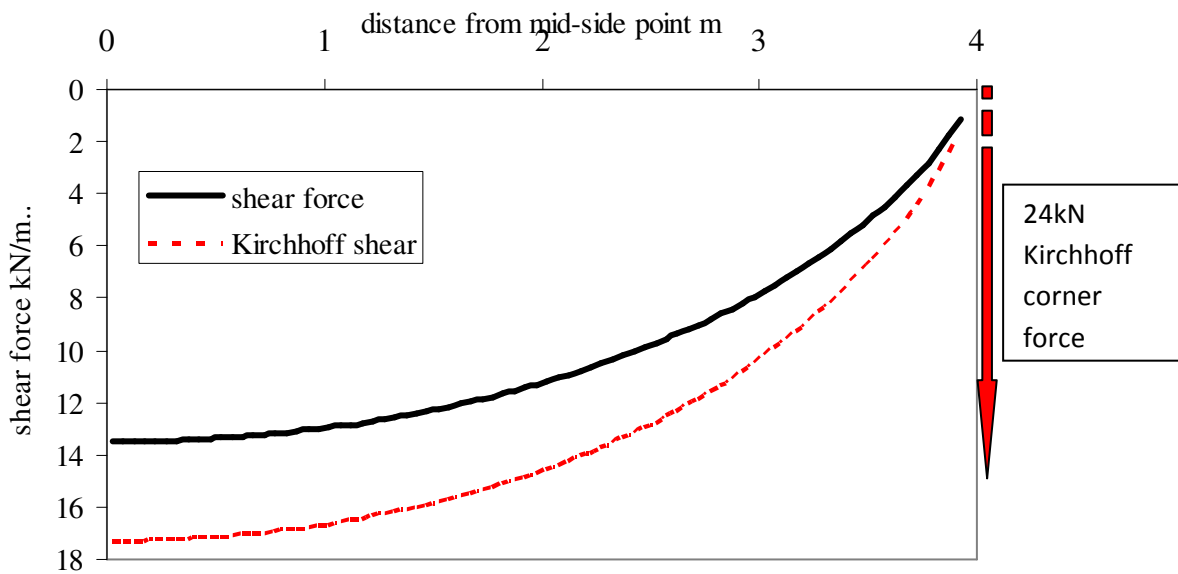


Figure 14: distributions of shear forces

Similar results are given in Timoshenko et al in Figures 63 and 81 [1].

The problem lies in our assumptions, we can assume zero shear deformation throughout most of the plate, but local to the boundaries the behaviour is really governed by 3D stresses and strains for which zero shear deformation is inconsistent.

A theory which begins to account for the 3D nature of the plate is due to Reissner-Mindlin, and their theory assumes that shear deformation can take place through the thickness of the plate – it is based on similar assumptions for shear as is used for relatively deep beams. As we will see we can then specify zero torsional moments at the supports, this produces the reactions and field of torsional moments within the plate as shown in Figure 15. We see that significant downward reactions act near the corner of the plate, which has some similarity to the Kirchhoff reactions shown in Figure 14.

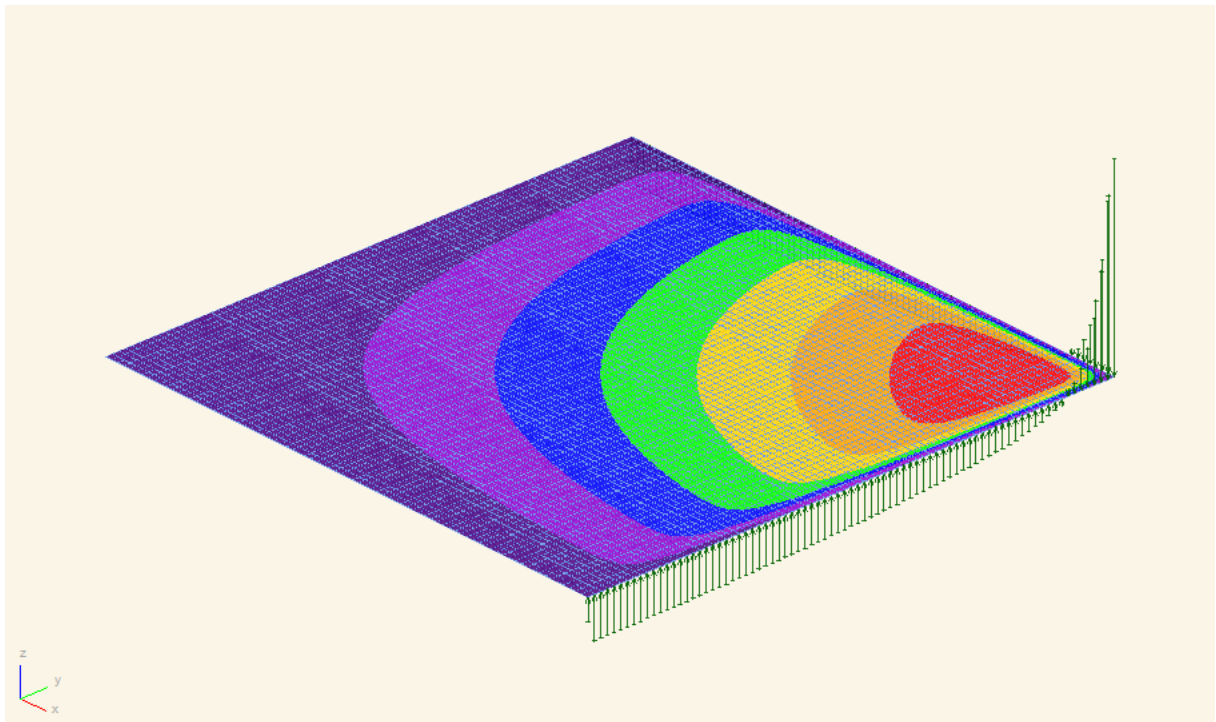


Figure 15: reactions and the internal field of torsional moments

We may deduce from all these alternative distributions of reactions that if we remove reactions near the corner, then we should expect the plate to lift. And indeed we show this effect in Figures 16 to 19 when reactions are released for 1m on both sides adjacent to a corner, whether we include torsional moments as reactions or not.



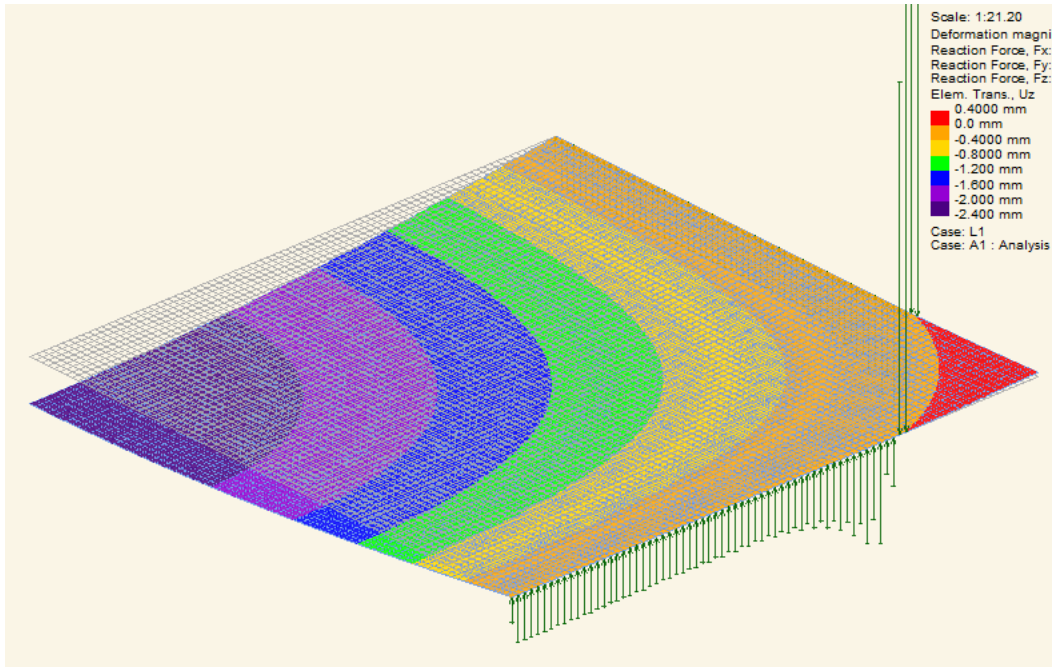


Figure 16: Deflection contours and vertical reactions after corner release.

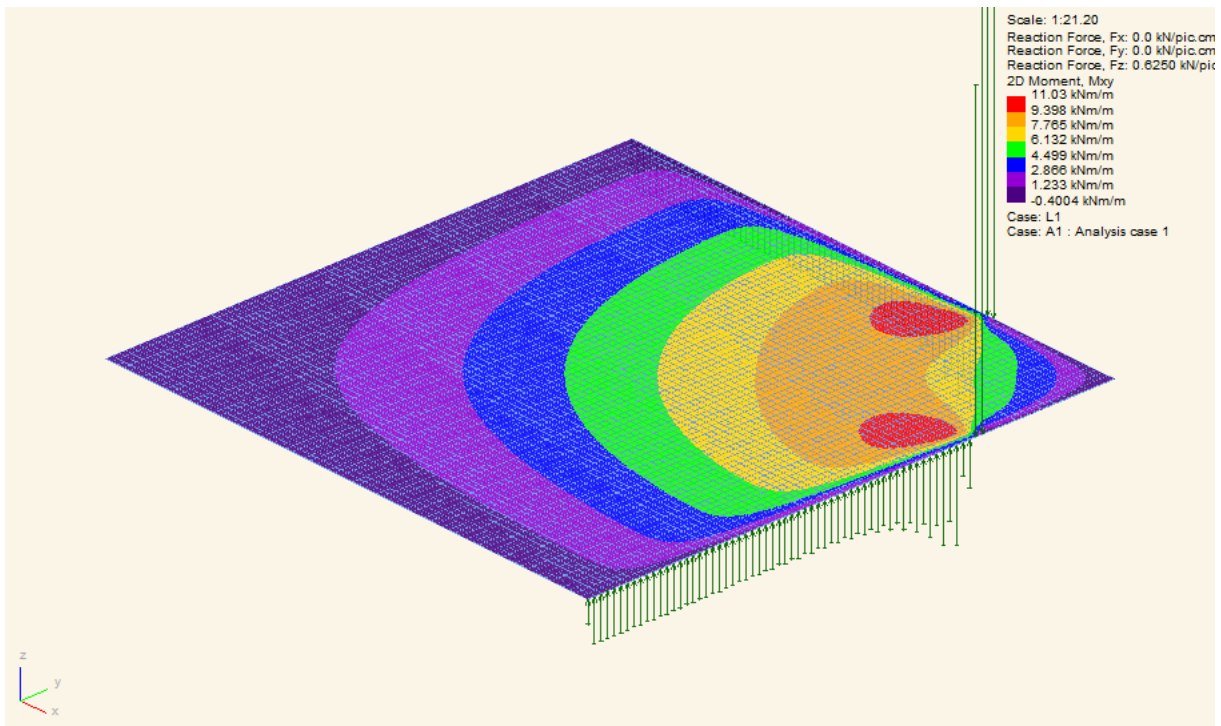


Figure 17: Contours of torsional moments and vertical reactions after corner release.

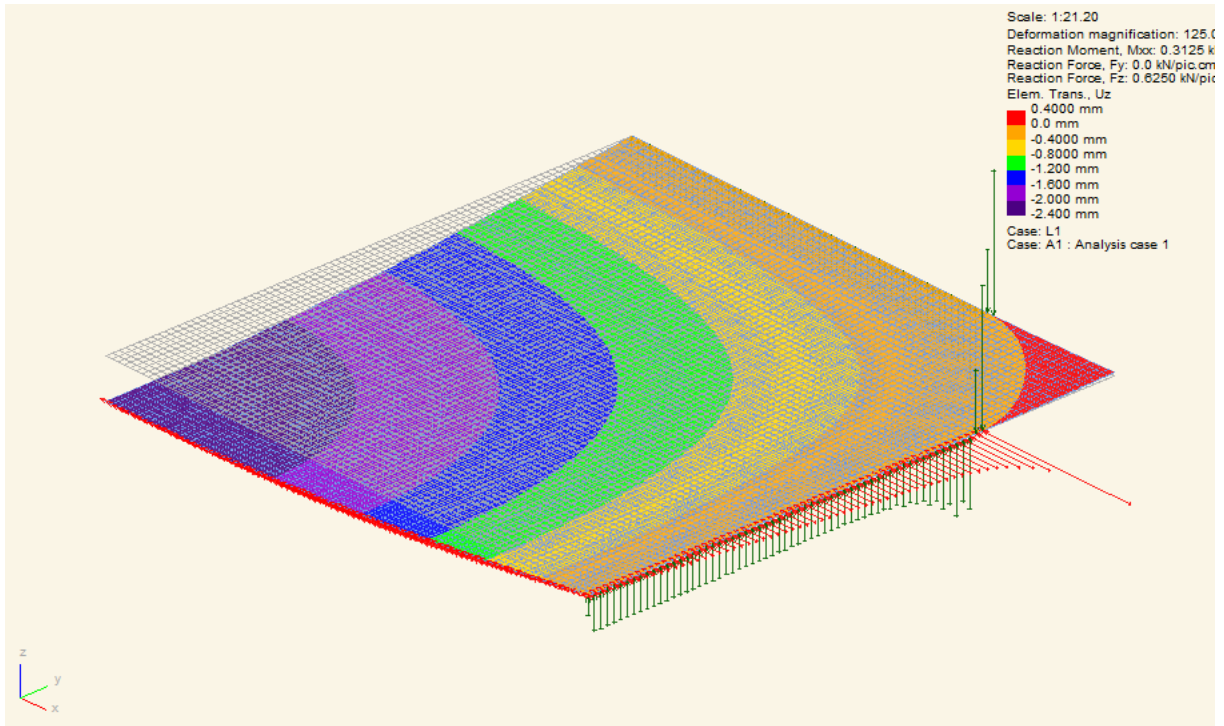


Figure 18: Deflection contours and reactions (shear and torsional moment) after corner release

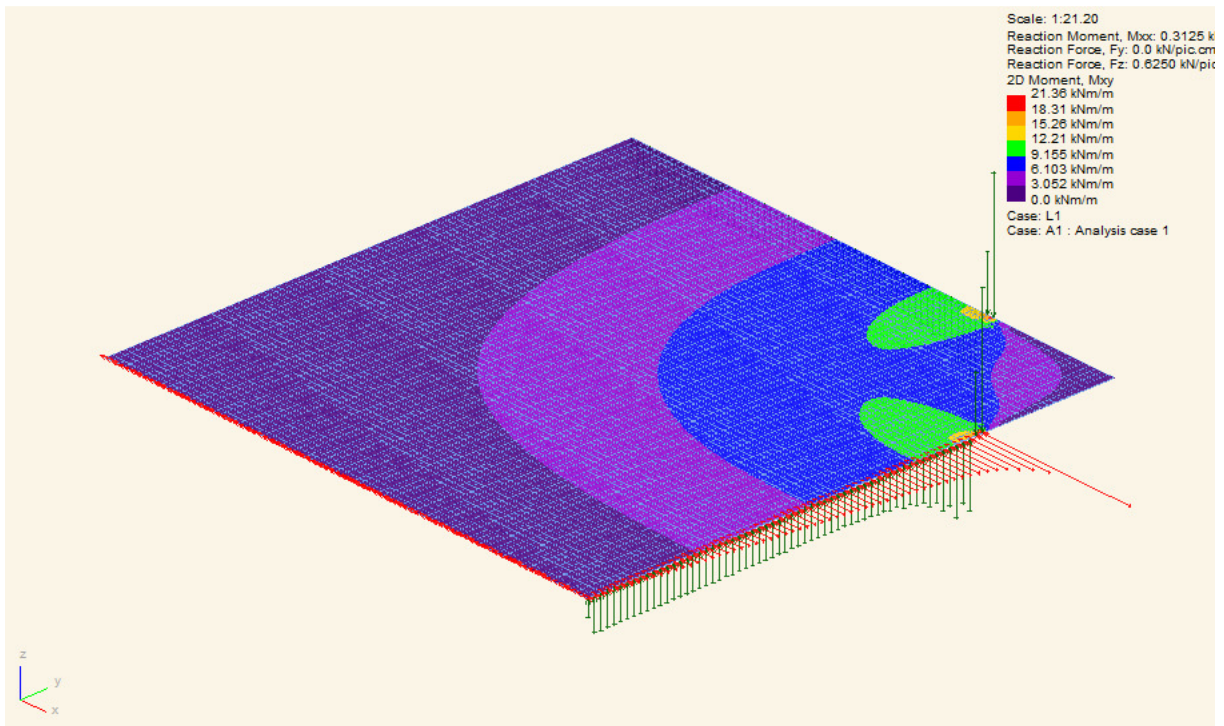


Figure 19: Contours of torsional moments and reactions after corner release.

## References

[1] Theory of plates and shells, S.P. Timoshenko & S. Woinowsky-Krieger, McGraw-Hill, 2<sup>nd</sup> ed., 1959.

[2] Concepts and applications of finite element analysis, R D Cook, D S Malkus, M E Plesha, R J Witt.  
4<sup>th</sup> ed Wiley 2002,

Section 15.1 for an introduction to plate bending behaviour.

[3] Mechanics of Structures, Variational and Computational Methods, W. Wunderlich & W.D. Pilkey,  
CRC Press, 2<sup>nd</sup> ed., 2003.

Sections 13.2.1 to 13.3.1 for classical plate theory based on Kirchhoff assumptions.

## Linear elastic theory of elastic plates - Reissner-Mindlin theory

In this theory we make the first step to account for the 3D nature of a plate by making allowance in an approximate way for shear deformation through the thickness of a plate as well as bending and twisting deformations. The “fibres” that are initially straight and normal to the mid-surface are still assumed to remain straight, but they are given independent degrees of freedom to rotate about axes in the plane of the plate. Thus each fibre is given 3 degrees of freedom: transverse deflection  $w$ , and two rotations  $\psi_x$  and  $\psi_y$ .

Curvatures are again defined by the first derivatives of the rotations in Figure 20, and the moment curvature relations as a form of Hooke’s law are unchanged, but remember that now we do not express curvatures as second derivatives of deflections. The additional aspect of Hooke’s law concerns the relations between shear forces and shear strains.

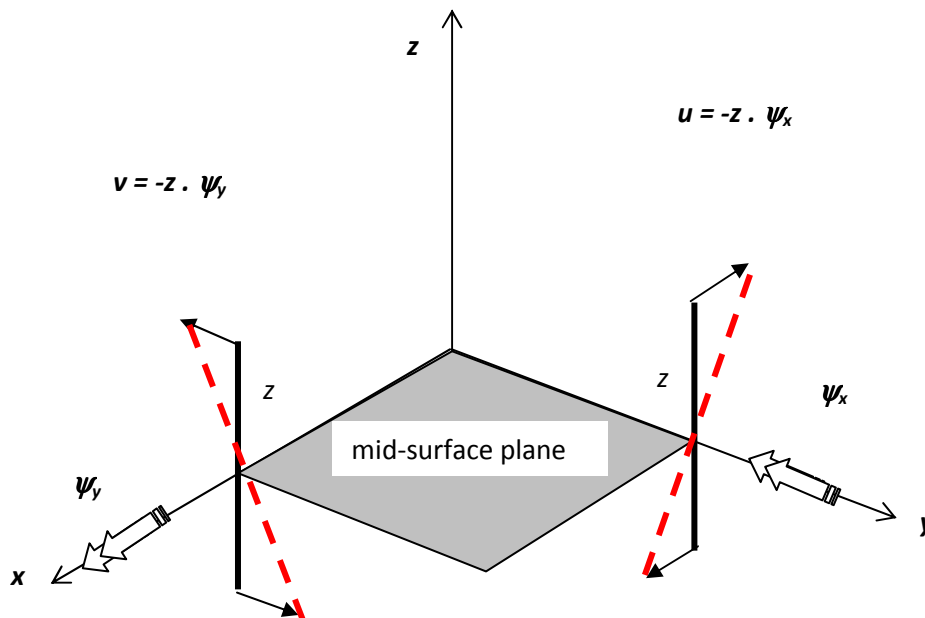


Figure 20: rotations of fibres through the thickness of a plate.

### Transverse shearing of plate

The distinction between Reissner-Mindlin and Kirchhoff plate theories rests on the inclusion or exclusion respectively of transverse shear deformation through the plate thickness. Both theories assume that normals to the midsurface remain straight. However Mindlin allows for a shear strain, i.e. a change of angle between the normal and the tangent to the midsurface, whereas Kirchhoff neglects such shear strains so that the normals remain perpendicular to the midsurface.

The shear strain

$$\gamma_{zx} = \left( \frac{\partial w}{\partial x} - \psi_x \right), \quad (13)$$

indicated by the symbol ● in Figure 21, is treated as constant throughout the plate thickness. In Kirchhoff theory it is assumed that  $\gamma_{zx} = 0$ , i.e. that  $\frac{\partial w}{\partial x} = \psi_x$ .

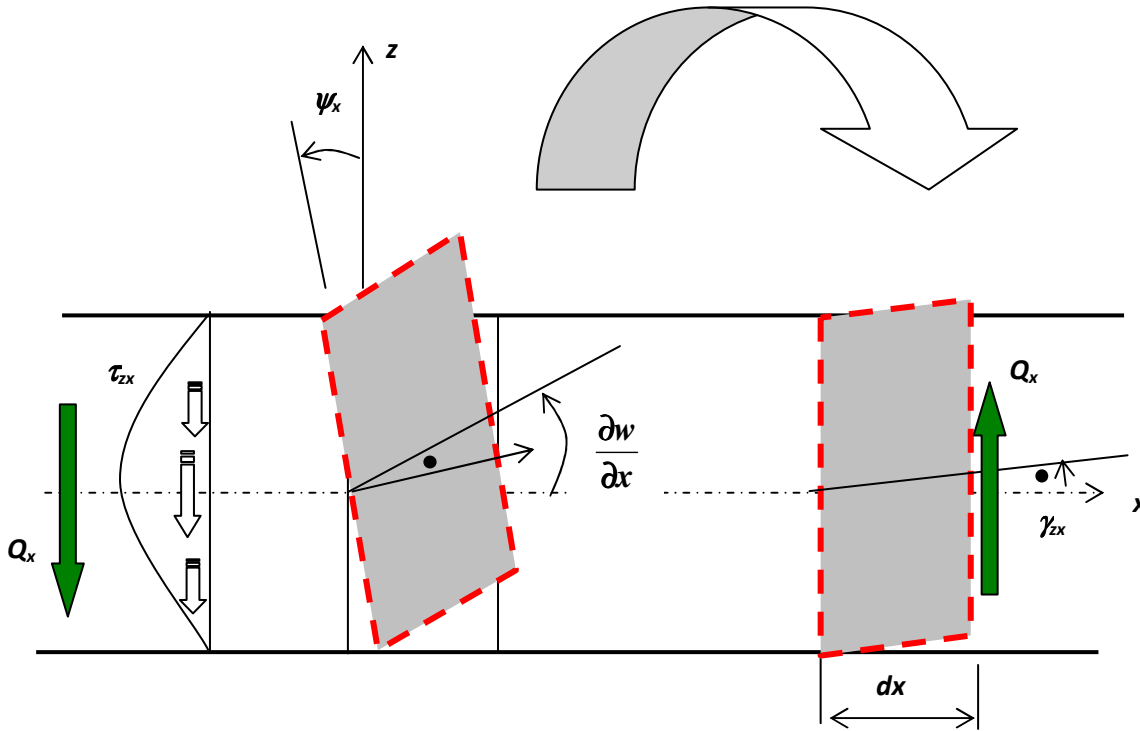


Figure 21: assumptions for shear stress and shear strain in Reissner-Mindlin theory

In Reissner-Mindlin theory the shear strain  $\gamma_{zx}$  is accounted for, but note that there is an inconsistency between the assumption of a constant shear strain and the parabolic distribution of shear stress  $\tau_{zx}$  as illustrated in Figure 21. The latter is required to satisfy equilibrium of stress according to engineer's beam theory.

$$\tau_{zx} = \frac{3Q_x}{2t} \left( 1 - \frac{2z}{t} \right) \left( 1 + \frac{2z}{t} \right) = \frac{3Q_x}{2t} \left( 1 - \frac{4z^2}{t^2} \right) \quad (14)$$

This inconsistency is resolved in a "weak" way by equating two expressions for virtual work developed in terms of the shear force stress-resultant  $Q_x$  per unit width of a beam strip and the shear stresses  $\tau_{zx}$ :

$$(Q_x)(\gamma_{zx} \cdot dx) = \left( \int_{-t/2}^{+t/2} \frac{\tau_{zx}^2}{G} \cdot dz \right) \cdot dx = \frac{1}{G} \left( \frac{6}{5} \cdot \frac{Q_x^2}{t} \right) \cdot dx$$

where  $G$  is the shear modulus defined by  $G = E/2(1 + \nu)$ .

Thus

$$Q_x = \frac{5}{6} \cdot Gt \cdot \gamma_{zx} \quad (15)$$

as indicated in Cook et al [1] Chapter 15, Equation (15.1-5) when  $k = 5/6$ .

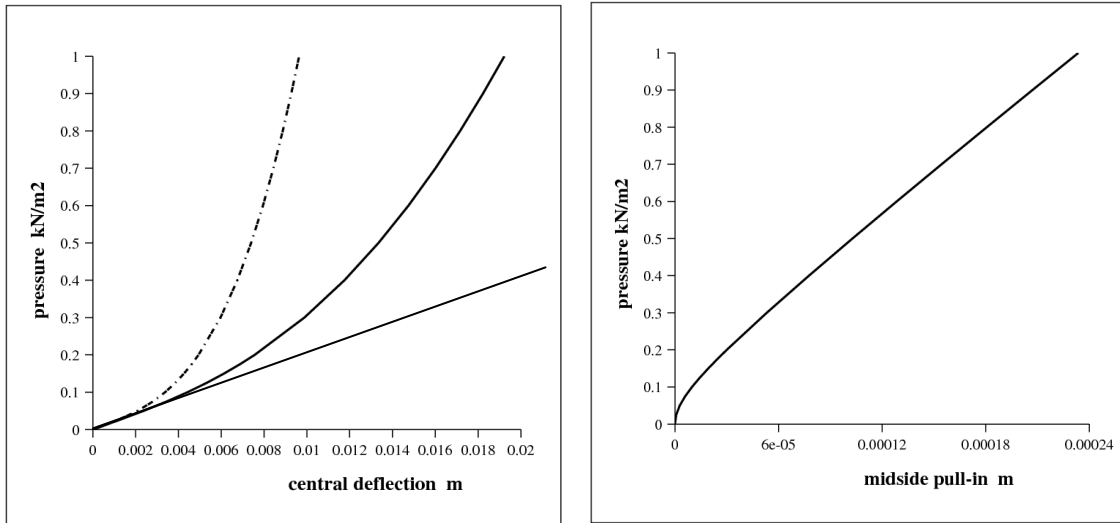
### Simple supported boundary conditions

Now that we have 3 independent degrees of freedom for each transverse fibre, the number of boundary conditions that can be specified at each point increases to 3. Thus at a loaded boundary, we can specify both components of moment (bending and twisting) and a shear force intensity. Furthermore at simple supports we specify zero transverse deflection  $w$  and bending moment  $M_n$  about the line of support, with a choice for the third condition. There are two alternative forms which result from using Reissner-Mindlin theory: termed “soft” and “hard”. “Soft” specifies zero twisting moment  $M_{ns}$ , whereas “hard” specifies zero rotation  $\psi_s$  about the normal to the boundary in the  $xy$  plane. Which type of support best represents the physical problem requires your decision – Cook has words of wisdom in Section 15.5 [1]!

It is important to appreciate that linear theory only works so long as the vertical deflections are very small. Otherwise in-plane forces can develop and plates tend to transmit loads in ways you may not have imagined [3]!

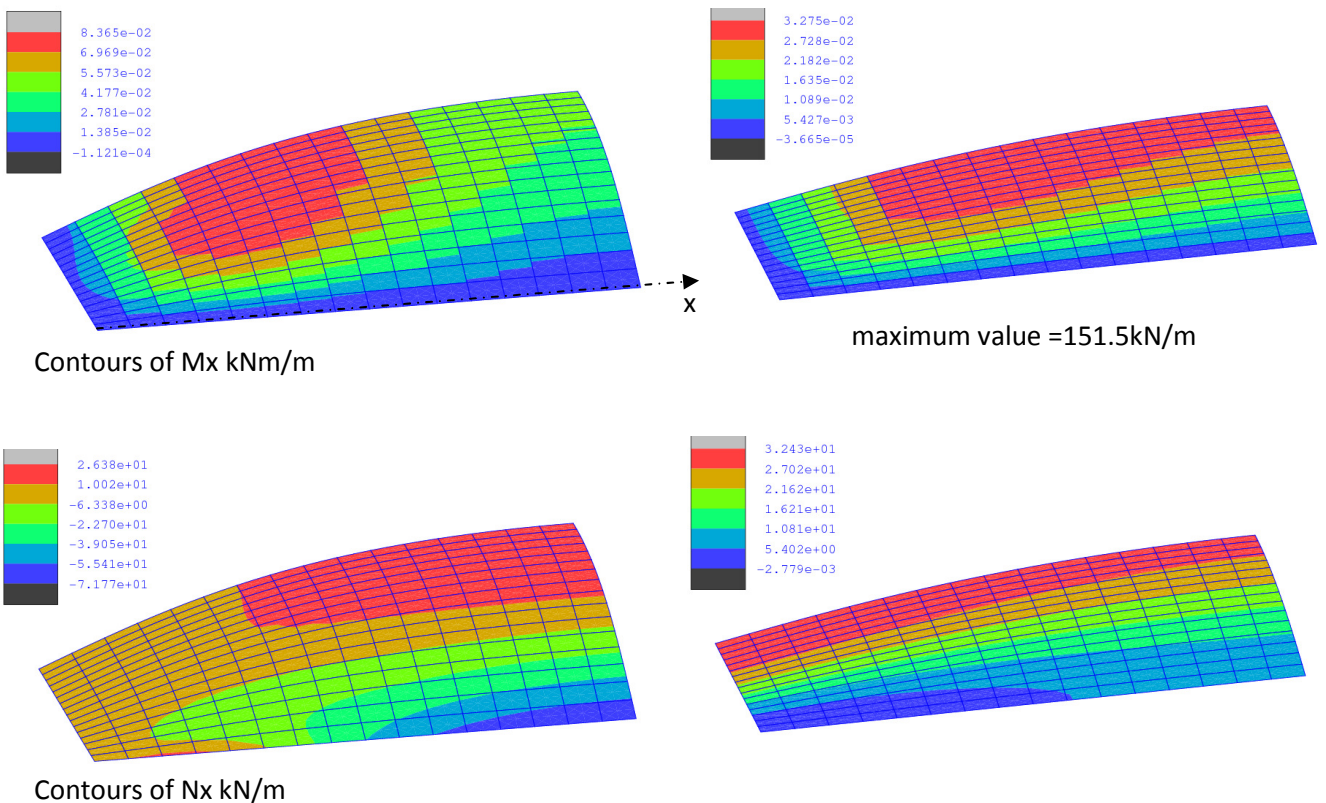
Figures 22 and 23 refer to the non-linear elastic behaviour of a 2m square vertical glass plate with 6mm thickness, simple supports and subjected to a uniform pressure of 1kN/m<sup>2</sup>. In this context “soft” implies that the edges have freedom to rotate in the torsional sense and freedom to move in the plane of the plate; whereas “hard” implies in this case that freedom of the edges to rotate is maintained but in-plane movement is fully constrained.





straight line for linear behaviour; soft conditions imply edge deflections, e.g. midside pull-in is unconstrained.

Figure 22: load deflection curves for non-linear behaviour due to large deflections



(a) contours for soft supports

(b) contours for hard supports

Figure 23: deflections (scaled x10) and contours of stress-resultants due to 1kN/m<sup>2</sup> pressure.

**References**

[1] Concepts and applications of finite element analysis, R D Cook, D S Malkus, M E Plesha, R J Witt. 4<sup>th</sup> ed Wiley 2002,

Chapter 15, various sections.

[2] Mechanics of Structures, Variational and Computational Methods, W. Wunderlich & W.D. Pilkey, CRC Press, 2<sup>nd</sup> ed., 2003.

Sections 13.4 for shear deformation effects.

[3] Structural Use of Glass, M. Haldimann, A. Liuble, M. Overend, International Association for Bridge and Structural Engineering (IABSE), 2008.



### Quad 4 element in Oasys GSA as a Reissner-Mindlin flat plate element.

The formulation of this 4 noded element follows the description in Cook et al in Section 15.3 with the same interpolation (or shape) functions for each component of deflection and rotation of the normals. These functions are those defined in page 97 of Cook, and repeated here for a rectangular element:

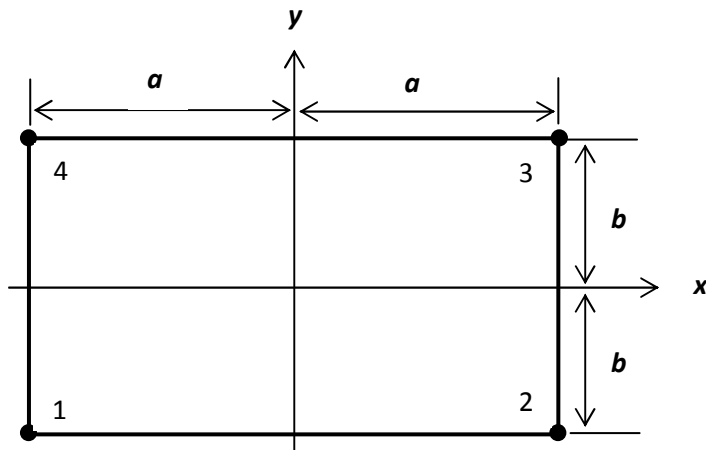


Figure 24: 4 noded plate element

The four shape functions (one for each corner node) are defined with bilinear forms:

$$\begin{aligned}
 N_1 &= \frac{(a-x)(b-y)}{4ab} & N_2 &= \frac{(a+x)(b-y)}{4ab} \\
 N_3 &= \frac{(a+x)(b+y)}{4ab} & N_4 &= \frac{(a-x)(b+y)}{4ab}
 \end{aligned}
 \tag{16}$$

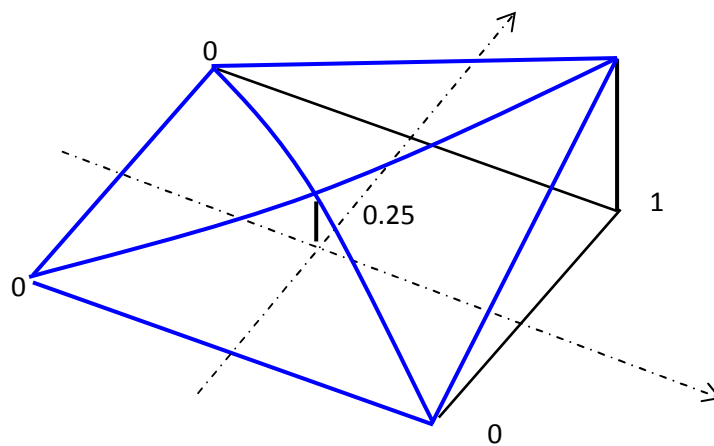


Figure 25: isometric view of a shape function with a unit value at a corner node

We interpolate deflections at internal points from the nodal displacements given by Oasys GSA:

$$w(x, y) = w_1 \times N_1 + w_2 \times N_2 + w_3 \times N_3 + w_4 \times N_4$$

$$\psi_y(x, y) = \theta_{x1} \times N_1 + \theta_{x2} \times N_2 + \theta_{x3} \times N_3 + \theta_{x4} \times N_4 \quad (17)$$

$$-\psi_x(x, y) = \theta_{y1} \times N_1 + \theta_{y2} \times N_2 + \theta_{y3} \times N_3 + \theta_{y4} \times N_4$$

where components of nodal rotation such as  $\vartheta_{x1}$  and  $\vartheta_{y1}$  at node 1 are defined by the right hand screw rule (their values are listed in output in columns headed Rxx and Ryy respectively), whereas components of rotation within an element are defined as in Figure 20. Thus at corner  $n$  of an element,  $\psi_x(x_n, y_n) = -\theta_{yn}$  and  $\psi_y(x_n, y_n) = \theta_{xn}$ .

Symbolically we express these relations in matrix form:  $\mathbf{u} = \mathbf{N} \cdot \mathbf{d}$  (ref Cook Equation (15.3-1)).

**What loads produce a deflected shape?** These are usually quantified and represented by “nodal forces/moments” and the element stiffness matrix, e.g. see Cook Equation (15.3-4):

$\mathbf{f} = \mathbf{k} \cdot \mathbf{d}$ , where the components of  $\mathbf{f}$  correspond to those of  $\mathbf{d}$ , and  $\mathbf{k} = \int \mathbf{B}_M^T \mathbf{D}_M \mathbf{B}_M dA$  where deformations  $\boldsymbol{\kappa}_M = \partial \mathbf{N} \cdot \mathbf{d} \equiv \mathbf{B}_M \mathbf{d}$ .

It should be clear that the stiffness matrix is symmetric and is in the form to yield the strain energy of a deformed element  $U = 0.5 \mathbf{d}^T \mathbf{k} \cdot \mathbf{d}$ .

The mathematical derivation of the stiffness matrix can however take another route which does not depend on concepts of strain energy, but deals directly with quantifying the internal forces and moments due to a deformation, and then quantifying the actual distributed loads which equilibrate with them. These loads can then be represented by integral quantities which we refer to as nodal forces/moments. The full mathematical story will not be told here, but at least we should understand how to derive the distributed loads using the assumed deformations, the constitutive relations and the equilibrium equations.

So now for the deformations:

$$\psi_{x,x}(x, y) = -\left(\theta_{y1} \times \frac{\partial N_1}{\partial x} + \theta_{y2} \times \frac{\partial N_2}{\partial x} + \theta_{y3} \times \frac{\partial N_3}{\partial x} + \theta_{y4} \times \frac{\partial N_4}{\partial x}\right) = -\sum_{i=1}^{i=4} \theta_{yi} \times \frac{\partial N_i}{\partial x}$$

$$\psi_{y,y}(x, y) = +\sum_{i=1}^{i=4} \theta_{xi} \times \frac{\partial N_i}{\partial y} \text{ and } (\psi_{x,y} + \psi_{y,x}) = -\sum_{i=1}^{i=4} \theta_{yi} \times \frac{\partial N_i}{\partial y} + \sum_{i=1}^{i=4} \theta_{xi} \times \frac{\partial N_i}{\partial x}$$

$$\frac{\partial w}{\partial x} = \sum_{i=1}^{i=4} w_i \times \frac{\partial N_i}{\partial x}; \quad \gamma_{zx} = \frac{\partial w}{\partial x} - \psi_x; \quad \frac{\partial w}{\partial y} = \sum_{i=1}^{i=4} w_i \times \frac{\partial N_i}{\partial y}; \quad \gamma_{zy} = \frac{\partial w}{\partial y} - \psi_y.$$

Note that first derivatives of shape functions for this element are simple linear functions:

e.g.  $\frac{\partial N_3}{\partial x} = \frac{(b+y)}{4ab}; \quad \frac{\partial N_3}{\partial y} = \frac{(a+x)}{4ab}$

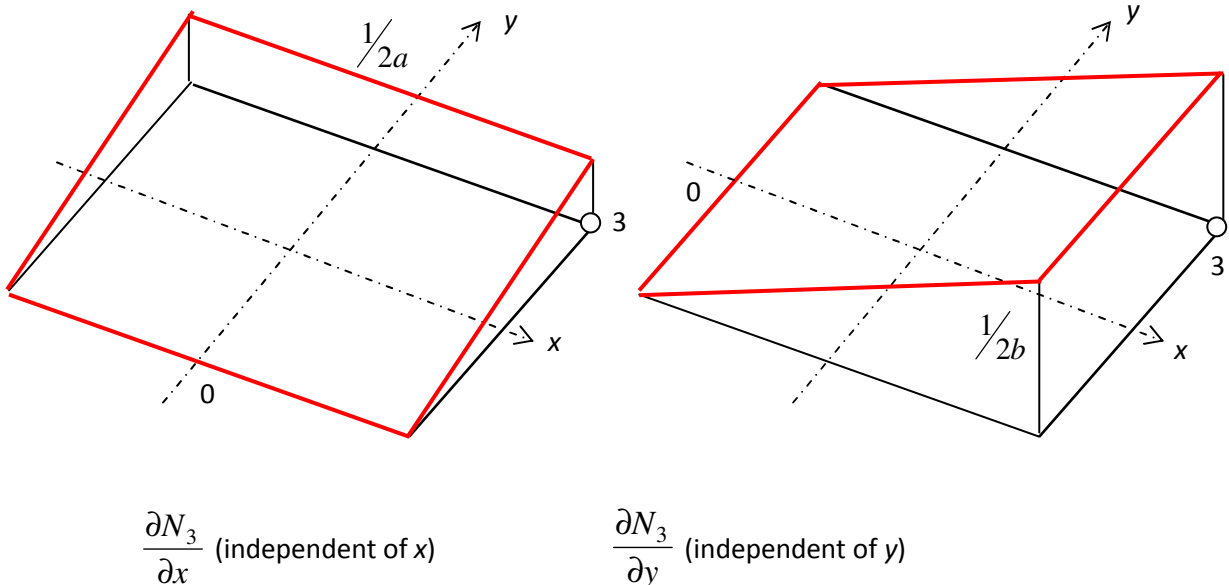


Figure 26: gradients of a shape function

For this simple element, the gradients (rates of change) of the deflection components are easily found, e.g. consider the gradient component:

$$\begin{aligned}
\frac{\partial w}{\partial x} &= w_1 \frac{(-b+y)}{4ab} + w_2 \frac{(b-y)}{4ab} + w_3 \frac{(b+y)}{4ab} + w_4 \frac{(-b-y)}{4ab} \\
&= \frac{1}{4ab} (b((w_2+w_3)-(w_1+w_4)) + y(w_3-w_4) - y(w_2-w_1)) \\
&= \frac{\left[ \frac{(w_2+w_3)}{2} - \frac{(w_1+w_4)}{2} \right]}{2a} + \frac{y}{2b} \cdot \frac{(w_3-w_4)}{2a} - \frac{y}{2b} \cdot \frac{(w_2-w_1)}{2a}
\end{aligned}$$

and this expression is independent of  $x$ . So the gradient along different  $y = \text{constant}$  lines is given for example by:

$$y = 0 \Rightarrow \frac{\partial w}{\partial x} = \frac{\frac{(w_2+w_3)}{2} - \frac{(w_1+w_4)}{2}}{2a}; \quad (18)$$

$$y = b \Rightarrow \frac{\partial w}{\partial x} = \frac{(w_3-w_4)}{2a}; \quad y = -b \Rightarrow \frac{\partial w}{\partial x} = \frac{(w_2-w_1)}{2a}. \quad (19)$$

The deformations, and the consequent forces/moments can thus be easily derived from knowledge of the nodal deflections.

### Check moments output by Oasys at the corners and centre of a typical element

This check requires evaluation of the curvatures and twists at the 5 points using the rotations at the nodes as data. Then for example:

$$\text{along side 12, } \psi_{x,x} = \frac{(\psi_{x2} - \psi_{x1})}{2a} \text{ and } \psi_{y,x} = \frac{(\psi_{y2} - \psi_{y1})}{2a}, \text{ and}$$

$$\text{along side 43, } \psi_{x,x} = \frac{(\psi_{x3} - \psi_{x4})}{2a} \text{ and } \psi_{y,x} = \frac{(\psi_{y3} - \psi_{y4})}{2a}, \text{ and similarly}$$

along side 14,  $\psi_{x,y} = \frac{(\psi_{x4} - \psi_{x1})}{2b}$  and  $\psi_{y,y} = \frac{(\psi_{y4} - \psi_{y1})}{2b}$ , and

along side 23,  $\psi_{x,y} = \frac{(\psi_{x3} - \psi_{x2})}{2b}$  and  $\psi_{y,y} = \frac{(\psi_{y3} - \psi_{y2})}{2b}$ .

From these values we can select or combine to obtain curvatures and twists at each corner, and the values at the centre are simply the average values.

Use Hooke's law to derive the moments at each point, and from the theory of the element the moments should conform with linear variations over the element.

**Check shear forces output by Oasys at the corners and centre of the element.**

Check two ways to derive shear:

(i) from the equilibrium conditions

$$\frac{\partial M_x}{\partial x} + \frac{\partial M_{xy}}{\partial y} = Q_x \quad \text{and} \quad \frac{\partial M_y}{\partial y} + \frac{\partial M_{xy}}{\partial x} = Q_y. \quad (20)$$

This only involves deriving the gradients of the linear moment field, again by taking differences between moments at two nodes and dividing by the distance between them. Thus the derivatives are constant over the element.

(ii) from the shear strains and Hooke's law, e.g. at the centre of the element where

$$\gamma_{zx0} = \left( \frac{\partial w}{\partial x} \right)_0 - \psi_{x0} = \left( \frac{w_6 - w_8}{2a} \right) - \left( \frac{\psi_{x1} + \psi_{x2} + \psi_{x3} + \psi_{x4}}{4} \right) \quad (21)$$

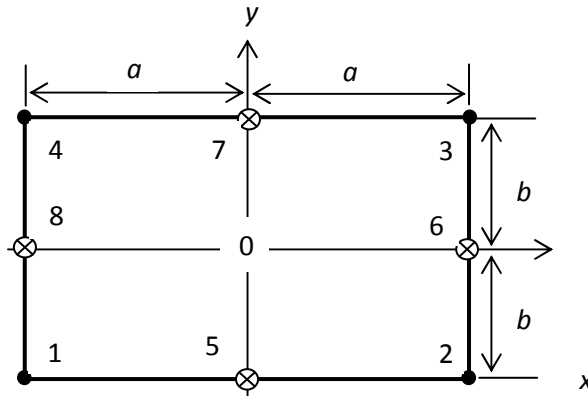


Figure 27: 4 noded element with centre and mid-side reference points.

and  $Q_{x0} = \frac{5}{6} Gt \cdot \gamma_{zx0}$ , similarly for  $Q_{y0}$ .

### Lack of equilibrium

Whilst the stiffness equations for a system of elements essentially enforce equilibrium, it must be realized that the quantities being equilibrated are the nodal forces/moments. No direct attempt is made to enforce complete equilibrium of the internal forces and moments within elements! If we could do that, then we would have found the unique correct solution to the problem. Finite element solutions are only approximations, and unfortunately the least accurate quantities are usually the derived forces/moments!!

To appreciate that equilibrium is not satisfied in a local sense it is necessary to evaluate quantities like:

$$\frac{\partial^2 M_x}{\partial x^2} + 2 \frac{\partial^2 M_{xy}}{\partial x \partial y} + \frac{\partial^2 M_y}{\partial y^2} + q \text{ and compare with zero;}$$

$$\left( \frac{\partial M_x}{\partial x} + \frac{\partial M_{xy}}{\partial y} - Q_x \right); \text{ and } \left( \frac{\partial M_y}{\partial y} + \frac{\partial M_{xy}}{\partial x} - Q_y \right) \text{ where moments and shears are derived}$$

from curvatures and shear strains respectively, and compare with zero;

or  $\left( \frac{\partial Q_x}{\partial x} + \frac{\partial Q_y}{\partial y} + q \right)$  where shears are derived from shear strains, and compare with zero.

Alternatively we could evaluate the loads for which equilibrium is exactly satisfied and hence for which the displacements and compatible deformations output by Oasys are the exact response. Such loads require in general a pressure  $\tilde{q}$  and two components of load in the form of couples per unit area about the x and y axes.

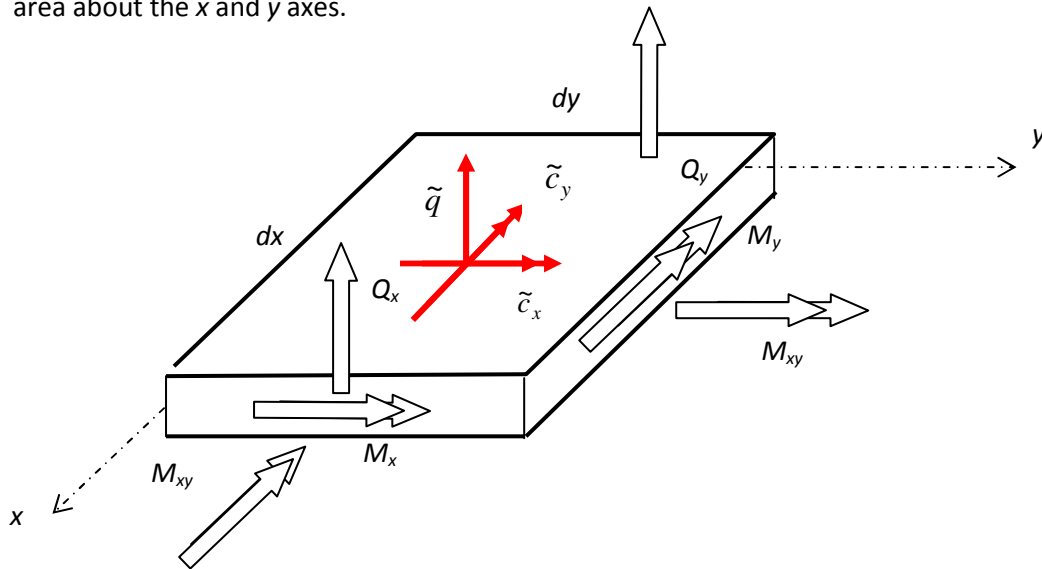


Figure 28: infinitesimal element including derived equilibrating loads

$$\tilde{q} = -\left( \frac{\partial Q_x}{\partial x} + \frac{\partial Q_y}{\partial y} \right) \text{ kN/m}^2, \quad (22)$$

$$\text{and } \tilde{c}_x = \left( Q_x - \left( \frac{\partial M_x}{\partial x} + \frac{\partial M_{xy}}{\partial y} \right) \right) \text{ kNm/m}^2, \quad \tilde{c}_y = \left( Q_y - \left( \frac{\partial M_y}{\partial y} + \frac{\partial M_{xy}}{\partial x} \right) \right) \text{ kNm/m}^2. \quad (23)$$

Such loads can be compared with the applied loads. In practice we can then decide whether the lack of equilibrium is acceptable for the job in hand (How accurate do we need to be? How well are the loads defined?), or needs to be improved. In the later case the size of elements should be considered and reduced, or a different type of element used.....

## Weak equilibrium

The weak form of equilibrium enforced by the finite element model involves balancing equivalent nodal forces and moments in vector  $\mathbf{f}$ .

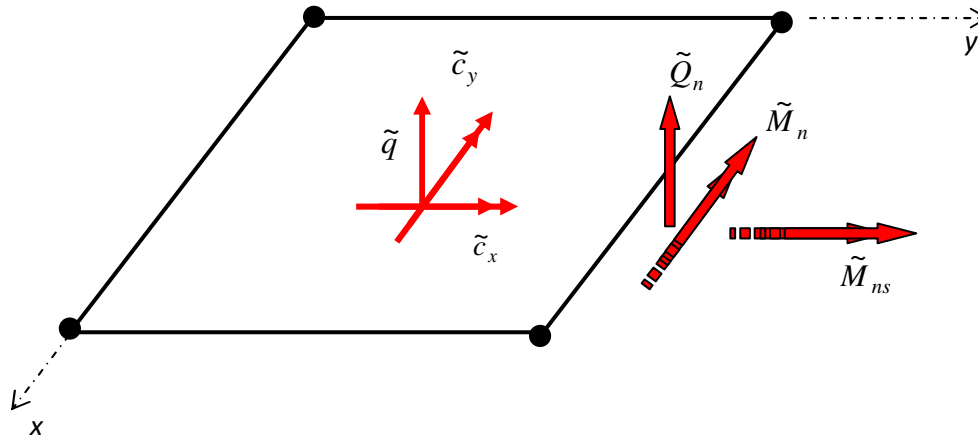


Figure 29: an element with derived surface loads and boundary tractions

Nodal forces that are statically equivalent to the derived loads are defined in Equation (24).

$$\mathbf{f} = \int \mathbf{N}^T \begin{Bmatrix} \tilde{q} \\ -\tilde{c}_x \\ -\tilde{c}_y \end{Bmatrix} dA + \oint \mathbf{N}^T \begin{Bmatrix} \tilde{Q}_n \\ -\tilde{M}_{ns} \\ -\tilde{M}_n \end{Bmatrix} ds \quad (24)$$

## Reference

Concepts and applications of finite element analysis, R D Cook, D S Malkus, M E Plesha, R J Witt. 4<sup>th</sup> ed Wiley 2002,

Section 15.3 for Reissner-Mindlin plate elements; Section 15.5 for boundary conditions.



**Advanced Structural Engineering**  
**Assignment: Linear elastic behaviour of plates**

**Use of finite element models**

For this Assignment use Oasys GSA to model the plate. This model is based on linear elastic behaviour with further properties tabulated in Table 1.

plate	thickness	Young's modulus	Poisson's ratio
Floor slab	0.250m	25e6 kN/m <sup>2</sup>	0.2
Road deck	1.0m	30e6 kN/m <sup>2</sup>	0.2
Granite slab	0.150m	35e6 kN/m <sup>2</sup>	0.2
Water tank	0.3	30e6 kN/m <sup>2</sup>	0.2
Retaining wall	0.4	30e6 kN/m <sup>2</sup>	0.2

Table 1: plate properties – real constants and material properties

- **Modelling with GSA**

- Create a uniform mesh of rectangular elements having side dimensions  $\leq 1/10^{\text{th}}$  of the lengths of the sides of the plate, i.e. split the initial quadrilateral into at least 10 divisions each way – to fit individual problems.
- Use explicit definitions of material properties.
- Use soft conditions first to simulate simple supports.

- **Results and reports**

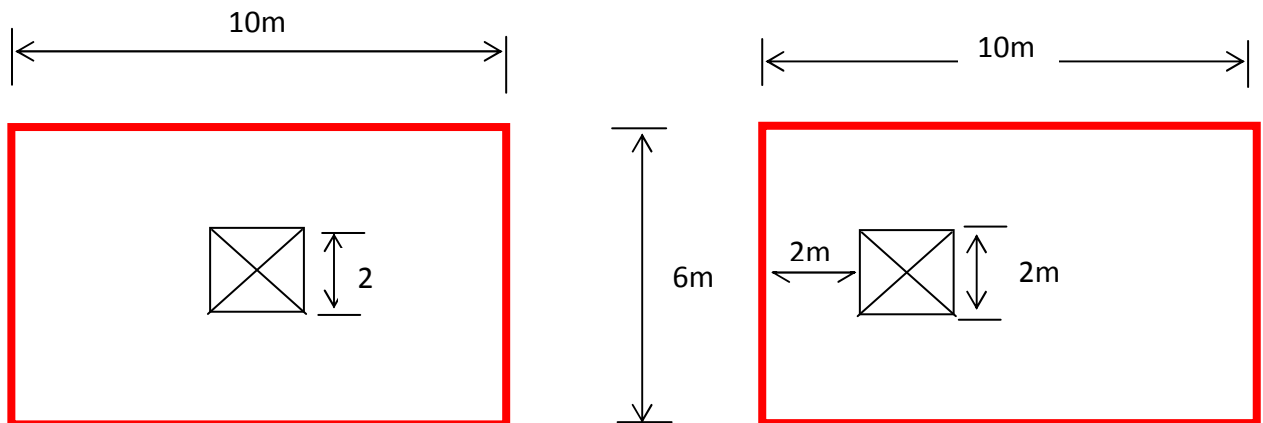
- Plot contour maps of deflections and/or vector plots at nodes, and indicate maximum values of deflections;

- Plot the distributions of reactions, and indicate maximum values;
- Plot contours of bending moments, torsional moments, and shear forces and indicate maximum values;

N.B. These plots describe the linear elastic behaviour of your plate, but they will also form useful references for the limit analyses in Assignment 4.

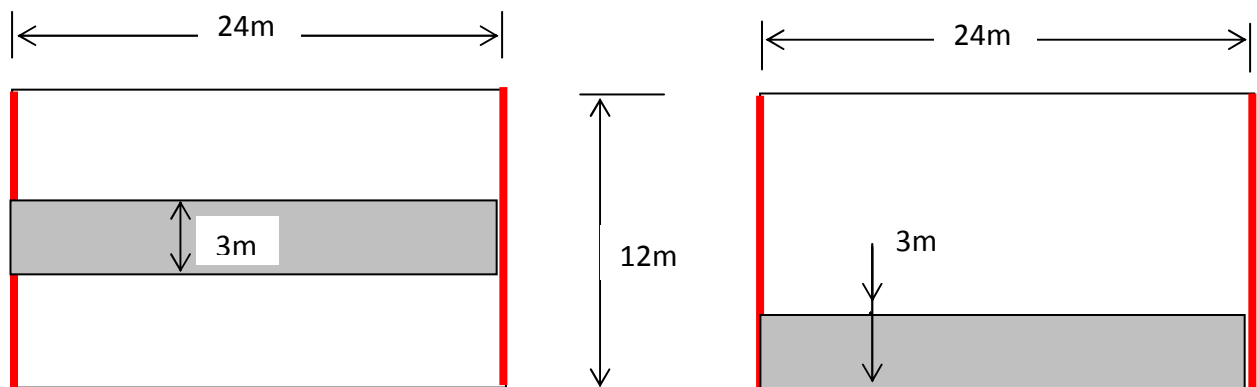
- Check the GSA results for ONE element (e.g. the one with the largest moments and indicate its location in the plate) as follows:
  - From the output of nodal rotations, derive by hand the curvatures and twists at the nodes and the centre of the element. Be aware of the differences between  $\psi_x$  and  $\psi_y$  and  $\theta_x$  (Rxx) and  $\theta_y$  (Ryy) as illustrated in Figure 15.1-4 in Cook.
  - Then using the  $\mathbf{D}_M$  matrix, derive the components of moment at these points and compare with the output from Oasys;
  - Then derive the derivatives of moments as constant values throughout the element to obtain:  $\left( \frac{\partial M_x}{\partial x} + \frac{\partial M_{xy}}{\partial y} \right)$  and  $\left( \frac{\partial M_y}{\partial y} + \frac{\partial M_{xy}}{\partial x} \right)$  as estimates of the shear forces;
  - From the output of nodal deflections, derive by hand the gradient of deflection  $w$  at the nodes and centre of the element and the rotations. Hence derive the transverse shear strains at the nodes and centre and the corresponding shear forces.
  - Compare the shear forces at the centre of the element as derived above and as output from Oasys.
- As a check on local equilibrium evaluate the load intensities in the form of a pressure and two components of couples at the centre of the element, corresponding to the shape of the deformed element compatible with the nodal displacements as output from Oasys. Compare with the applied load. Reflect and comment on the significance of these values.
- Do not be surprised if local equilibrium appears to be violated. Violations indicate that the finite element model is not completely accurate for the purposes of simulating linear elastic behaviour, it is only an approximation.
- Re-compute with Oasys GSA using hard simple supports, and reflect and comment on any significant differences between using soft or hard supports. These comments should be based on inspection of graphical output, there is no need to re-check the single element!

- floor slab with an opening, simply supported on 4 edges



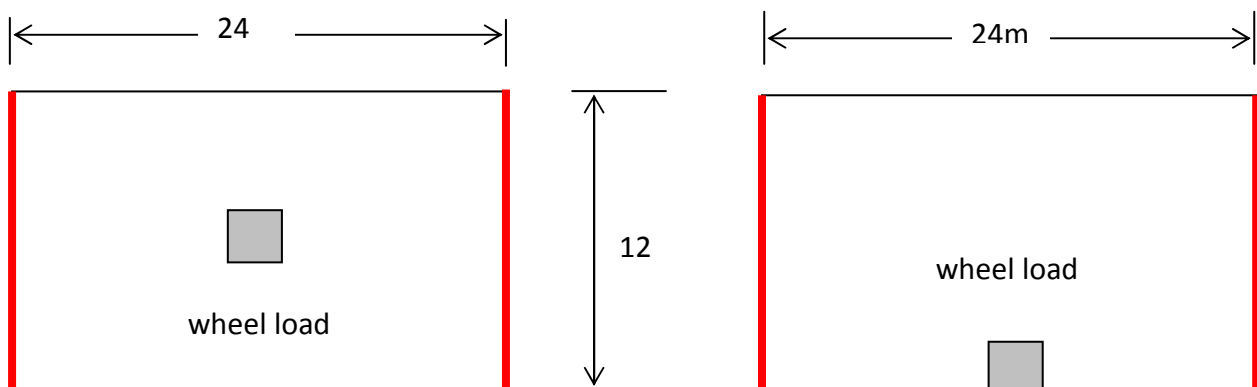
- (1)  $5\text{kN/m}^2$  UDL with a central square opening      (2) as (1) but with an off-centre opening

- road bridge deck simply supported on two opposite edges, free on the other two edges



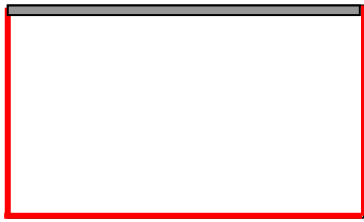
- (3)  $10\text{kN/m}^2$  centre lane load      (4) as (3) but with lane load next to a free edge

- road bridge deck simply supported on two opposite edges, free on the other two edges



- (5)  $40\text{kN}$  UDL on a  $1\text{m}\times 1\text{m}$  central patch      (6) as (5) but with position moved to a free edge

- 10m × 5m floor slab simply supported on 3 edges

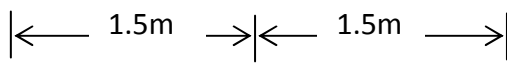


(7) 5kN/m edge load

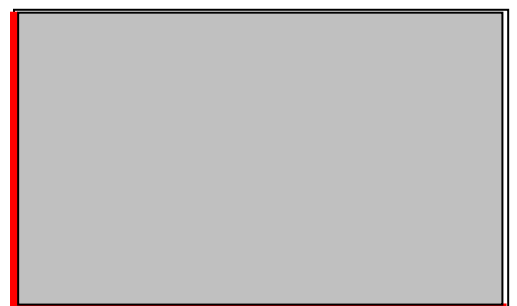
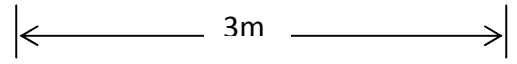
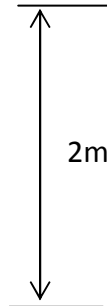


(8) 4kN/m<sup>2</sup> UDL

- granite landing slab simply supported on two adjacent edges, free on the other two edges

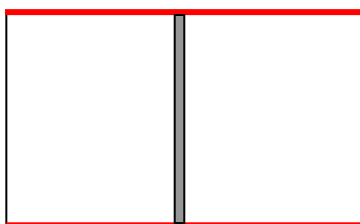


(9) 12kN/m line load applied on part of a free edge



(10) 5kN/m<sup>2</sup> UDL over the entire slab

10m × 5m floor slab simply supported on 2 edges




(11) 5kN/m central load

## Guidance document for using Oasys GSA version 8.3 in modelling rectangular plates.

### ○ Create a finite element model

- Select Structure Type: **Space**, and check default units or select different ones.
- Note re axes and definition of 4 corner nodes and element topology as for the plane stress demonstration.
- Define the material properties explicitly under Properties: Materials: User Defined
  - Input values of Young's Modulus and Poisson's Ratio; use only the one material which will be referenced as material number 1 and by name, e.g. "stone".
- Define 2D Element Properties
  - Input 2D element property number 1, Type as Flat Plate; Material by name; and Thickness.
- Split element as demonstrated for the plane stress model.
- Delete elements as necessary to create an opening in the plate.
  - Select elements for deletion, then select Edit and Delete. Check by viewing a "shrink" view.
- Define supports (e.g. simple or fixed)
  - Activate the "Select nodes" icon in the left hand menu, then select nodes on the boundary (e.g. surround with a box and use Ctrl key for multiple boxes).
  - Select Edit from the top menu, and then Save Selection As List..., give a name to the list for future reference.
  - Under Constraints select the Generalised Restraints option to specify common restraints to each node in a list – remember the distinction between soft ( $w = 0$ ) and hard supports ( $w = 0$  AND  $\theta_x = 0$  when the supported edge is parallel to the y axis). For each named list choose "Yes" to apply zero values of vertical deflection or rotation under the headings x,y,z and/or xx,yy,zz respectively. You must realize here that, for example, "xx" denotes rotation about the x axis as illustrated in Figure 15.1-1. in Cook using the symbol  $\theta_x$ .
- Define loads
  - Select elements in order to specify a common value of a UDL. Selection may be done by enclosing elements within a box and using the Edit, Save Selection As List... feature.
  - Under Loading, 2D Element Loading, select Face Loads:
    - Input lists of elements, and Pressure at Position. Just one value is required for a UDL, or different values at the nodes when appropriate. Remember that a negative value is required to specify a pressure in the downwards direction when the z axis is positive upwards!
  - Line loads on a boundary must be specified under Loading, Nodal Loading, Node Loads.
    - Input lists of nodes, and Value of a vertical force. This value should represent a uniform intensity of line load in a statically equivalent way, e.g. in the same way that you would represent a distributed load on a beam element. In this case, note that the values of vertical forces for the end nodes of a line should be half that for the nodes in between the ends.

- **Analyse the model**
  - Use the  $\Sigma$  icon on the top menu.
- **Examine the output**
  - Deflected shape, use the  button – try 3D views by rotating the viewing direction, and animation.
  - Display nodal reaction forces/moments by activating the **Diagram settings button** in right hand menu, then select Reactions from the dialogue box and select a component of force or moment. Note that reactions can also be displayed by selecting the “reaction” button in the menu on the right hand side of the screen.
  - For numerical values select Output from the left hand menu, then:
    - Nodal Results, Displacements for a table of components. Save those of interest by selecting with the mouse and Copy under the Edit menu. It appears that you cannot restrict the saved results to particular components but only to particular lines of output. Note that the relevant components will be Uz, Rxx, and Ryy. The copied output may then be pasted into a word or Excel document. In this context it may be better to opt for the Grid style Output View.
    - Nodal Results, Reactions for a table of components. List and note reactions – save in a file for later editing. Note that the relevant components will be Fz, Mxx, and Myy; be careful with the notation and sign conventions, e.g. Mxx denotes a moment at a node which corresponds to a rotation Rxx (or  $\theta_x$ ).
    - Display contour maps of components of interest, e.g. vertical deflections and “projected” moments and shear forces:
      - Activate Contour settings icon in right hand menu, then select from the dialogue box: 2D Element Displacements (select a component), 2D Element Projected Moments (for 2D Moment, Mx, My, or Mxy) or Forces (for 2D Through-Thk Shear, Qx or Qy).
      - Graphic views can be saved in different formats such as PNG or JPEG by selecting Graphics and then SaveImage, or use “Copy” and “Past Special” buttons, and choose Bitmap.
    - List components of interest, e.g. moments and shears in each selected element at node positions and at the centre point – save in a file for later editing:
      - Select 2D Element Results, 2D Element Projected Moments or Forces. Note that contour maps of shear forces are displayed as if they were constant for each element, and the Force components listed include in-plane components Nx etc which should all be zero! Check that results are displayed using Global Axes. For notation and sign conventions refer to Figure 15.1-3 in Cook, but note that output for shear forces appears to use the opposite sign convention – which just goes to show how careful you must be when interpreting computer output!!

- Output can also be printed directly using File and Print commands.
  
- **Reanalysis after modifications to the model or the loads**
  1. Modifications can only be made after selecting Delete All Results under the Analysis item of the top menu.

**Acknowledgements:**

These notes were prepared for the Advanced Structural Engineering Module in the College of Engineering, Mathematics and Physical Sciences at the University of Exeter. This is a fourth year module undertaken by MEng and MSc students. These were presented by Edward Maunder in the academic year 2009/10. For this presentation the finite element software OASYS was used and there is some reference to this software in the text and figures. The geometric non-linear example used the finite element software ADAPTIC at Imperial College, London.

## Limit analysis: bounds on ultimate loads for plates.

### Introduction

Whilst linear elastic analyses are widely used in practice (a rough estimate has been made that some 90% of structural analyses are based on linear elastic assumptions), it is vital to understand how structures may collapse, and at what loads (the ultimate loads). One way to address this problem is to carry out a sequence of analyses that recognise from stage to stage that material becomes inelastic and/or the deflections become large – this is normally referred to as an incremental non-linear analysis. It needs to make many assumptions along the way, and can become very expensive in terms of computational effort. An alternative approach, termed limit analysis, exists based on theorems of plasticity when the material exhibits sufficiently ductile behaviour [1]. Limit analyses aim to predict collapse loads directly without the need for incremental analyses. The first type of limit analysis we consider leads to lower bound estimates of collapse loads, and hence it is on the safe side. The second type of analysis leads to upper bound estimates of collapse load, and hence it is on the unsafe side!

### Yield in the context of reinforced concrete slabs - Nielsen's yield criterion [2].

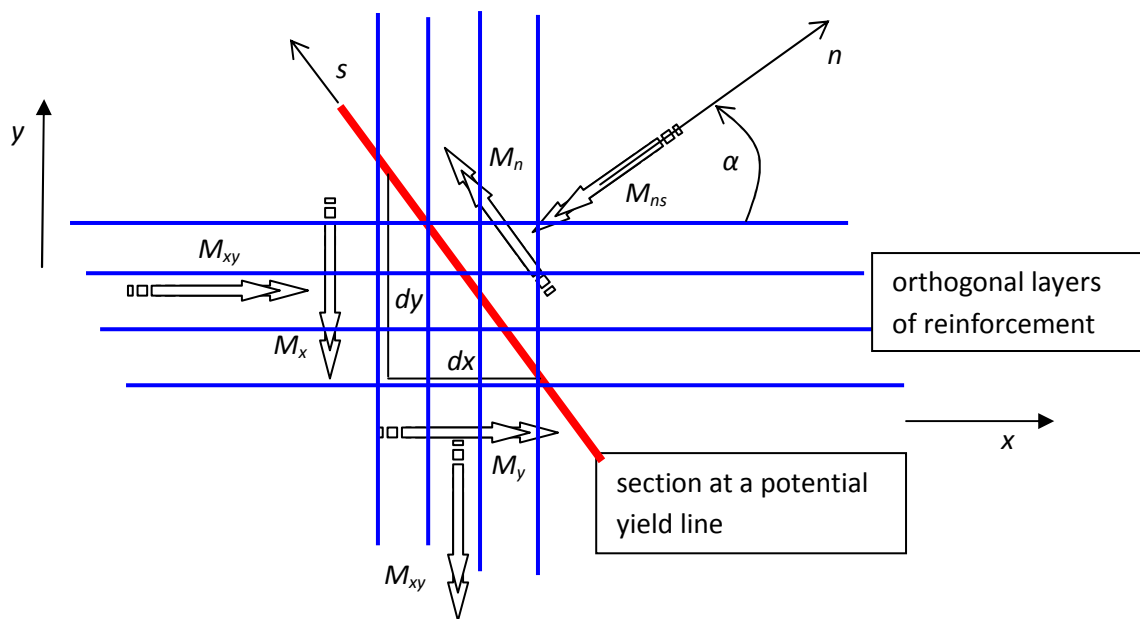


Figure 1: yield in orthogonal reinforcement

The yield criterion is derived from the assumption due to Johansen that the bending moment that can be mobilised to resist  $M_n$  is provided by the tension at yield in the reinforcing bars that cross the section. Resolving the tensile forces in the reinforcement parallel to the normal direction  $n$  gives a yield moment intensity  $M_{Yn}$  defined by:

$$M_{Yn} = M_{Yx} \cos^2 \alpha + M_{Yy} \sin^2 \alpha, \text{ and } M_n = M_x \cos^2 \alpha + M_y \sin^2 \alpha + M_{xy} \sin 2\alpha.$$

We then require that the bending moment  $M_n \leq M_{Yn}$  for all values of  $\alpha$ .

It can be shown that this is achieved with top/bottom layers of reinforcement when the principal moments corresponding to:



$$\left\{ \begin{array}{l} M_x \mp M_{Yx} \\ M_y \mp M_{Yy} \\ M_{xy} \end{array} \right\} \text{ just become sagging/hogging moments, i.e. } \left| \begin{array}{cc} (M_x \mp M_{Yx}) & M_{xy} \\ M_{xy} & (M_y \mp M_{Yy}) \end{array} \right| = 0. \quad (1)$$

Note that the minus sign is associated with yield moments provided by the top layers of reinforcement and the plus sign is associated with the yield moments provided by the bottom layers of reinforcement – using the standard sign convention for moments as in elastic theory. In general yield occurs with orthogonal reinforcement when the three components of moment  $M_x$ ,  $M_y$ , and  $M_{xy}$  lie on the yield surface in 3D space. The surface corresponding to Equation (1) is formed from two cones (hence the term “biconic”) as shown in Figure 2.

Note also that in the absence of torsional moments, the requirements for yield moments are simplified to  $M_x \leq \pm M_{Yx}$  and  $M_y \leq \pm M_{Yy}$

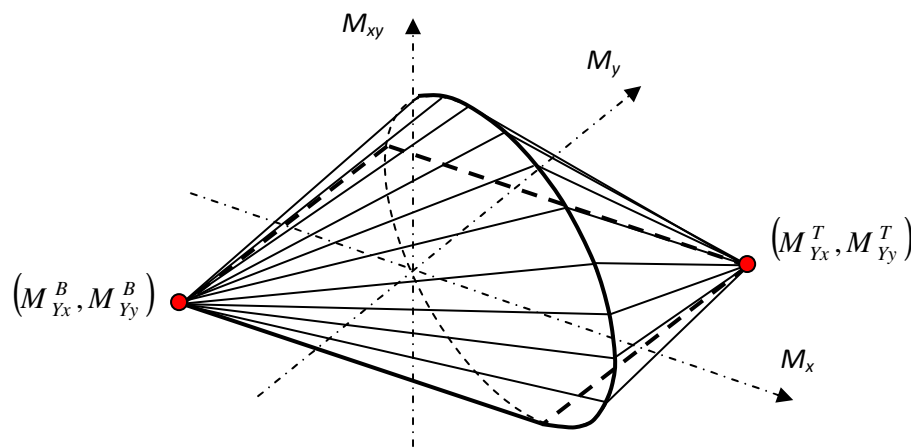


Figure 2: yield surface, superscripts  $T$  and  $B$  refer to yield moments due to top or bottom layers of reinforcement.

## Limit analysis for lower bounds

### The master safe theorem

Equilibrium analysis and the “**master safe**” theorem: “**if any equilibrium state can be found, that is, one for which a set of internal forces is in equilibrium with the external loads, and, further, for which every internal portion of the structure satisfies a strength criterion, then the structure is safe**” [1,3]. This wording is a way of expressing the lower bound theorem in the theory of plasticity, and assumes that collapse by buckling or the development of large deflections is unlikely. It can be used in the context of **design or assessment**, e.g. a new structure can be safely designed to resist any internal forces which equilibrate with the external loads, and an existing structure can be assessed for its safety to carry (new) loads by seeking a state of equilibrium of the internal forces which nowhere violates local strength criteria. This all sounds straightforward, but the determination of equilibrium solutions for a plate where there are an unlimited number of such solutions has not yet been automated, as far as we know, within commercially available software – it requires thought, imagination, and experience! However the rewards are considerable, and may enable you to sleep at night!! NB: Ramsay Maunder Associates are currently developing software tools (part of EFE) for limit analyses of plates [4].

### An example of a rectangular plate with continuous fields of moments [2].

We can illustrate the application of the master safe theorem to a rectangular slab supporting a line load on one edge when two adjacent edges are simply supported as shown in Figure 3. We need to devise suitable expressions for moment fields, i.e. the components  $M_x$ ,  $M_y$ , and  $M_{xy}$  as functions of coordinates  $x$  and  $y$ . In general this may pose quite a challenging problem, and we will demonstrate later that the application of equilibrium elements as in EFE opens a systematic way of approaching it. However for the moment we will propose some fields and see what we can achieve with them.

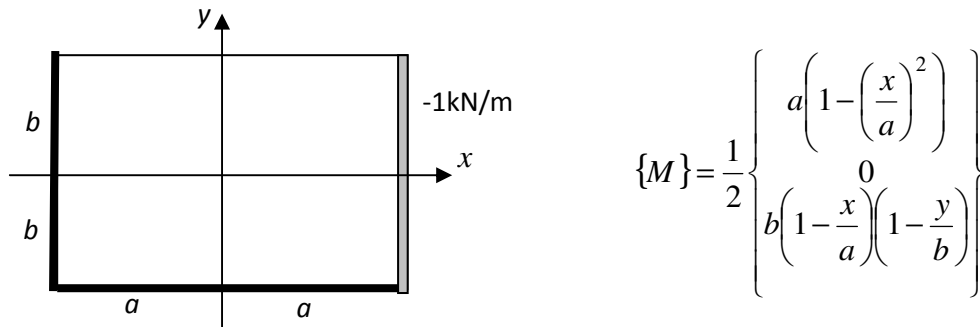


Figure 3: simply supported plate and a moment field.

We can verify that equilibrium is satisfied as follows: clearly bending moments are zero along all four edges, and

$$\{Q\} = \frac{1}{2a} \begin{Bmatrix} -a-x \\ -b+y \end{Bmatrix} \Rightarrow Q_x = -1 \text{ when } x = a, Q_y = 0 \text{ when } y = b, \text{ and } q = 0.$$

Thus the loads are correctly accounted for, and the reactions are as shown in Figure 4:

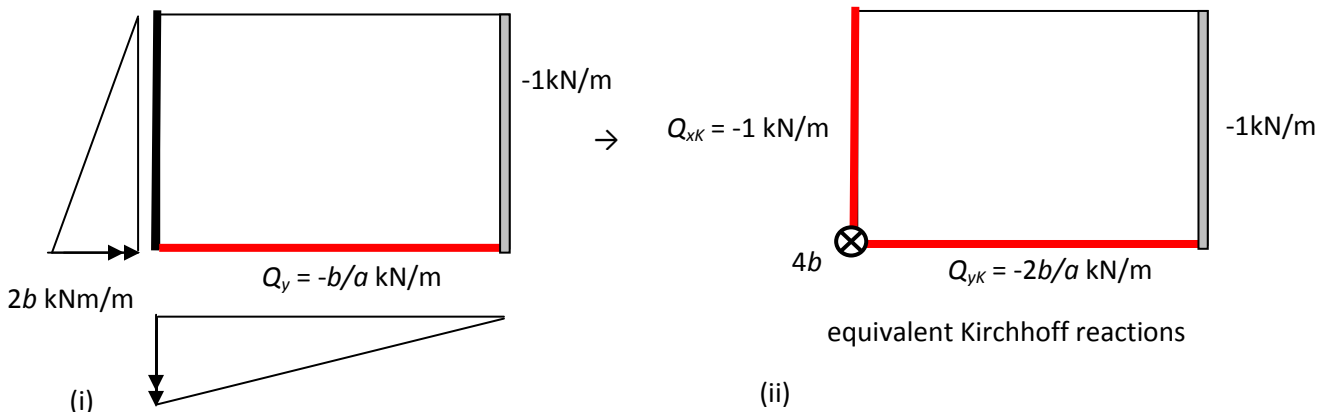


Figure 4: distributions of reactions, including the Kirchhoff equivalent form.

This solution leads the load to the lower edge support, and requires torsional moment reactions. We can adapt this solution to comply with “soft” supports, i.e. without torsional reactions, by invoking the concept of equivalent Kirchhoff shear forces. From the physical point of view we argue that narrow edge strips have unlimited shear strength, and hence have the capacity to transfer the Kirchhoff reactions to the stress-resultants defined by the moment field [5].

In Figure 5 the edge strips are shown in an exploded view in order to show clearly the forces and moments applied to the external and internal faces of each strip. Each strip is in equilibrium, and although there are shear forces within the strips, there are no bending moments! The external reactions now include a concentrated corner force.

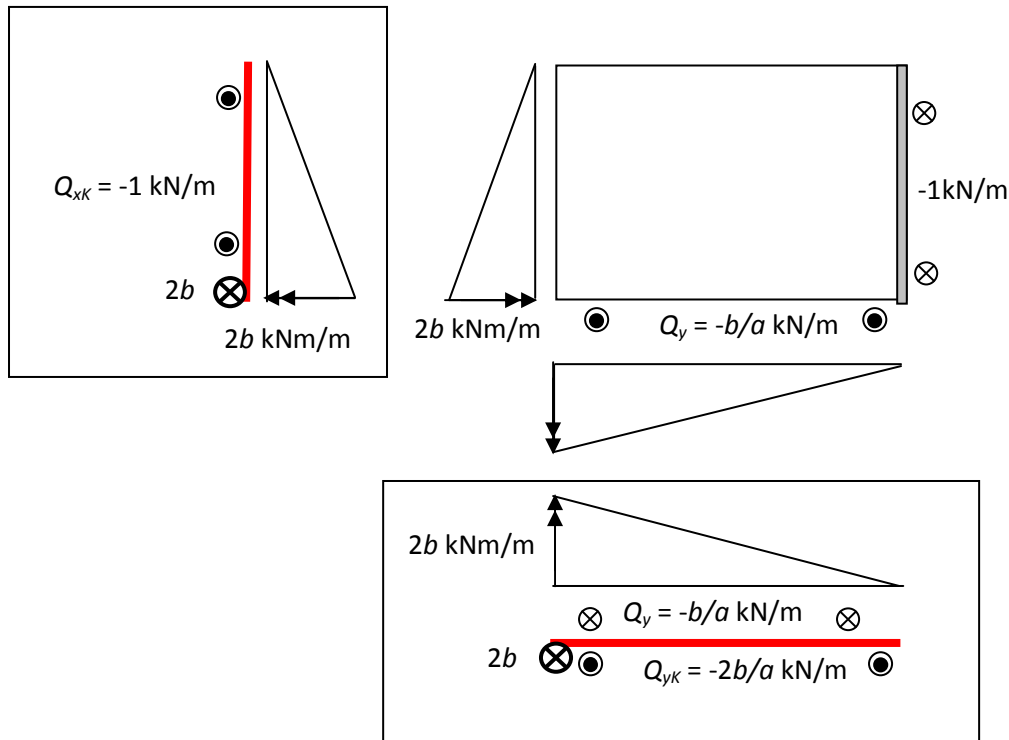


Figure 5: exploded view of the simply supported plate without torsional reactions.

However, even if we only restrict ourselves to simple quadratic moment fields, the field equilibrating with the load is not unique. In the present example, by exploiting Kirchhoff equivalent forces, we can define two fields in Equations (2) and (3) that equilibrate with zero applied loading, e.g.:

$$\{M\} = c \begin{Bmatrix} 1 - \left(\frac{x}{a}\right)^2 \\ 0 \\ \frac{x}{a^2}(-b + y) \end{Bmatrix}; \quad \{Q\} = \frac{c}{a^2} \begin{Bmatrix} -x \\ -b + y \end{Bmatrix}; \quad q = 0, \quad (2)$$

and the edge reactions are shown in Figure 6.

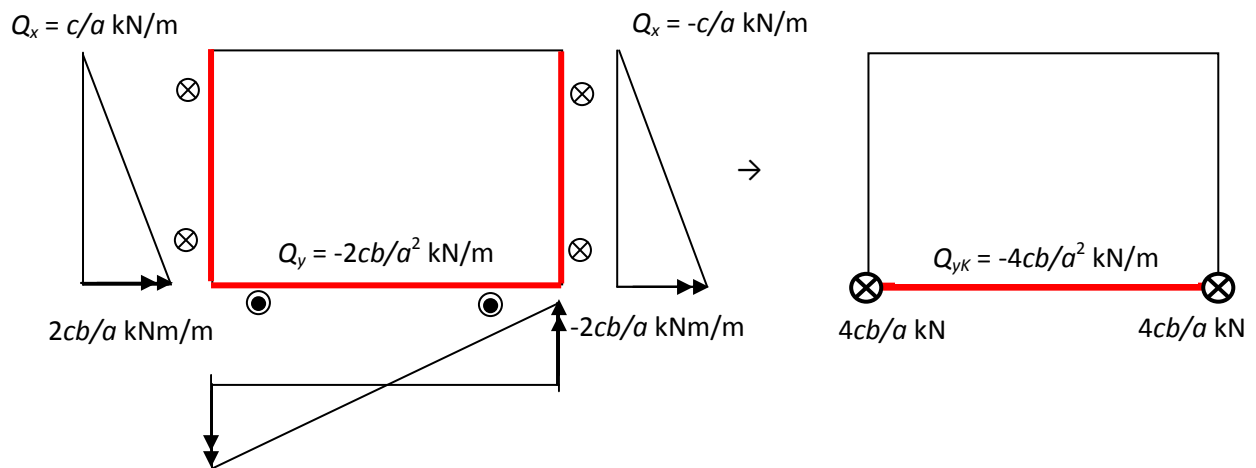


Figure 6: edge reactions for a hyperstatic moment field.

After transforming to the Kirchhoff reactions, the reactions are essentially contained along the lower supported edge, and hence they become self-balanced and independent of any external load. This moment field is statically indeterminate, otherwise termed hyperstatic. Once more an exploded view, in Figure 7, clarifies the structural function of each edge strip:

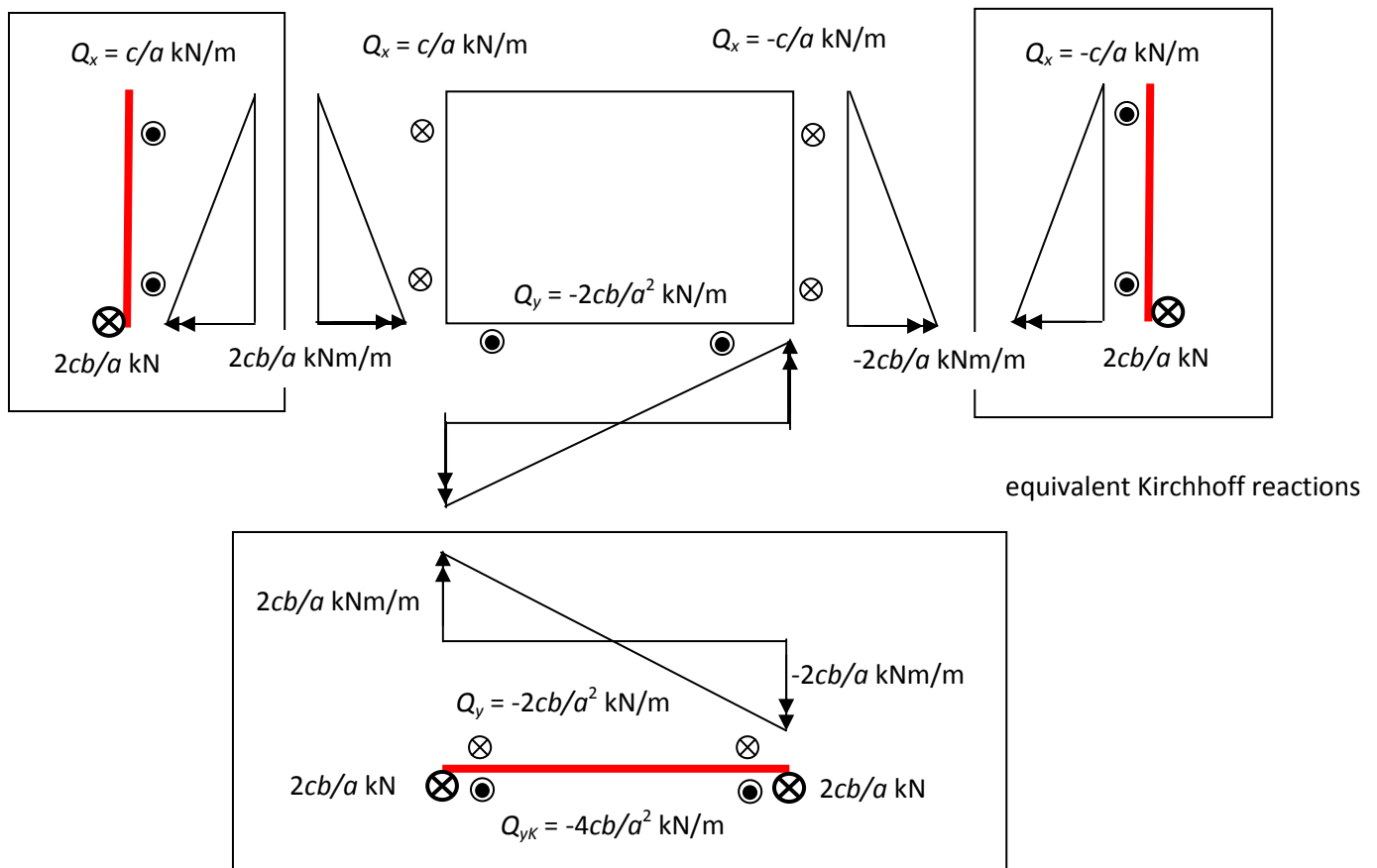


Figure 7: exploded view of hyperstatic reactions.

A second hyperstatic moment field is similarly defined in Equation (3):

$$\{M\} = d \begin{Bmatrix} 0 \\ 1 - \left(\frac{y}{b}\right)^2 \\ \frac{y}{b^2}(-a+x) \end{Bmatrix}; \quad \{Q\} = \frac{d}{b^2} \begin{Bmatrix} -a+x \\ -y \end{Bmatrix} \quad (3)$$

and this field has reactions as shown in Figure 8.

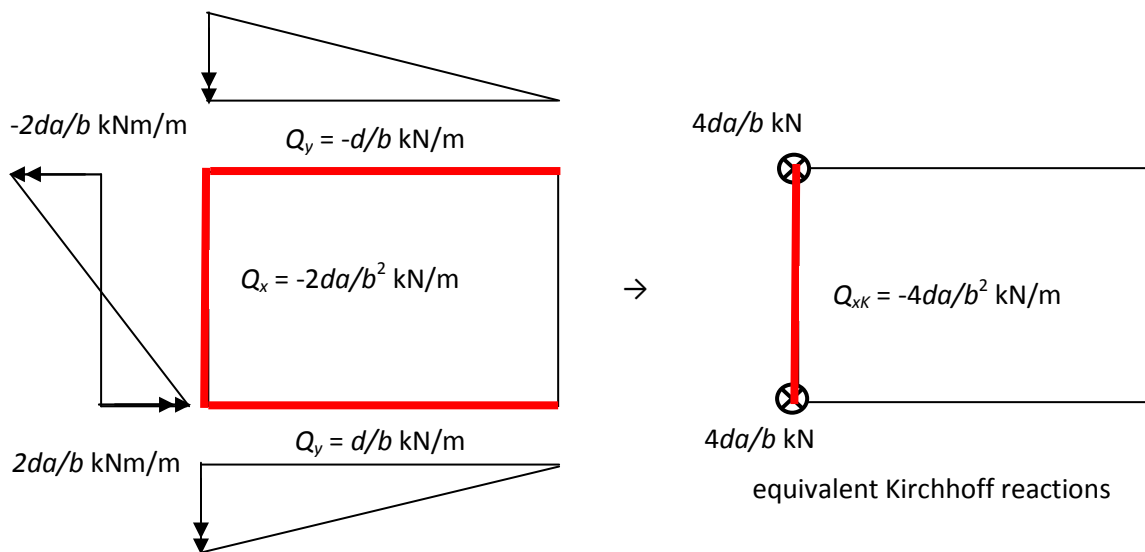


Figure 8: hyperstatic reaction corresponding to moments in Equation (3).

Now we have 1 particular moment field and 2 hyperstatic, or complementary, ones. If we are assessing the capacity of a slab with a given yield strength, then we have the freedom to combine the 3 fields with the aim of maximising the load factor that can be applied to the unit edge load. On the other hand, if we are designing a new slab to support a specified load, then we can aim to minimise the yield strength required. These are basic problems of optimisation.

### Hillerborg's strip method

The previous example is meant to indicate how a systematic method may be developed as a computational tool. However, equilibrium solutions can often be generated manually by exploiting further the concept of modelling a slab as interconnected families of beam strips which act in a similar way to floor planks as illustrated in Figure 9.:

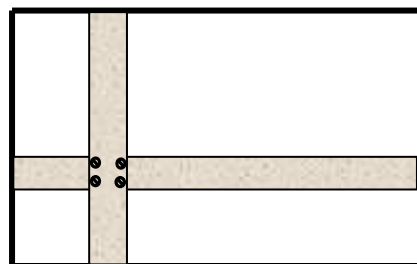


Figure 9: beam strips as floor planks.

In the context of reinforced concrete slabs, Hillerborg's strip method [6,7] considers the way a slab transfers load as a 2D extension of beam concepts. At its simplest a slab can be thought of as **two orthogonal families of contiguous strips (rather like floor planks placed edge to edge, but in two layers or directions)**, whose directions coincide with the directions of the reinforcing bars. The beam strips transfer load directly placed on them to supports, or orthogonal strips interact with each other to provide mutual support. Loads or interactions are equilibrated in each strip by distributions of shear forces and bending moments – these quantities and the reactions at supports need to be evaluated in order to specify an equilibrium solution. With more complicated cases it may be necessary for equilibrium to include torsional moments within beam strips as well as bending moments. It is generally simpler to avoid these if possible.

Some guidelines are given here to supplement the example in CALcrete [8] and the rather brief notes in Mosley et al [9], MacGregor [10] and Nilson et al [11], and should be considered in relation to the individual problems included in Assignment 4. All these problems are based on rectangular slabs with edges which are either free (unsupported), or simply supported (able to resist vertical shear forces and torsional moments if required).

- Define two orthogonal families of beam strips – normally these would be aligned parallel to the lines of support and/or the directions of the reinforcement. The beam strips can be infinitesimal in width, or of finite width, but must recognise the occurrence of openings (beam strips should “frame” round openings) and concentrated loads spread over a small area (strip widths should be such as to coincide with the dimensions of the loaded area). It should be noted that the division of a slab into strips is similar to the subdivision (discretisation) involved in the finite element models (rectangular elements can be identified by the overlap of two orthogonal strips) for Assignment 3.
- Identify lines of support (concentrated supports are also used in practice in the form of columns with flat slabs – such cases are not considered in this module).
- Define load routes for the pattern of loading being considered – three alternative ways to divide the load are described by MacGregor [10] for a rectangular slab with each edge simply supported and loaded with a UDL (uniformly distributed load). For this particular problem there is no need for the strips to interact, you decide how to divide the load between them. Basically the ways described by Macgregor either share the load in the same proportion at each point (e.g. as illustrated in later examples), or subdivide the area of the slab (favoured by Hillerborg [6,7] and impose all the load in an area onto one or other of the families of strips as designated by arrows, for example in Figure 10.

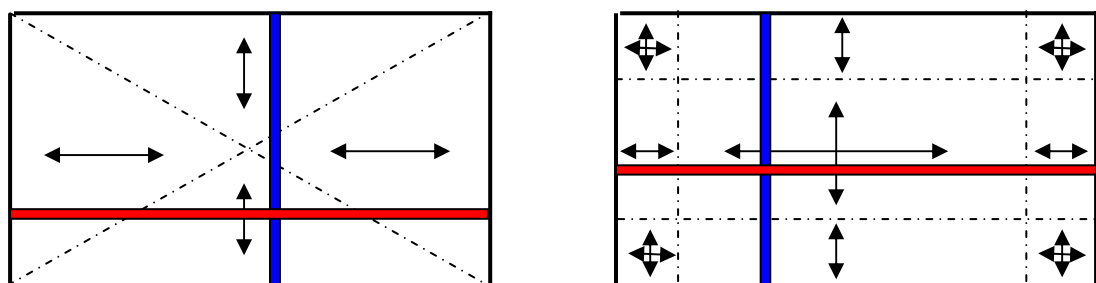


Figure 10: load routes designated by location.

A summary of the procedure for exploiting beam strips:

- identify supports
- identify families of beam strips
  - 2 families generally: for reinforced concrete slabs, their alignment usually agrees with the alignment of the reinforcing bars.
- load sharing and/or interactions between strips
- for simplicity, keep torsional moments zero if possible
- infinitesimal or finite width of strips?
- lateral thinking and imagination
- explain your structural system, follow the load paths so as to define distributions of reactions, and form moment and shear force diagrams for a typical strip from each family.
- **EXAMPLES**
- **4 simply supported sides with a UDL**

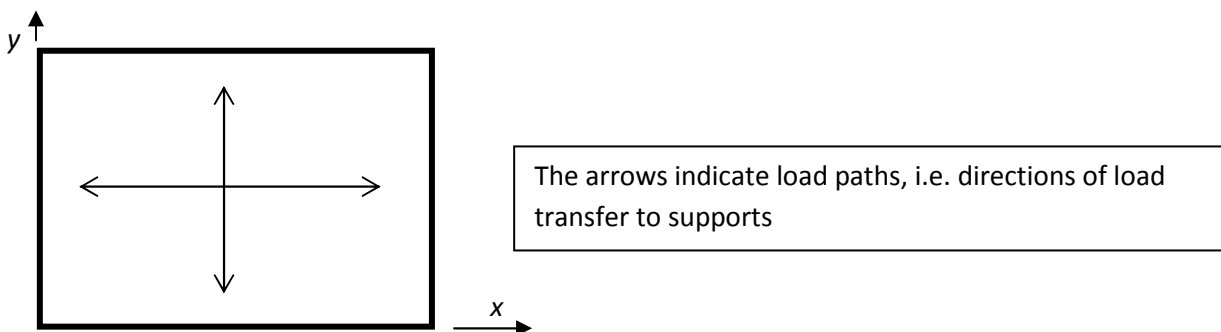


Figure 10: rectangular plate with simple supports and a UDL

Share load  $q$  between 2 families of beam strips parallel to the sides (and the  $x$  and  $y$  axes). How might we proportion the loads?

For an isotropic design we can equate the maximum midspan bending moments:

$$\frac{q_x(2a)^2}{8} = \frac{q_y(2b)^2}{8} \Rightarrow \frac{q_x}{q_y} = \left(\frac{b}{a}\right)^2. \quad (4)$$

Or we could aim to make deflections equal at the centre, and this would imply that:

$$\frac{q_x(2a)^4}{384EI} = \frac{q_y(2b)^4}{384EI} \Rightarrow \frac{q_x}{q_y} = \left(\frac{b}{a}\right)^4. \quad (5)$$

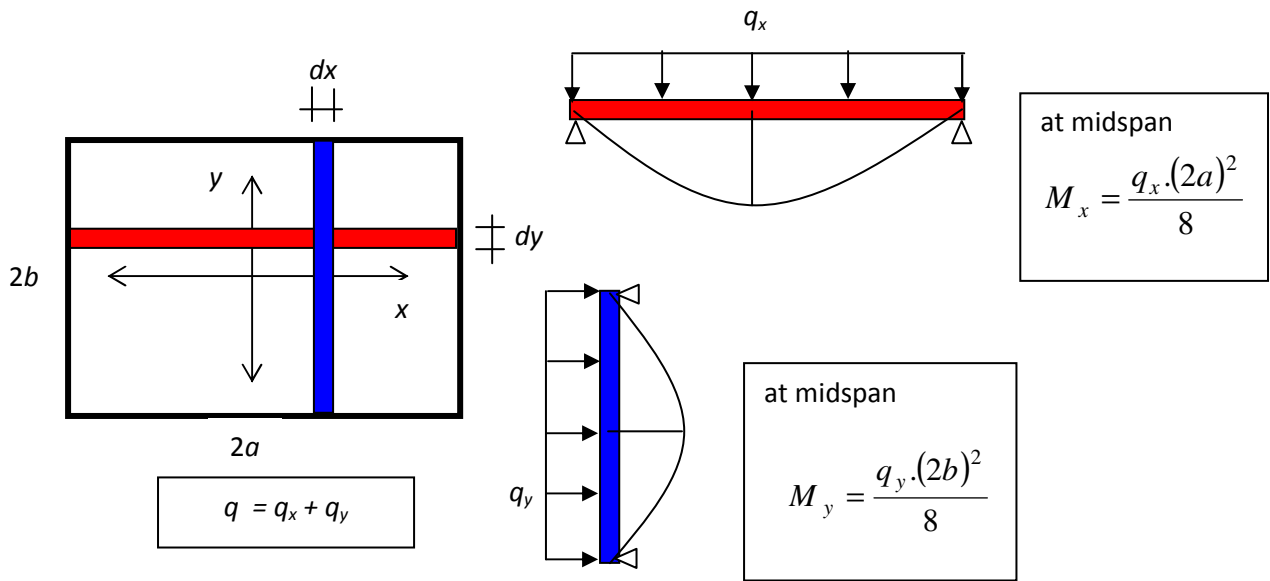


Figure 11: beam strip solutions for figure 10.

- **2 simply supported sides with a line load in a perpendicular direction , e.g. a wall**

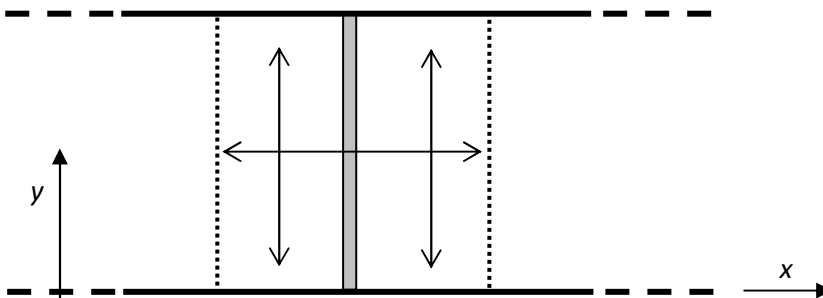


Figure 12: line load perpendicular to two lines of support.

In this case the two families of beam strips interact when we consider  $y$ -strips support the  $x$ -strips. We decide on a width of support  $2a$  and require  $W \cdot dy = q_x(2a) \cdot dy$  and  $q_y = -q_x$  for equilibrium. The line load from the wall is then dispersed laterally over an “effective” width  $2a$  by the  $x$ -strips and then transferred by the  $y$ -strips to the 2 lines of support perpendicular to the wall.



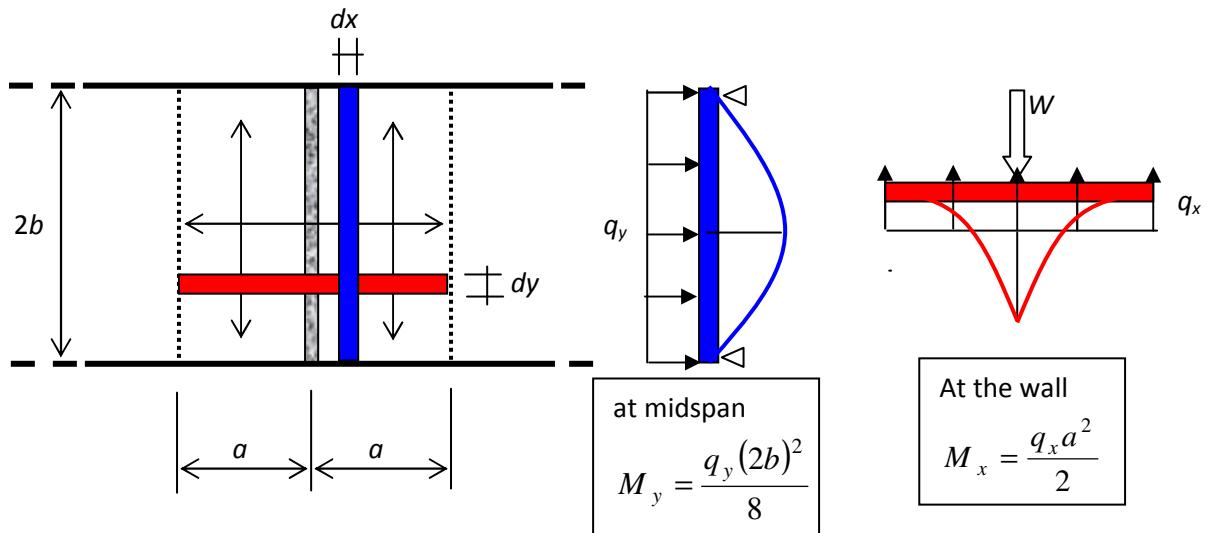


Figure 13: beam strips for Figure 12.

- **2 adjacent simply supported sides, line load along an unsupported side**

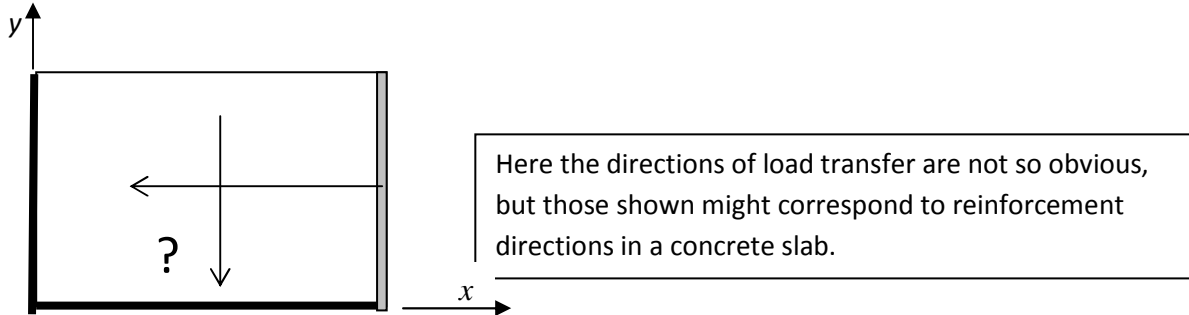


Figure 14: slab simply supported on 2 adjacent sides.

Like the previous example we might expect interaction between strips to disperse the line load to remote supports. However because individual strips are only supported at one end, rotational equilibrium becomes problematic! A way to overcome this problem is to imagine that the strips not only interact via pressures  $q_x = -q_y$ , but also via distributions of couples which restore moment equilibrium via torsional couples as indicated in Figure 15.

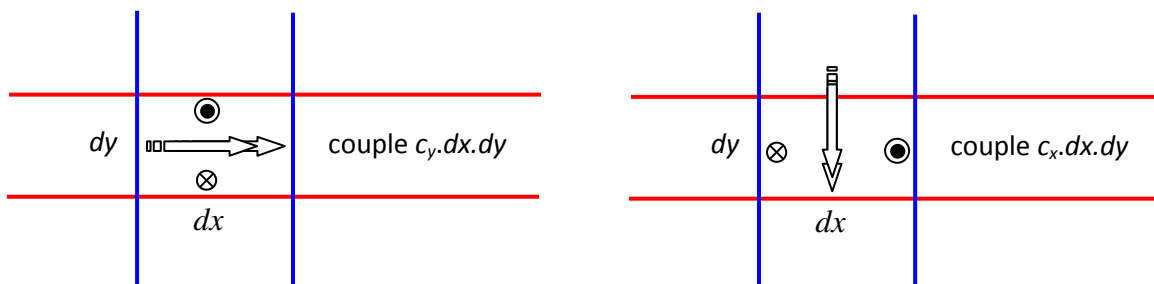


Figure 15: Interactive couples (imagine as transferred between planks by nails or screws)

An interactive couple such as  $c_y dx dy$  can be imagined to be activated by a couple of nails connecting two perpendicular planks as beam strips. The couple then acts as a bending load on the  $y$ -strip and a torsional load on the  $x$ -strip, and these types of load must be transferred to the two lines of support. Whilst the concept of interacting floor planks is a useful way to

describe load transfer (or load paths), it still treats the planks in one particular family as independent parts of a structural system. Figure 16 illustrates this case.  
 NB The definition of the interactive forces and couples in the above example are by no means unique – as usual the structural system is highly statically indeterminate!

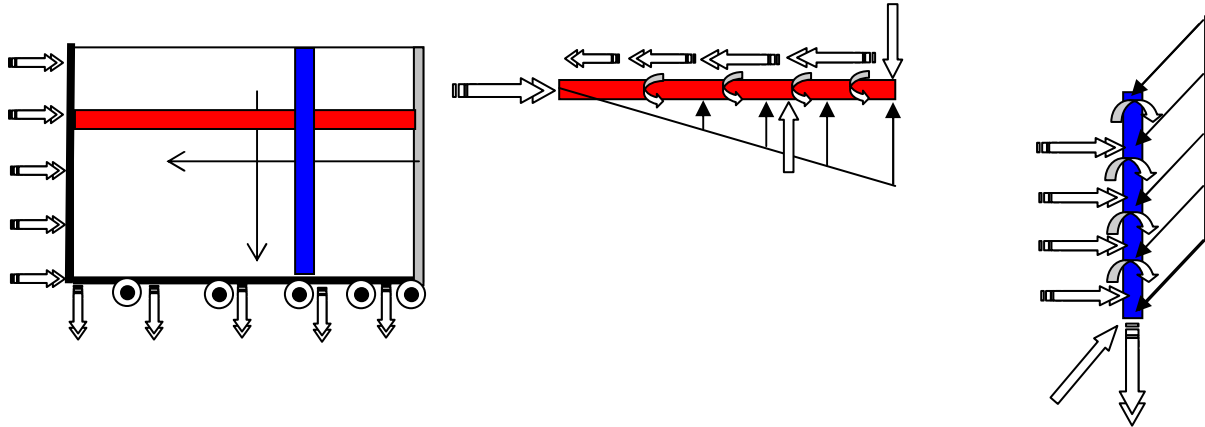


Figure 16: Beam strips with an example of interactive loads in the form of pressures and couples.

- **dispersal of a concentrated load on a small area to a larger area**

This example illustrates strip interactions when concentrated loads need to be dispersed over a larger area as indicated in Figures 17 and 18.

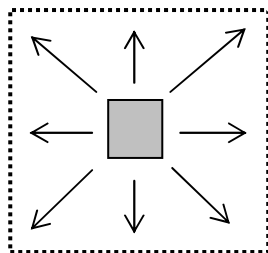


Figure 17: a concentrated load to be dispersed.

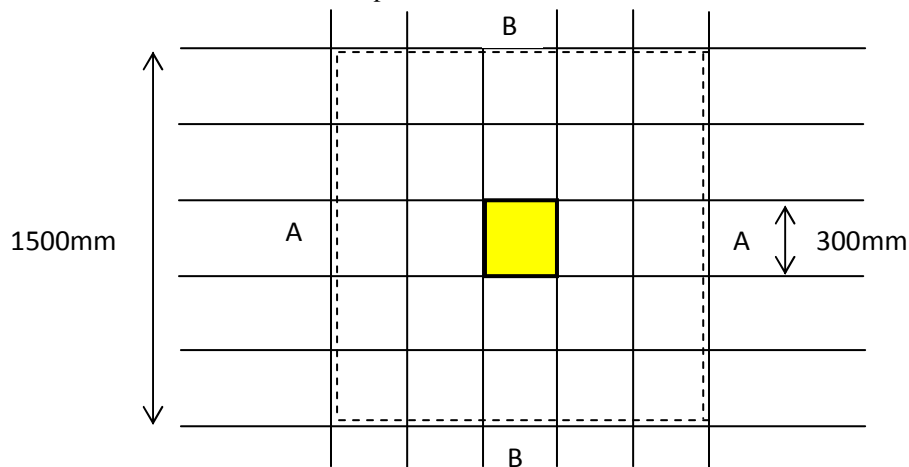


Figure 18: 100kN uniformly distributed over 300mm by 300mm area

The first stage could be to share the load equally onto the two central strips A-A and B-B that are supported by uniform upward pressures of  $\frac{50}{1.5 \times 0.3} = 111.11 \text{ kN/m}^2$ :

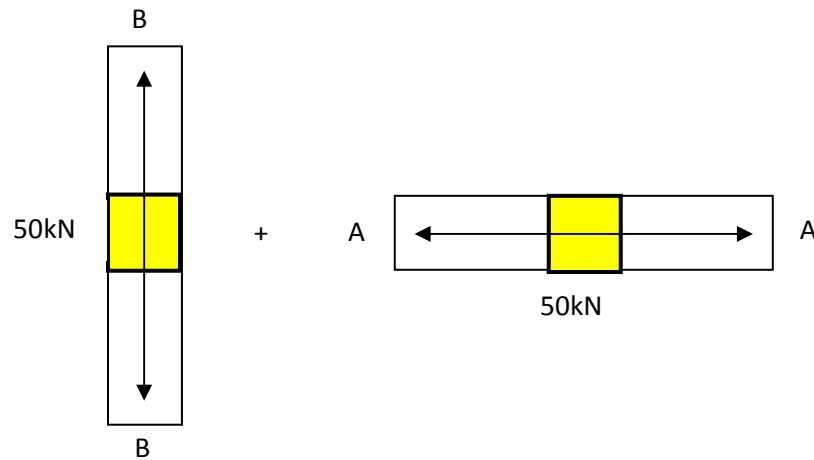


Figure 19: load shared between two orthogonal strips.

The downward pressure of  $111.11 \text{ kN/m}^2$  is imposed on transverse strips that extend over a 1.5m length. Thus each transverse strip is loaded over its central  $300 \text{ mm} \times 300 \text{ mm}$  area by a force of 10kN. This force is, in turn, supported by a uniform upward pressure of  $\frac{10}{1.5 \times 0.3} = 22.22 \text{ kN/m}^2$ . The downward pressure from each family of strips leads to a total downward pressure of  $2 \times 22.22 = 44.44 \text{ kN/m}^2$  i.e.  $\frac{100}{1.5 \times 1.5} = 44.44 \text{ kN/m}^2$  onto the larger area.

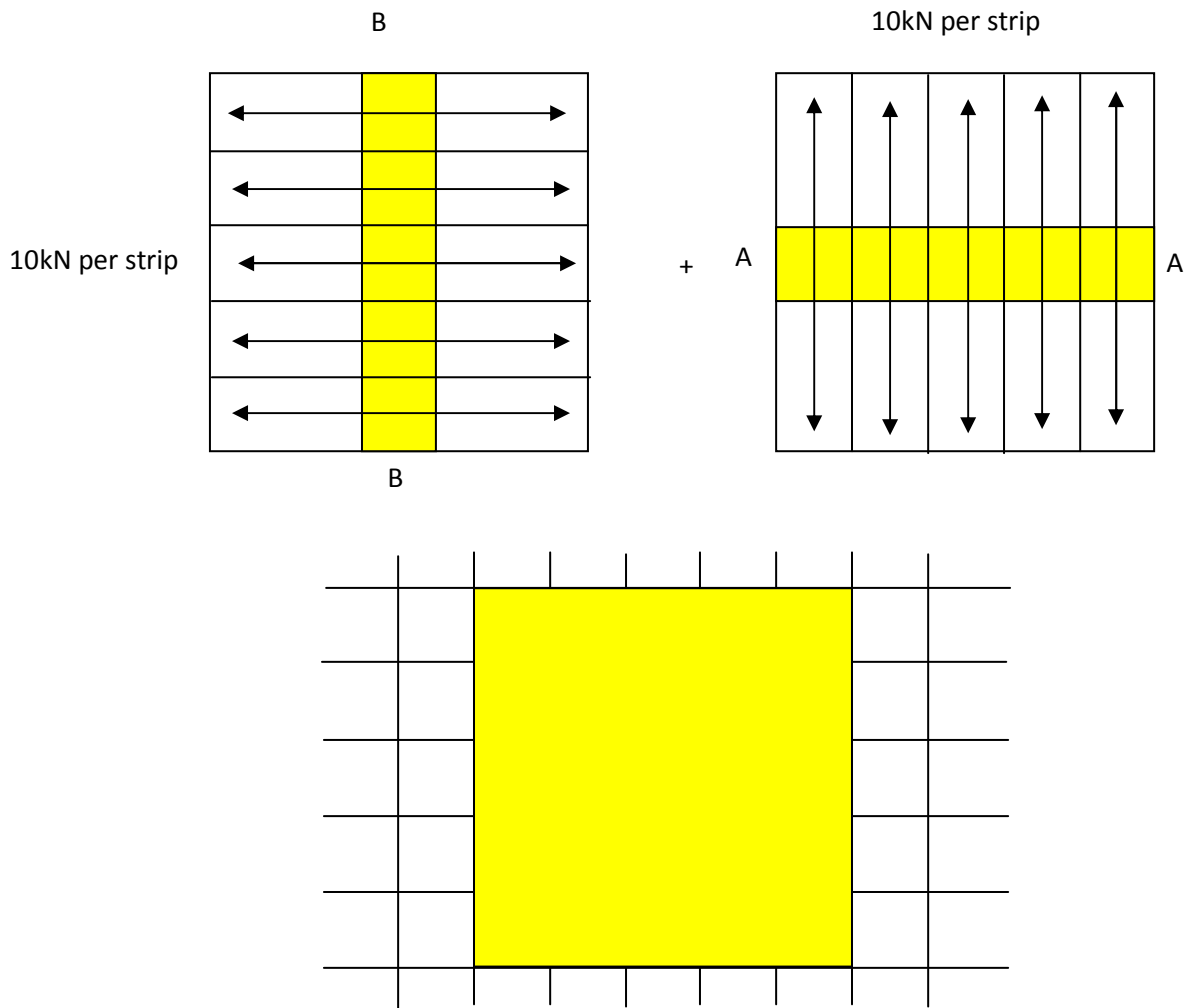


Figure 20: 100kN uniformly distributed over 1500mm by 1500mm area

We can now calculate shear force and bending moment diagrams for typical strips. The loads and internal forces in strip A-A are illustrated in Figure 21.

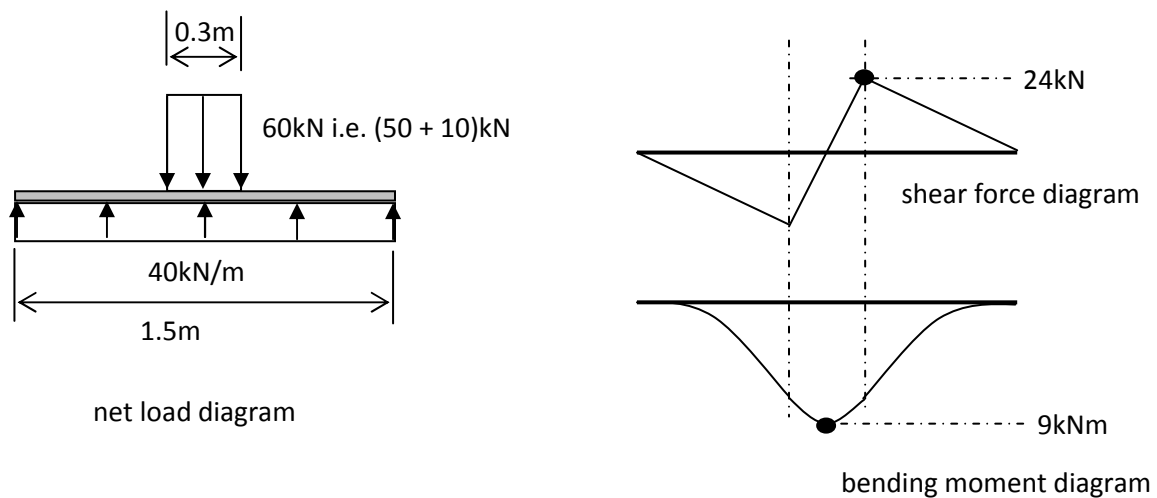


Figure 21: loads and internal shear force and bending moment diagrams.

Note that parallel adjacent strips have similar shear force and bending moment diagrams, but they support a smaller load, i.e. only 10kN. Further dispersion could be defined by continuing with similar stages, and superimposing the total internal actions.

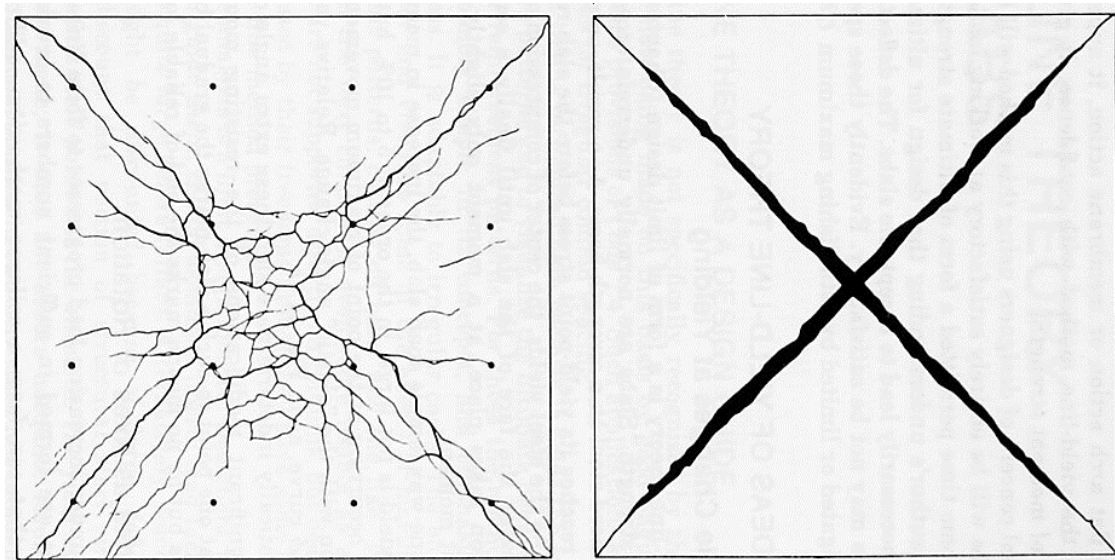
### Limit analysis for upper bounds

The dual aspect to limit analysis involves predicting/imagining the possible modes of collapse, e.g. as shown in Figures 22 and 23, and then ensuring that collapse doesn't occur before the load has reached a value above that normally expected – the ratio of the collapse load to the normal load is termed the load factor.

In the case of plates we will restrict ourselves to those modes of collapse that involve the formation of zones of local yielding due to flexural actions as indicated in Figure 23.



Figure 22: Collapse of Pipers Row car park – mainly a shear mode of collapse. [12]



(a) Crack patterns on soffit of a simply supported square slab, (b) simplified pattern of yield lines [13]

Figure 23: example of a flexural mode of collapse.

This mode of collapse tends to develop by the gradual formation of “plastic hinges” that extend to form “yield lines”, and when these lines connect to complete a mechanism, the slab collapses. The art is then to predict the most likely pattern of yield lines for a given slab with its supports and a given pattern of loading. If we happen to choose a different pattern of yield lines i.e. another mode of collapse, then the determination of the corresponding collapse load, and its load factor, will be theoretically too high, i.e. we obtain an upper bound to the collapse load (or we may say that we obtain an unsafe result). We need to determine the least upper bound if possible.

The nature of this bound follows from the upper bound theorem of plasticity, and although it is theoretically unsafe, experience has given engineers the confidence to exploit the yield line method [14], and it is always useful to know if upper bounds can be found close to lower bounds.

Yielding of the reinforcement to form hinge lines tends to concentrate deformations into zones along the yield lines, and deformations outside these zones are relatively insignificant. So we generally idealise the pattern of yield lines so as to partition a slab into **rigid regions** (or elements) **between yield lines**, and we neglect shear modes of collapse. For each region we should identify an axis of rotation – this will usually coincide with a line of support. Consequently the compatibility of transverse deflections along interfaces between regions implies that:

- yield lines remain straight between intersections with other yield lines,
- the alignment of a yield line along an intersection between two regions must be such as to be coincident with the point of intersection of the axes of rotation of the adjacent regions.

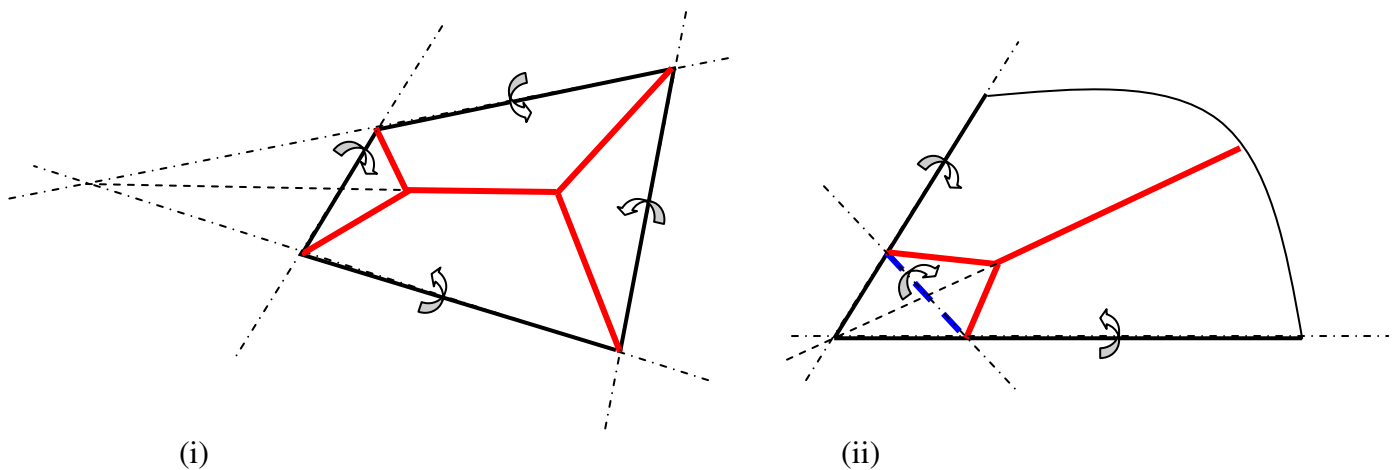


Figure 24: Some illustrative examples to illustrate yield lines and axes of rotation.

(ii) includes a so-called corner lever where a triangular corner region is held down with no deflection or rotation.

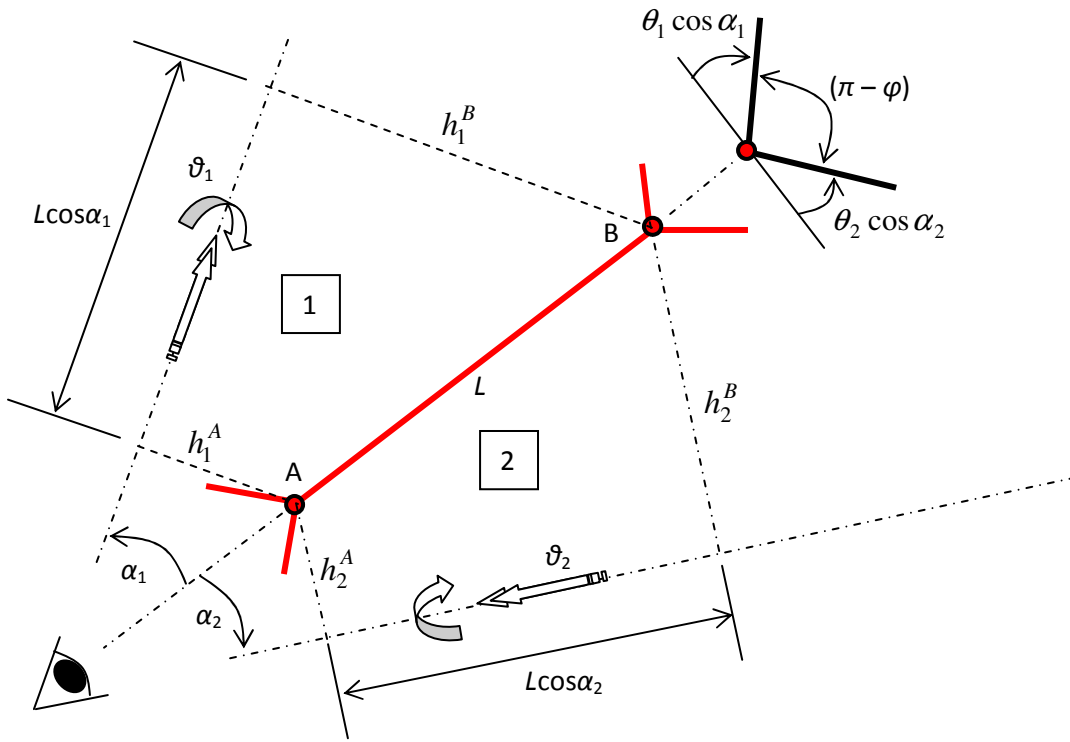


Figure 25: rotations or regions and rotations in yield lines.

To ensure compatibility of vertical deflections along yield line AB,

$$\theta_1 \times h_1^A = w_A = \theta_2 \times h_2^A \quad \text{and} \quad \theta_1 \times h_1^B = w_B = \theta_2 \times h_2^B, \quad (6)$$

and this is only achieved when continuation of the line B to A passes through the point of intersection of the axes of rotation of regions 1 and 2. Thus via the commonality of deflections  $w$  at each “node”, i.e. where 3 or more yield lines intersect, we obtain relations between the rotations of the regions about their axes of rotation. In fact each mechanism must have a unique relation between the nodal deflections, and so all the rotations of the regions can be expressed in terms of just one controlling parameter – which we may choose as one particular nodal deflection. NB, deflections of a mechanism are only known relative to each other – there are no absolute values.

So much for rotations of the regions, now we need to understand how to obtain the angle of rotation  $\varphi$  (or “fold” angle) as observed along a yield line. Small angles of rotation can be treated as vectors and resolved in different directions, so

$$\varphi = (\theta_1 \times \cos \alpha_1 + \theta_2 \times \cos \alpha_2) \quad (7)$$

Now we enforce a weak type of equilibrium by equating the internal work done within yield lines to the external work done by the loads applied to the regions, or more succinctly:

$$\text{Internal work } \sum (M_Y \times L \times \varphi) = \text{external work } \sum (P \times w) \quad (8)$$

where the summation for internal work is taken over all yield lines and the summation for external work is taken over all regions.

NB, in the case of homogeneous isotropic slabs (equal yield moments across yield lines in any direction at all points of the slab) we can simplify the evaluation of internal work as follows:

$$M_Y \times L \times \varphi = M_Y \times L(\theta_1 \cos \alpha_1 + \theta_2 \cos \alpha_2) = (M_Y \times L \cos \alpha_1) \times \theta_1 + (M_Y \times L \cos \alpha_2) \times \theta_2 \quad (9)$$

So then we could sum the work done by projected lengths of yield lines onto associated axes of rotation of the adjacent regions when they rotate.

The external work is evaluated for each region  $j$ . A load that is distributed in some way, e.g. uniformly, has a resultant force  $P_j$  with a corresponding line of action. Since each region is assumed rigid, it suffices to calculate the vertical deflection  $w_j = d_j \times \theta_j$  of the point on the line of action of  $P_j$ , where  $d_j$  is the perpendicular distance from the point to the axis of rotation. Then the work done by the load on region  $j$  is simply expressed as  $P_j \times w_j$ .

Since rotations  $\varphi$  and deflections  $w$  are functions of  $\theta_j$  which in turn can be expressed in terms of single controlling parameter  $\delta$ , the work equation leads us to a relation between the yield strength of the slab and the loads corresponding to a particular mode of collapse. NB, this relation provides us with results that are theoretically unsafe. It can be used in one of two ways: (i) given the load determine the flexural strength required to support it, or (ii) given the flexural strength determine the load that it can support. (i) is the design situation for a new structure, but the result is unsafe and hence gives a lower bound for the strength needed, and (ii) is the assessment situation of an existing structure, but the result is unsafe and hence gives an upper bound to the load capacity.

The use of the work equation will be demonstrated in a simple example. Consider a 5m by 10m slab as illustrated in Figure 26, simply supported on side AD, and supported with moment continuity on sides AB, BC, and CD. It supports a UDL  $q$  kN/m<sup>2</sup>, and is reinforced so as to have a yield moment  $M_Y$  kNm/m that is the same in all directions and at all positions, i.e. the slab is isotropic and homogeneous.

First we find relations between  $q$  and  $M_Y$  for 3 possible yield line patterns, each of which involves hogging along the lines of continuous support.

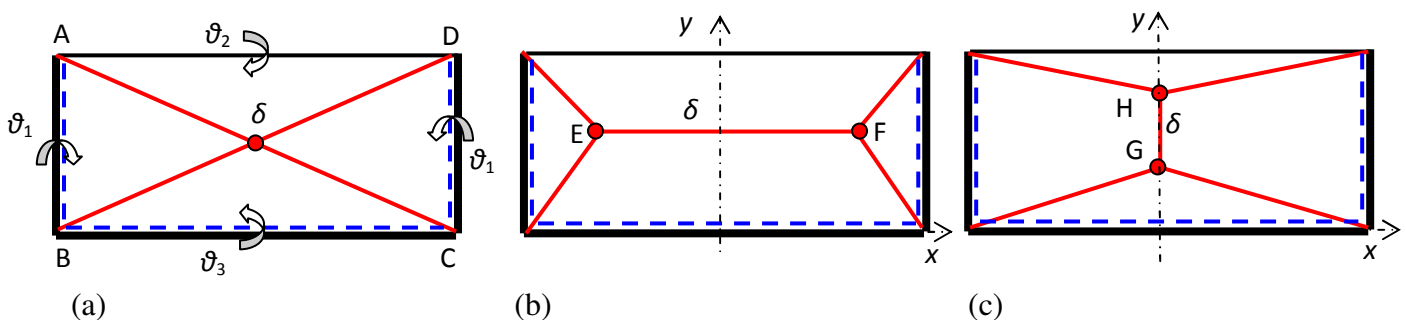


Figure 26: some possible yield line patterns

In pattern (a) the 4 sagging yield lines converge at the centre of the slab.

The work done in the sagging yield lines =  $M_Y(2.5\theta_1 + 5\theta_2) \times 2 + M_Y(2.5\theta_1 + 5\theta_3) \times 2$

The work done in the hogging yield lines =  $M_Y(2 \times 5 \theta_1 + 10 \theta_3)$

Compatibility requires  $5\theta_1 = 2.5\theta_2 = 2.5\theta_3 = \delta$



Thus total internal work =  $2M_Y \left( \frac{2.5}{5} + \frac{5}{2.5} \right) \times 2\delta + M_Y \left( \frac{10}{5} + \frac{10}{2.5} \right) \times \delta = 16M_Y \delta$

The external work done by the UDL on each triangular region =  $q \times \frac{5 \times 10}{4} \times \frac{\delta}{3} = \frac{50}{4} q \frac{\delta}{3}$

The work equation becomes:  $50q \frac{\delta}{3} = 16M_Y \delta$ , i.e.  $q = 0.96M_Y$  or  $M_Y = 1.04167q$ . (9)

Pattern (b) contains 2 geometric parameters which can be taken as the coordinates of  $F(a,b)$ , when symmetry about the y-axis is assumed. The work done in the sagging yield lines =

$$M_Y(2a(\theta_2 + \theta_3)) + 2M_Y((5 - b)\theta_1 + (5 - a)\theta_2) + 2M_Y(b\theta_1 + (5 - a)\theta_3)$$

The work done by the hogging yield lines =  $10M_Y(\theta_3 + \theta_1)$ , and the total internal work done =  $10M_Y(2\theta_1 + \theta_2 + 2\theta_2)$ .

Compatibility requires  $(5 - a)\theta_1 = (5 - b)\theta_2 = b\theta_3 = \delta$ , from which we deduce that

the internal work =  $10M_Y \frac{(50 - 10a + 5b + ab - 2b^2)}{(5 - a)(5 - b)b} \delta$ .

The external work =  $q(2a \times 5) \frac{\delta}{2} + 2q(5(5 - a)) \frac{\delta}{3} = q \frac{5(10 + a)}{3} \delta$ .

$$\text{Work balance then leads to: } q = 6M_Y \left[ \frac{(50 - 10a + 5b + ab - 2b^2)}{(10 + a)(5 - a)(5 - b)b} \right]. \quad (10)$$

Since we expect to derive an upper bound solution for  $q$ , we should minimise the expression in square parentheses to find the least upper bound for this pattern.

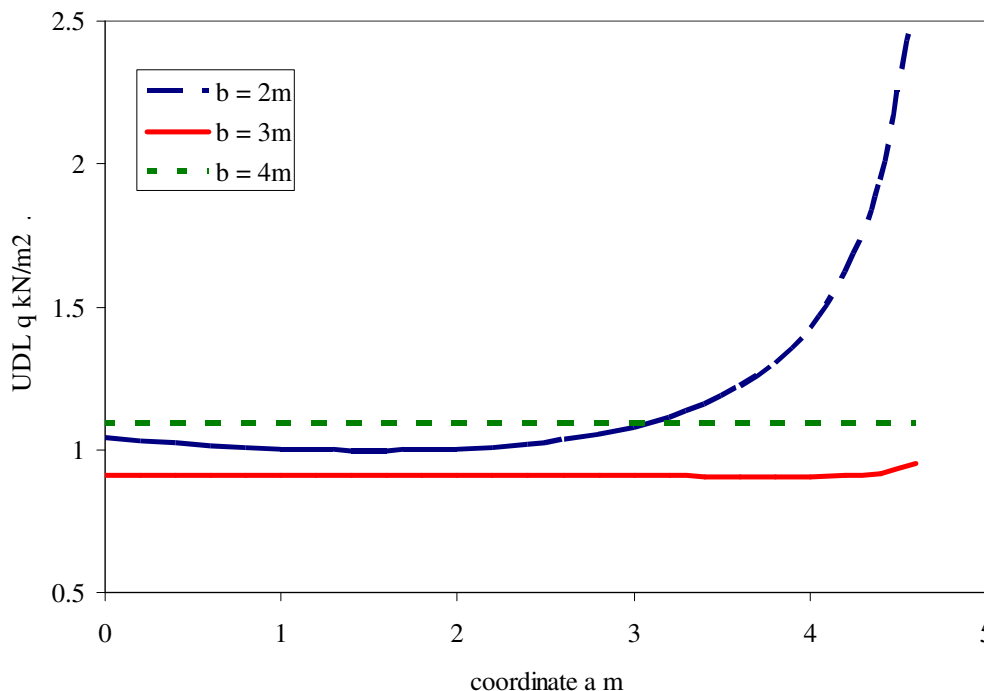


Figure 27: variation of  $q$  dependent on coordinates ( $a, b$ ) for a unit value of  $M_Y$ .

Figure 27 indicates that the value of  $q$  is not very sensitive to the value of  $a$  in the range  $0 \leq a \leq 3\text{m}$ , and the minimum value of  $q \approx 0.9059M_Y$  occurs when  $F$  is at (1.36, 2.93).

Pattern (c) appears to have a minimum value of  $q$  occurring when  $G$  and  $H$  coincide at the centre of the plate, and this indicates that the pattern is not the critical one in this case.

Comparison is now made with a lower bound from an equilibrium solution based on simple beam strips shown in Figure 28.

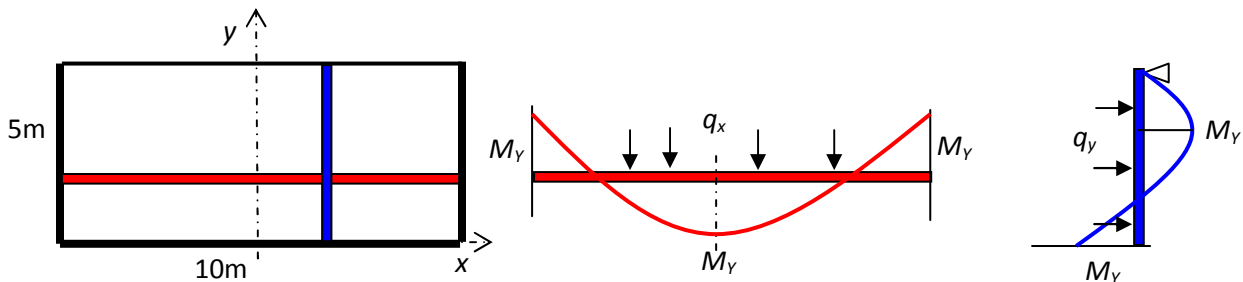


Figure 28: beam strips with simple and continuous supports.

The maximum UDL's on each type of beam strip satisfy  $\frac{q_x 10^2}{8} = 2M_Y$ ,  $q_y 5^2 = \frac{2M_Y}{(3 - 2\sqrt{2})}$

and then  $q = q_x + q_y = (0.16 + 0.466)M_Y = 0.626M_Y \text{ kN/m}^2 < 0.9059M_Y$ . The true theoretical collapse load lies somewhere inbetween the lower and upper bound values!

Further examples of yield line solutions can be found in references [8 to 11,14,15]. A more systematic approach, using patterns based on triangular FE meshes, is exploited in EFE [4], and this is illustrated in the Appendix.

## References

- [1] The establishment of plastic design in the UK, J. Heyman, Proceedings of the Institution of Civil Engineers: Engineering History and Heritage, EH1, 7-11, February 2009.
- [2] Limit analysis and concrete plasticity, M.P. Nielsen, Prentice-Hall, 1984.
- [3] The Stone Skeleton, Jacques Heyman, CUP, 1995.
- [4] [www.ramsay-maunders.co.uk](http://www.ramsay-maunders.co.uk)
- [5] Design of Concrete Slabs for Transverse Shear, P. Marti, ACI Structural Journal, **87**, No 2, March-April, 1990, 180-190.
- [6] Strip method of design, A. Hillerborg, Viewpoint, 1975
- [7] Strip method design handbook, A. Hillerborg, E & FN Spon, 1996.

- [8] CALcrete, RC design part 2, section 6: Slabs, 2005
- [9] Reinforced Concrete Design to Eurocode 2, W. Mosley, J. Bungey, R. Hulse, 6<sup>th</sup> ed, Palgrave, 2007.
- [10] Reinforced Concrete – Mechanics and Design, J.G. MacGregor, Prentice Hall, 3<sup>rd</sup> ed., 1997. Chapter 15: Two-Way Slabs: Elastic, Yield Line, and Strip Method Analysis.
- [11] Design of Concrete Structures, A.H.Nilson, D.Darwin, C.W.Dolan, McGraw-Hill, 13<sup>th</sup> ed., 2003.
- [12] [www.hse.gov.uk/research/misc/pipersrow.htm](http://www.hse.gov.uk/research/misc/pipersrow.htm)
- [13] Reinforced Concrete Fundamentals, P.M. Ferguson, 4<sup>th</sup> ed. Wiley, 1981.
- [14] Practical yield line design, G. Kennedy & C.H. Goodchild, The Concrete Centre, 2004  
See also [www.brmca.org.uk/downloads/PYLD240603a.pdf](http://www.brmca.org.uk/downloads/PYLD240603a.pdf), 2003
- [15] [www.sbe.napier.ac.uk/projects/yield-line-analysis](http://www.sbe.napier.ac.uk/projects/yield-line-analysis)
- [16] Collapse analysis of reinforced concrete slabs: are the up and down roads one and the same?, D. Johnson, in Advances in Engineering Structures, Mechanics & Construction, M. Pandey et al. (eds.), 823-831, Springer, 2006.

Assignment: Limit analysis in the design of reinforced concrete slabs specified in Previous Assignment

**(a) Equilibrium analysis of slabs**

Use two families of beam strips to estimate the maximum design moments for the specified loads, preferably without torsional moments, although you may find it easier to include torsion in cases (9) and (10).

- The diagrams for Assignment 3 are not to scale, so a first step in designing families of beam strips is to draw a plan to scale, and then consider “load routes” to the supports.
- Assume simple supports to mean zero vertical deflection with no normal bending moments. Twisting moments could be included, but you need to think about the physical nature of the supports!
- Determine by statics a distribution of support reactions, and sketch load, bending moment and shear force diagrams for the strips with greatest bending moments in each family.

Complete part (a) for presentation and discussion at a seminar on 2<sup>nd</sup> December 2008.

**(b) Yield line analysis of slabs.**

- Use the proposed yield line patterns in the following Table to calculate the flexural strength, or yield bending moment  $M_Y$  kNm/m, required to support the specified load. The yield line pattern defines one possible collapse mechanism for the slab, there are an infinite number of possibilities! However many mechanisms are considered in practice, the one which minimises the collapse load for a given strength (least upper bound) gives the best solution. You can assume for simplicity that the slab is homogeneous and isotropic.
- Propose an alternative yield line pattern which should be considered for analysis, but do not carry out the analysis!

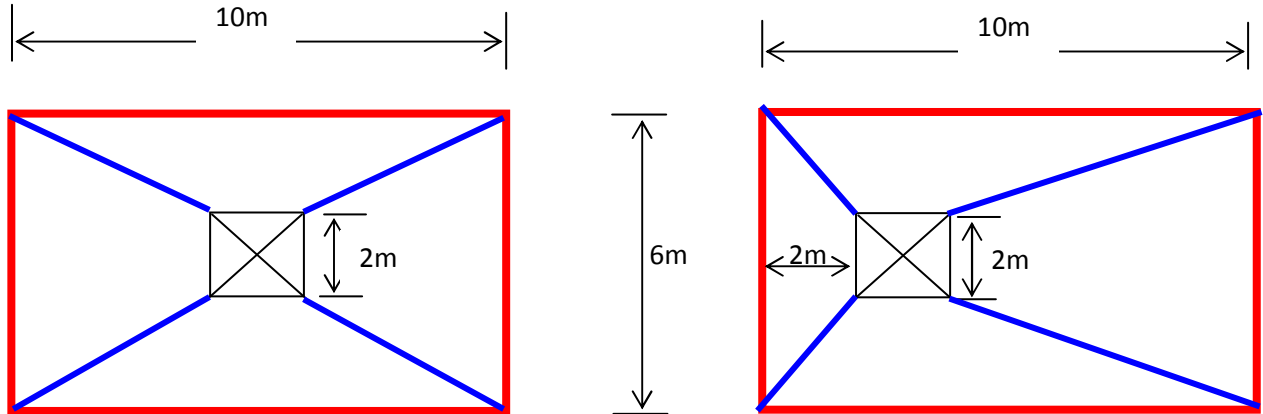
Note that yield line analysis is “unsafe” in that, for a given slab with a given strength, a yield line analysis leads to an upper bound of the collapse load; **conversely for a given load a yield line analysis leads to a lower bound of the flexural strength required to support the load!**

On the other hand for limit analysis of “plastic” structures, equilibrium analysis, where you define stresses or stress-resultants to be in a state of equilibrium with specified loads in a way which does not allow moments to exceed yield bending moments, leads to a “safe” prediction of the flexural strength, i.e. an upper bound of the flexural strength required. Note that the linear elastic finite element analysis provides a pseudo-equilibrium analysis that could lead to another “safe” prediction provided you are satisfied with the lack of equilibrium involved!

- **You should compare the design flexural strengths you obtain from parts (a) and (b), and the strengths required from the linear elastic finite element analysis in**

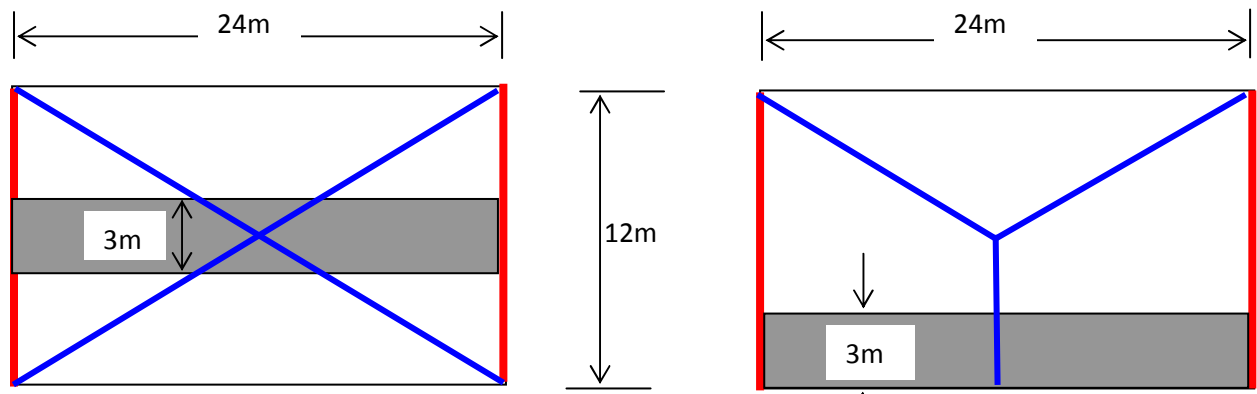
**Assignment 3. In the latter analysis you can observe the range of principal moments by plotting contours of derived moments termed  $M_{max}$  and  $M_{min}$  in Oasys GSA.**

- floor slab with an opening, simply supported on 4 edges



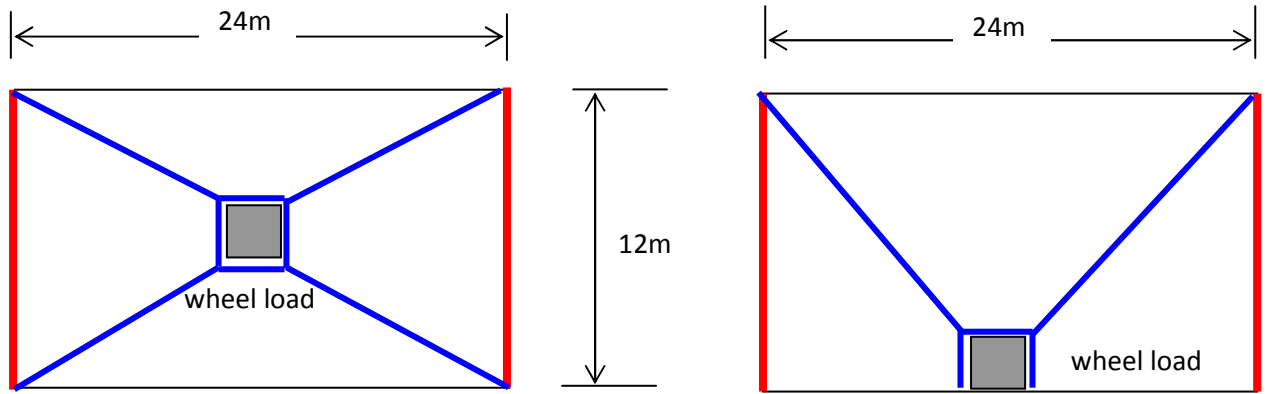
(1)  $5\text{kN/m}^2$  UDL with a central square opening      (2) as (1) but with an off-centre opening

- road bridge deck simply supported on two opposite edges, free on the other two edges



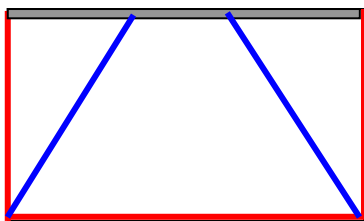
(3)  $10\text{kN/m}^2$  centre lane load      (4) as (3) but with lane load next to a free edge

- road bridge deck simply supported on two opposite edges, free on the other two edges

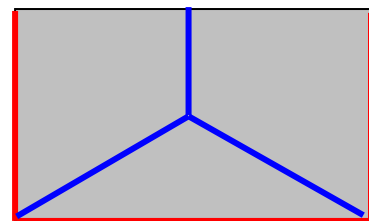


1. (5) 40kN UDL on a 1m×1m central patch      (6) as (5) but with position moved to a free edge

- 10m × 5m floor slab simply supported on 3 edges

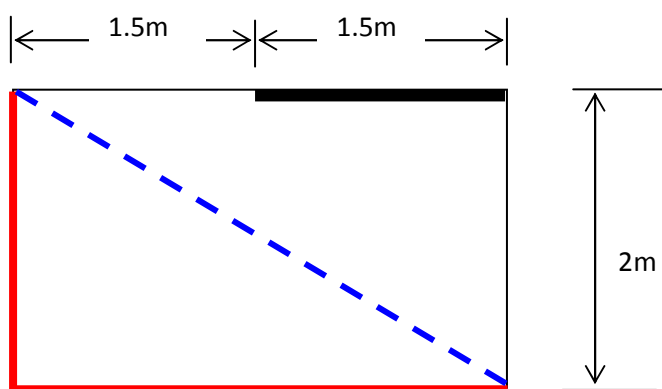


(7) 5kN/m edge load

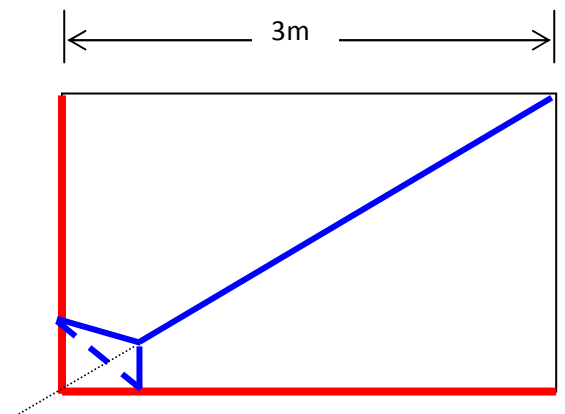


(8) 4kN/m<sup>2</sup> UDL

- granite landing slab simply supported on two adjacent edges, free on the other two edges

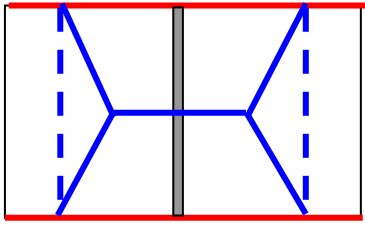


2. (9) 12kN/m line load applied on part of a free edge



(10) 5kN/m<sup>2</sup> UDL over the entire slab

- 10m × 5m floor slab simply supported on 2 edges      Table of student problems



(11) 5kN/m central load

## Appendix: Automated Yield Line Technique – Demonstration of EFE-YL

### Introduction

A demonstration of an automated or computerised technique for the yield line analysis of ductile plates is to be given as implemented in the software EFE-YL. The example chosen for consideration is problem 4 from Assignment 4 for this module and is shown in Figure 1. The reinforcement is isotropic (equal strength in all directions both in sagging and hogging). Two edges are simply supported and a UDL is applied to a strip as shown in the figure.

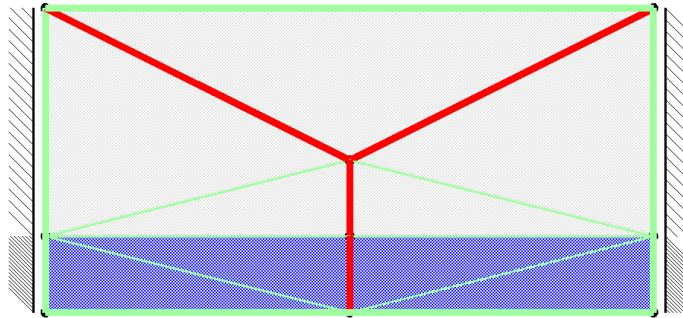


**Figure 1:** Geometry, boundary conditions and loading (Problem 4 from Assignment 4)

The yield line pattern assumed for the assignment, which may not be the correct pattern, is as shown in Figure 1 and comprises a symmetric 'Y' pattern of sagging (red) yield lines.

### Model Construction

The automated technique used in EFE-YL requires that the model be meshed with triangular elements – see underlying mesh in Figure 1. The edges of the elements form potential yield lines and the particular configuration chosen by EFE-YL on solution is that which minimised the collapse load – recall that the method is an upper-bound technique.

### Geometric Optimisation

The suggested yield line pattern of Figure 1 has a number of potential geometric degrees of freedom. The bifurcation point can move in the plane, i.e. it can have two degrees of freedom, and the bottom point can move along the edge, i.e. it can have a single degree of freedom. To maintain a 'Y' pattern with a vertical stem the horizontal degree of freedom of the bottom point should be coupled or made a slave of the horizontal position of the bifurcation point. Figure 2 shows the geometric variables used.



— Point Master Bound  
— Point Slave Bound  
 PM-1 (Non-Polygonal) (Number of Grouped Points =1)  
 $-4.00E+00 < \text{Global}(X) < 4.00E+00$   
 $4.00E+00 < \text{Global}(Y) < 10.00E+00$   
 PS-1 (Number of Grouped Points =2)  
 $\text{Global}(X)=\text{PM-1}, \text{Global}(X), 1.00E+00$

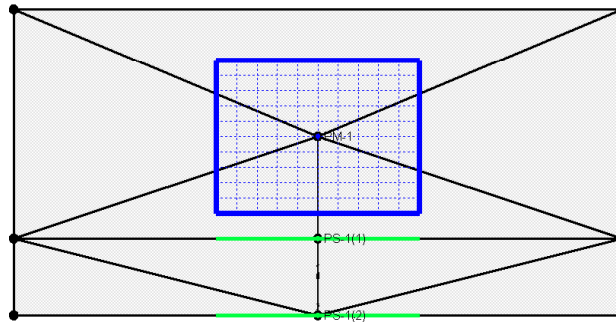


**Figure 2:** Geometric variation of ‘Y’ yield line pattern

A geometric optimisation problem has now been defined where the x and y position of the bifurcation point are variables (bounded by the blue box). For each x,y position there will be a different collapse load (load factor)but the optimum position for the bifurcation point is that which minimises the collapse load.

EFE-YL can perform this optimisation automatically but it is useful to obtain a feel for the nature of the objective function, i.e. the objective function terrain. This has been done by setting the bifurcation point in the centre of the bounding box (as in Figure 2) and independently varying the two geometric variables between their respective bounds. The resulting plot of load factor against position is shown in Figure 3. The values in this figure are normalised so that all results fit onto a single plot. The load factors and collapse mechanisms at various key points are shown in the figure.

When the x position of the bifurcation point is varied the result is symmetric with a minimum at the central value of x. This is to be expected as the problem (reinforcement, loading and boundary conditions are symmetric. The variation of load factor with the y position of the bifurcation point appears to be a composite curve of two parts which join some three-quarters of the way between the minimum and maximum values of y. The two parts of the composite curve correspond to different collapse mechanisms with the mechanism for higher y values involving hogging yield lines (green) and no longer being a ‘Y’ pattern.

The results shown in Figure 3 were generated by moving the bifurcation point to the desired position and then performing an analysis. The results indicate a minimum value of the collapse load to occur for a central value of x and a minimum value of y. EFE-YL can conduct such optimisation automatically and if this is done the procedure converges to the optimum solution just identified.

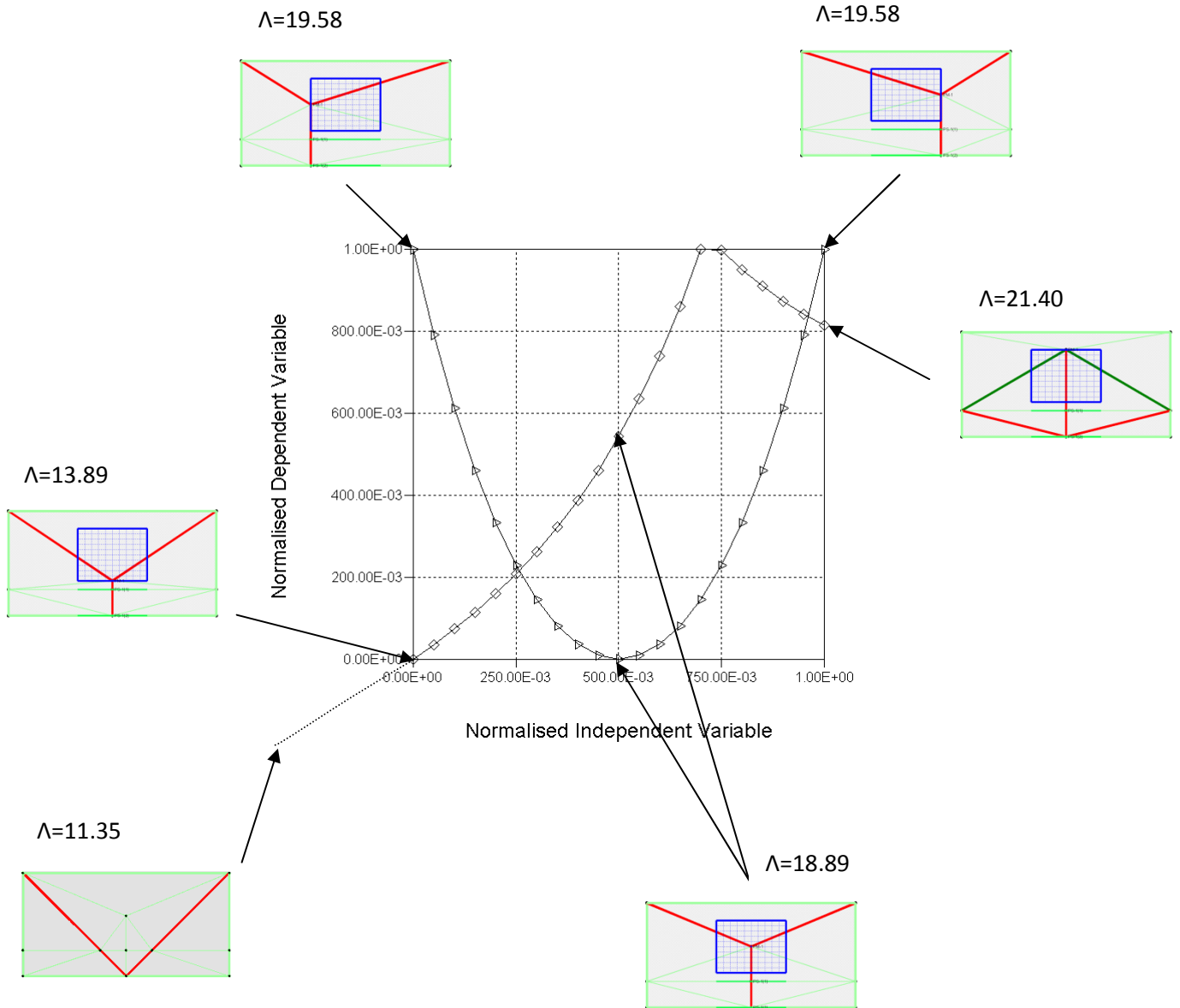


**Figure 3:** Plot of Load Factor  $\Lambda$  against geometric variable

Thus far we have assumed a mode of collapse mechanism (the 'Y' shaped mode) and, recognising that it possesses some geometric variability, we have found the optimum position for the bifurcation point. A question remains as to whether or not the chosen mode of collapse was actually the correct one – in other words is there another collapse mechanism lurking in the wings that has a lower collapse load?

## Mesh Refinement as a Method for Locating the Critical Collapse Mode

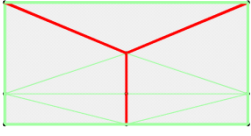
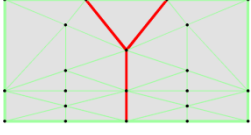
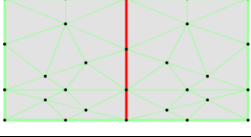
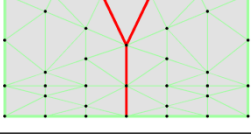
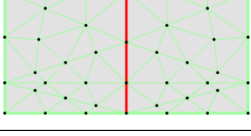
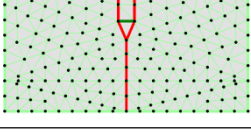
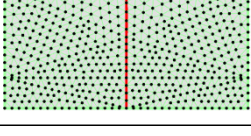
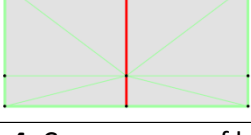
In the absence of any knowledge of the critical collapse mechanism, mesh refinement can be a useful although, as will be demonstrated, not foolproof technique. The idea here is that we mesh the model with some initial mesh then observe the way in which the collapse mechanism changes as the mesh is progressively refined. Experience with other numerical techniques, e.g. elastic finite element analysis, may condition us to expect a monotonic convergence of load factor with mesh refinement. However, such monotonic convergence is not generally obtained with the yield line technique since the element themselves are rigid and it is the position and orientation of the yielding edges that describes the collapse mechanism. Different meshes will have different patterns of element edges which may or may not allow the series of meshes to converge.

A convergence run using mesh refinement is shown in Figure 4. The first column of the figure shows the mesh and resulting yield line pattern. The second column lists the number of elements specified to the mesh generator and the actual number of elements produced whilst the final column lists the load factor. The initial mesh uses the geometry of the previous model for the 'Y' shaped collapse mode with the bifurcation point located at the centre of the bounds.

The 'convergence' observed in Figure 4 is not monotonic with the load factor oscillating with increasing numbers of elements. A number of meshes (20 and 40 specified elements) give the same results which has a load factor below that achieved with the other meshes. The collapse mechanism for these is a very simple one comprising a sagging yield line across the centre of the slab. Two highly refined meshes of 300 and 1000 specified elements were considered but as neither admits the simple central yield line in the mesh neither produces is able to better the lowest load factor. A 'minimal' mesh using the minimum number of elements possible to discretise the geometry whilst admitting the simple central yield line is shown in the last row of Figure 4 and is able to produce the lowest load factor.

The results of the mesh refinement study indicate that the critical collapse mechanism is that of the simple single sagging yield line running across the centre of the slab. This mechanism produces a significantly lower (approximately 50%) load factor than that of the assumed 'Y' pattern (5.56 as opposed to 11.35) and highlights the necessity for considering a range of possible collapse mechanisms when using the yield line technique.

Is the single sagging yield line running across the centre of the slab the correct (true or exact) mechanism? It seems likely but this question may only be answered by somehow confirming that the moment distribution within the rigid regions nowhere violate the yield criterion. Since the yield line technique provides no information regarding the moment distribution within the elements this can be neither confirmed nor denied with this technique. In order to obtain the moment distribution within elements resort needs to be made to a lower-bound technique in which the moment field for the entire slab is defined. Such lower bound elements exist and are currently being incorporated into EFE with a view to providing bounded solutions to the limit analysis of ductile plate structures.

Mesh	Number of Elements specified (actual)	Load Factor
	1 (9)	18.89
	10 (29)	7.04
	20 (40)	5.56
	30 (49)	6.09
	40 (64)	5.56
	300	5.88
	1000	5.69
	1 (8)	5.56

**Figure 4:** Convergence of load factor with mesh refinement

## A Case Study – St John’s Wood

The yield line technique is recommended by the Concrete Centre [10] as being admissible for the design of reinforced concrete slabs and being acceptable through the appropriate Euro Codes.

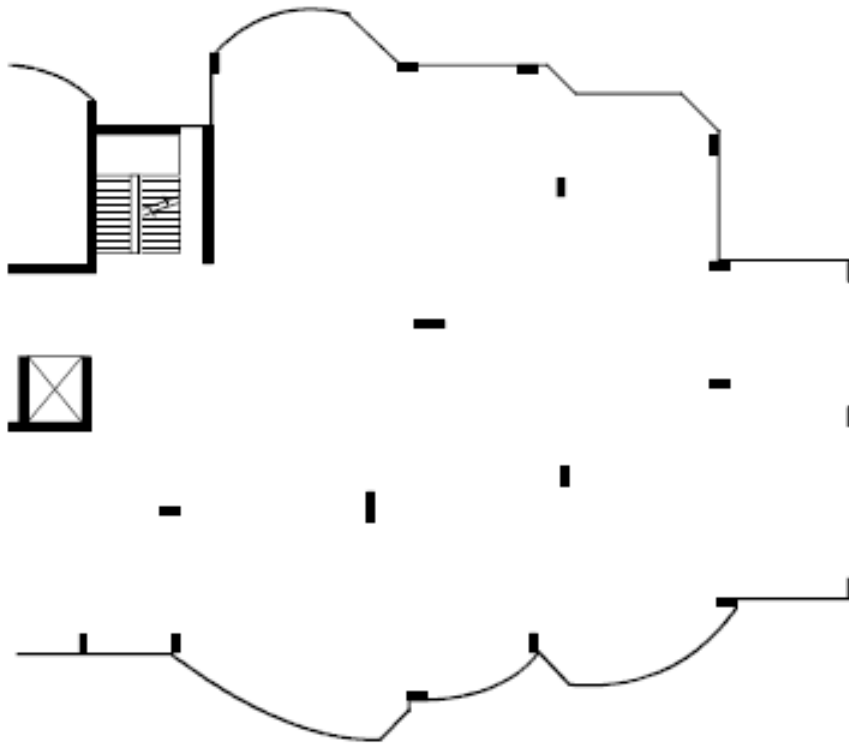


**Figure 5:** part floor plan of a typical floor at St John’s Wood.

Figure 5 shows a part floor plan of a 7-storey block of flats in London. The flat slab has a constant thickness of 250mm. The floor has an irregular geometry and an irregular array of support columns and column dimensions. The maximum span is about 7.5m.

Yield analyses were carried out using EFE-YL assuming a uniform slab with isotropic yield moments and a uniformly distributed load. Figure 6 summarises results with a unit applied load intensity and a moment capacity of 50kN/m obtained for a range of meshes, the specified numbers of elements ranged from 100 to 2000. The upper bound nature of the load factors is apparent, and we look for the least upper bound.

The results are then used to derive lower bounds for the moment capacity to support a specified load at ULS, i.e. 21.7kN/m<sup>2</sup>. Now we look for the greatest lower bound.

Number of elements specified	Load factor for $m = 50\text{kNm/m}$	Required moment capacity $\text{kNm/m}$ for a total design load of $21.7\text{kN/m}^2$
100	27.392	
200	25.437	
300	24.092	
400	23.688	45.80
500	24.033	
600	23.175	46.82
700	23.884	
800	23.732	
900	23.052	47.07
1000	22.651	47.90, which compares to 47.2 from David Johnson [16]
1200	23.444	
1400	22.868	
1600	23.433	
1800	23.005	

**Figure 6:** results for a range of meshes with a UDL =  $1\text{kN/m}^2$  and a notional isotropic yield moment of  $50\text{kNm/m}$  for both sagging and hogging moments.

### Closure

The yield line technique offers a useful method for estimating the limit load of ductile plates such as reinforced concrete slabs. The method relies heavily on the engineer being able to correctly predict the critical collapse mechanism. For simple cases critical collapse mechanisms are well known and documented. For non-standard cases the engineer needs to be prepared to study a range of potential mechanisms in order to home-in on the critical one. Automated techniques such as EFE-YL make this exploration simpler and less prone to error but neither the hand technique nor the automated technique protect the engineer from assuming a non-critical collapse mechanism. As seen in the simple example shown in this document the difference between the collapse load for critical and non-critical mechanisms can be very significant and with the yield line technique a non-critical mechanism always gives an unsafe prediction of the collapse load.

Further research and development work is being conducted by RMA into providing complimentary lower bound solutions so that even where the true collapse mechanism is unknown the true collapse load may be bounded – hopefully with sufficient tightness to be of practical value.

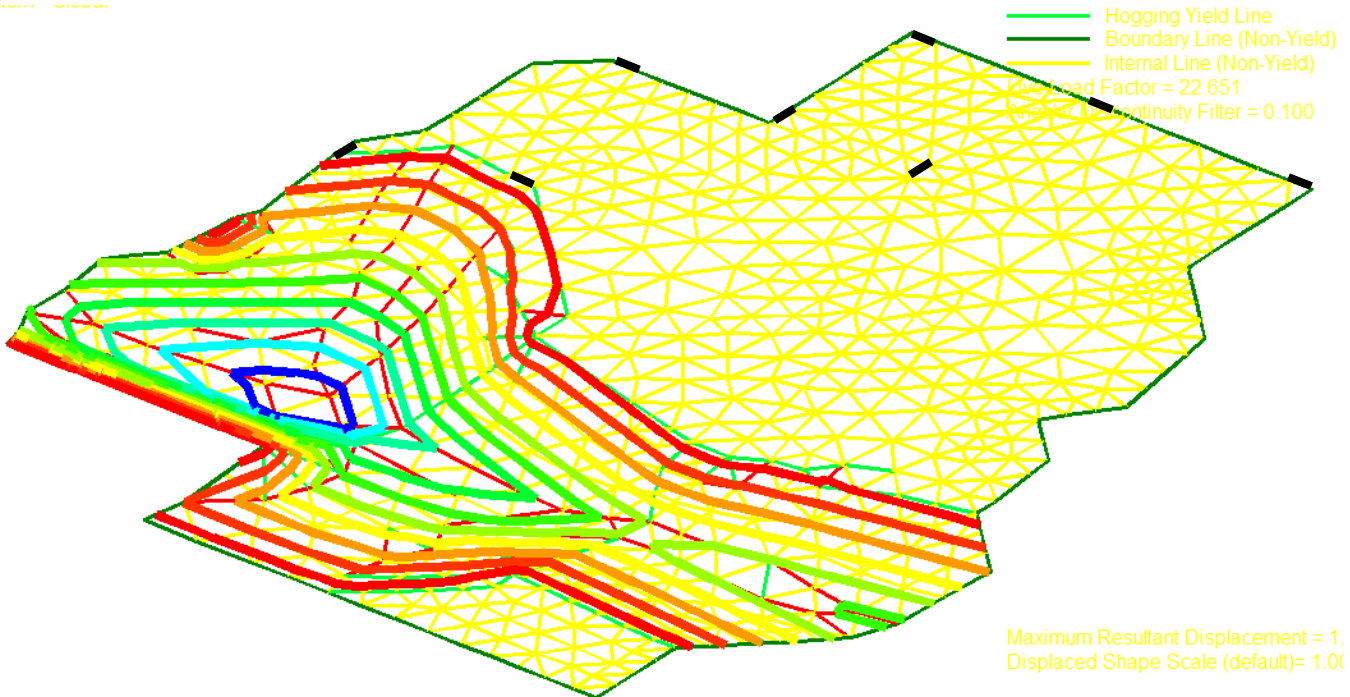


**Figure 7:** an isometric view of a collapse mechanism of the slab with column positions included

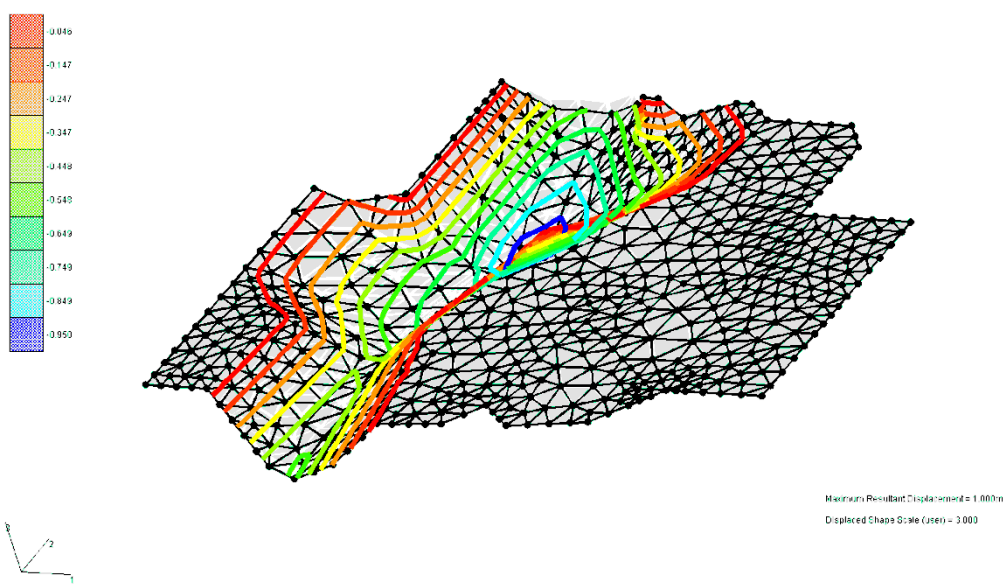


**Figure 8:** another isometric view of a collapse mechanism

Figures 7 and 8 show different views of the deflected form of a collapse mechanism together with contour lines of vertical deflection.

**Acknowledgements:**

These notes were prepared for the Advanced Structural Engineering Module in the College of Engineering, Mathematics and Physical Sciences at the University of Exeter. This is a fourth year module undertaken by MEng and MSc students. These were presented by Edward Maunder in the academic year 2009/10. The finite element yield line solutions were produced by RMA's software EFE.